The variations in the profiles of strong Fraunhofer lines along a radius of the solar disc

THE VARIATIONS IN THE PROFILES OF STRONG FRAUNHOFER LINES ALONG A RADIUS OF THE SOLAR DISC

J. HOUTGAST

THE VARIATIONS IN THE PROFILES OF STRONG FRAUNHOFER LINES ALONG A RADIUS OF THE SOLAR DISC

Diss Utrecht 1942

THE VARIATIONS IN THE PROFILES OF STRONG FRAUNHOFER LINES ALONG A RADIUS OF THE SOLAR DISC

PROEFSCHRIFT

TER VERKRIJGING VAN DE GRAAD VAN DOCTOR IN DE WIS- EN NATUURKUNDE AAN DE RIJKS-UNIVERSITEIT TE UTRECHT, OP GEZAG VAN DEN WAARNEMENDEN RECTOR MAGNIFICUS L. VAN VUUREN, HOOGLERAAR IN DE FACULTEIT DER LETTEREN EN WIJSBEGEERTE, VOLGENS BESLUIT VAN DE SENAAT DER UNIVERSITEIT TEGEN DE BEDENKINGEN VAN DE FACULTEIT DER WIS- EN NATUURKUNDE TE VERDEDIGEN OP MAANDAG 22 JUNI 1942, DES NAMIDDAGS TE 3 UUR

DOOR

JAKOB HOUTGAST

GEBOREN TE ASSEN

1942

DRUKKERIJ Fa. SCHOTANUS & JENS — UTRECHT

Aan de nagedachtenis van mijn Vader
Aan mijn Moeder
Aan mijn Vrouw

Wanneer ik bij de voltooiing van dit proefschrift de voorafgaande jaren overzie, waarbij ook mijn studietijd is inbegrepen, dan word ik mij bewust van een gevoel van grote dankbaarheid jegens allen, die het mij mogelijk hebben gemaakt het gestelde doel te bereiken.

U, Hoogleraren en Oud-Hoogleraren in de Faculteit der Wis- en Natuurkunde, ben ik zeer erkentelijk voor het hoogstaand wetenschappelijk onderwijs, dat ik van U heb ontvangen, en dat mij telkens weer te stade komt.

Mijn wetenschappelijke arbeid onder Uw leiding, Hooggeleerde Minnaert, Hooggeachte Leermeester, begon nu reeds bijna tien jaar geleden. Zeer veel heb ik in die tijd van U geleerd, diepe sporen heeft de samenwerking met U in mij achtergelaten, niet alleen door de wetenschappelijke en didactische gaven die Gij bezit, maar evenzeer door de bezielende wijze, waarop Gij in het werk pleegt vóór te gaan. Om U heen heeft zich een steeds groeiende School, een ware symbiose tussen physica en astronomie ontwikkeld, waarvan ook dit proefschrift getuigenis aflegt. Met hoeveel spanning en vreugde hebben wij deze dag, die een nieuw tijdperk in onze samenwerking op de Sterrewacht zou inluiden, verbeid. Nu neemt Gij, bij de plechtigheid, die voor ons een feest had kunnen zijn, niet de plaats in, waar ik U in mijn verbeelding zo dikwijls heb gezien — een diepe teleurstelling, die ik steeds zal blijven gevoelen.

Het stemt mij tot grote dankbaarheid, dat Gij, Hooggeleerde Rosenfeld, Hooggeachte Promotor, de zo plotseling leeg gekomen plaats hebt willen innemen. Bij de besprekingen over enkele questies betreffende dit proefschrift waren wij reeds nader met elkaar in aanraking gekomen, en, wetende dat Gij de astrophysica een warm hart toedraagt, hoop ik ook in de toekomst nog meermalen op Uw hulp te mogen rekenen.

Hooggeleerde Pannekoek, Uw uitgebreide kennis van de astrophysica en Uw systematische en kritische behandeling van haar problemen, waarvan ik op de gemeenschappelijke colloquia der Amsterdamse en Utrechtse astrophysici zoveel heb kunnen leren, is mijn wetenschappelijke vorming in hoge mate ten goede gekomen.

Ein Aufenthalt von über einem Jahr an dem Astrophysikalischen Observatorium zu Potsdam bot mir nicht nur die Gelegenheit das Beobachtungsmaterial für diese Dissertation mit wertvollen Ergebnissen zu bereichern, er ist auszerdem von grószter Bedeutung geworden für meine Ausbildung. Das danke ich an erster Stelle der ungezwungenen Zusammenarbeit mit Ihnen, Hochgelehrter ten Bruggencate. Mehrere Untersuchungen haben wir zusammen einem guten Ende zuführen können, und ich werde immer eine angenehme Erinnerung an eine Zeit behalten, in der es unser einziges Ziel war, die Kentnisse hinsichtlich des physikalischen Geschehens auf der Sonne zu vermehren. Hochgelehrter von Klüber, auch Ihrer vielseitigen Hilfe in oft schwierigen Umständen, die sowohl für mich, wie auch für meine Familie unentbehrlich war, gedenke ich mit Dankbarkeit.

In elk stadium van de bewerking van dit proefschrift, van de waarnemingen tot de drukproeven, heb ik de hulp gehad van mijn Vrouw; haar belangstelling en medeleven zijn voor mij een grote steun geweest.

INTRODUCTION AND SURVEY OF THE INVESTIGATION

§ 1. Introduction.

The sun is the only star of which the radiation from the various points of its surface can be studied separately. One part of the detailed study of the sun's disc consists in the investigation of the variation in the solar radiation arising from a centre-limb shift of the observed point. As this point approaches the limb, the radiation emerges at continually greater angles with the normal and originates on the average in continually higher layers of the sun's atmosphere, providing us thereby with the means to obtain some information concerning the variation with depth of various quantities and processes in that atmosphere. From the darkening of the continuous spectrum towards the limb important conclusions have indeed been already drawn.

In order to investigate the variation with depth of the *selective* properties, we must refer to the Fraunhofer lines which can for various reasons provide the necessary information. In the first place, because the region where they originate varies from one line to another, and in the second place, because along the intensity-profile of a strong Fraunhofer line the average depth from which the light reaches us varies gradually, while, finally, for every frequency within a Fraunhofer line, the depth differs whenever the light arrives from points located at different distances from the centre of the sun's disc. Let us hope that from observations combining these possibilities for investigating the depth, we may reap such a wealth of information as to enable us to determine the run with depth of a few of the most important selective properties.

§ 2. Outline of the investigation.

The testing by means of centre-limb observations, of the various conceptions concerning the constitution of the solar atmosphere and the processes acting in the formation of the Fraunhofer lines, will be the

more rigorous, the more widely the observational material varies; the fact that previous investigations in this field have not led to any general results, must be largely ascribed to the invariably too scanty observational data used.

In the first place, it is of importance to trace the variation over the complete extent of the line-profile, but in order to do this properly, the profiles must be exempt from deformations due to the spectral apparatus. That is why only strong lines were examined, the profiles of these being only slightly deformed and then only in the inner parts. The observational material was obtained partly at Utrecht and partly at Potsdam. The instrumental curve for the latter being known [1]), the profiles obtained from it could be corrected for finite resolving power, so that for a number of lines the centre-limb variations of the corrected central intensities have been determined.

In the second place, a suitable model of the sun's atmosphere will have to account for the observed centre-limb variations of lines belonging to different elements and atomic states, and also to explain the gradually changing behaviour from the ultra-violet to the infra-red region of the spectrum.

Finally, in order to accurately locate the variations over the sun's disc, it will be necessary to determine the profiles in a fairly large number of points and as these variations become considerable on approaching the limb, it is advisable to take these points, more in particular in its immediate neighbourhoud, near to each other and as close up to the limb as possible.

In consideration of the above requirements 23 strong Fraunhofer lines were selected belonging to different elements and with wave lenghts between 3800 and 8700 A. The hydrogen lines were excluded, because with them the Stark-effect would give rise to extra complications. The line profiles were determined for 7 or 8 points of the sun's disc, from the centre up to 0.005 R from the limb.

§ 3. Comparison of the observations with theory.

The way in which the centre-limb variations can be explained is examined in detail in the theoretical part. To this end the observed results are investigated with the aid of a schematic model of the solar atmosphere, comprising the Schuster-Schwarzschild- and the Milne-

---

[1]) A number like this indicates that the reader is to turn to the references (p. 141) for further information.

Eddington model as extreme cases *). We shall see that by means of this model we are able to draw important conclusions as regards the thickness of the layers in which the various lines originate.

The centre-limb variations of the central intensities of the observed lines can be explained in conformity with A. Unsöld's [2]) and B. Strömgren's [3]) theoretical investigations concerning their formation.

The question as to what extent selective coherent scattering and true selective absorption contribute separately to the formation of the lines has been extensively dealt with. It turns out that these two processes do not furnish a satisfactory explanation of the observed behaviour of the wings.

It appears, however, to be possible to explain this behaviour by means of non-coherent scattering by disturbed atoms, which, owing to the difference of radiation-density in the inner and outer parts of a Fraunhofer line, causes an exchance of radiation to take place between the wings and the central parts of the line. A more detailed study is then made of this exchange, but whether it can occur to the required extent in the case of damping by collisions without energy transfer (the process, which plays such a prominent part in the formation of the Fraunhofer lines), remains partly a question for theoretical physics to decide.

The conditions prevailing in the sun's atmosphere are in some respects favourable for the study of non-coherent scattering. These conditions can, however, not be reproduced artificially, but this does not exclude the carrying out in the laboratory of certain definite experiments, which would provide much valuable information concerning the scattering of light by disturbed atoms.

---

*) With this nomenclature I conform to A. Unsöld, *Physik der Sternatmosphären*, Kapitel XII.

OBSERVATIONAL PART

CHAPTER I

OBSERVATIONS

§ 4. Previous observations.

G. E. Hale and W. S. Adams [4]) were the first to photograph and visually to compare the spectra of the centre and of the limb of the sun's disc. In agreement with Hastings' results from visual observations, they stated that the wings of the strong lines disappear for the greater part at the limb, whereas they found, on the other hand, that the central parts of some of them are strengthened. The former statement has turned out to be indeed one of the characteristic features of lines in the limb-spectrum, the latter does not hold any longer for the lines investigated by them and can safely be ascribed to the effect of contrast.

To K. Schwarzschild [5]) we owe the first photographic-photometric determinations of intensity-profiles of Fraunhofer lines. He investigated the H- and the K line of Ca^+ in the centre and at the limb of the sun's disc; from the fact that these lines do not vanish at the limb he inferred that in the formation of Fraunhofer lines it is selective scattering and not selective absorption that plays the most important part.

In 1927 A. Unsöld explained the profiles of strong Fraunhofer lines by means of scattering and damping; applying Schuster's formula, he obtained an agreement between theory and observation, satisfactory for the time being, as regards the profiles in the centre- and limb spectra of the H- and the K line [6]),measured by Schwarzschild and the D lines of Na [7]), measured by himself.

H. H. Plaskett [8]) investigated in particular the centre-limb variation of the Mg b triplet, photographed at three different points of the sun's disc. He tried to explain this variation with the aid of various models of the sun's atmosphere and found that, in this respect, Eddington's

model for combined absorption and scattering, though giving rise to some difficulties, was the most successful.

Centre-limb variations of the Mg triplet were also observed by G. Righini [9]), who investigated the lines Mg 5183.6 and Mg 5172.7 at six points of the sun's disc, and by E. Cherrington [10]), including a careful determination of the central intensities, while Righini compared also the equivalent widths in the spectra of the centre and of the limb of the sun's disc [11]) of some hundred Fraunhofer lines between λ 5288 and λ 5472. T. Royds and A. L. Narayan [12]) investigated the H- and the K line of Ca^+, the line Ca 4226.7 and the hydrogen lines Hα to Hδ for seven points on the sun's disc, while Miss M. G. Adam [13, 14]) examined the behaviour of numerous weak Fraunhofer lines in the spectra photographed by H. H. Plaskett.

The wings of a few strong lines (H- and K line of Ca^+, Fe 4045.8 and Ca 4226.7 at six points of the sun's disc) are the subject of an investigation by M. Minnaert and the present writer [15]), who did not succeed in explaining with the aid of A. Pannekoek's [16]) model of the sun's atmosphere the observed behaviour on the assumption of selective scattering. The observational results from 20 strong Fraunhofer lines photographed at the Heliophysical Institute at Utrecht has already been communicated by the writer in abbreviated form [17]). These measurements constitute a considerable part of the material on which the present thesis is based.

C. W. Allen [18]) measured the D lines of Na in the centre and close to the limb of the disc, paying special attention to the central intensities. The latest publication dealing with centre-limb variations, that came to my knowledge, is the one by D. S. Evans [19]), who determined the profile of the line Hα in 5 points of the sun's disc. *)

Centre-limb variations in the spectra of the stars can be observed in the case of eclipsing variables, though we are not in a position to obtain, as in the case of the sun, the spectra of separate points of the star's surface. The various phases yield, each, the integrated spectrum of the non-eclipsed part of the principal star, and it will be clear that the centre-limb variation deduced from these spectra cannot be so accurate as for the sun. With these stars it is in the most favourable case only of the limb that we can obtain a pure spectrum. Photographs of this kind have been taken by R. O. Redman [20]), who observed the eclipsing

*) While reading the proofs I received C. D. Shane's publication concerning the Na D lines [19a]).

variables U Cephei and U Sagittae; his observations will, no doubt, be valuable, once we have understood the centre-limb variations in the case of the sun.

It appears from this survey that much work has already been done in the field of centre-limb observations, but we shall see that what is needed for a satisfactory checking of theory by experiment is a very extensive and, above all, homogeneous material.

§ 5. Introductory remarks on the observations on which the present thesis is based.

The distinguishing feature of the observations discussed in the present thesis is the more extensive scale on which they are planned; in the first place by using a greater number of Fraunhofer lines, and in the second place by increasing, if necessary, the number of points on the sun's disc. This second feature is especially important in connection with the peculiar run of the centre-limb variations which is not continually in one and the same sense from centre to limb, so that it cannot be determined by measurements in only a few points.

The number of Fraunhofer lines to be selected is greatly restricted, if one wants to determine the true profile, as any interfering spectral apparatus causes a deformation for which the observed profile cannot easily be corrected. As the investigation was started with the grating spectrograph of the Heliophysical Institute at Utrecht, possessing only a moderate resolving power, I had to restrict myself to some twenty of the stronger lines in the solar spectrum. The finite resolving power, however, affects the inner part of strong lines always to such an extent that, even if it should amount for a spectrograph theoretically to 100,000, the measured central intensities may very well deviate rather considerably from the true ones. For a judicious use of the Utrecht measurements, this must be taken into account. For the exposures at Potsdam the large grating spectrograph of the Institut für Sonnenphysik was used, possessing a much higher resolving power and of which, moreover, the instrumental curve was determined, so that the observed central intensities could be corrected for its influence.

In selecting the strong lines, the hydrogen lines were rejected, because their profiles are determined by the linear Stark effect, and are, therefore, likely to give rise to extra complications in interpreting the results. The more obvious thing to do was to examine first the other strong lines, of wich the wing profiles are determined by damping by collisions

(M. Minnaert and J. Genard [21]), A. Unsöld [22]), P. ten Bruggencate and the writer [23])), and of which the shape of the profile for large values of $\Delta\lambda$ (= distance from centre of line) is rendered so beautifully by Minnaert's formula [24]), according to which the depression $i_0 - i$ is proportional to $i/\Delta\lambda^2$. The lines remaining in this way belong to different elements and to different atomic states and they lie in different parts of the spectrum (see Table 1a, p. 21), a fortunate variety of which full advantage has been taken for determining the influence of these factors on the centre-limb variations.

The next point to be considered was for which points of the sun's disc the profiles should be determined. Following Prof. Minnaert's suggestion, I started with six points, from the centre of the disc to 0.98 R; in an image of the sun of about 12 cm diameter, the size of the one at Utrecht, the latter point lies at only 1.2 mm from the limb. In our opinion, this was the extreme position for obtaining with an ordinary technique of exposure a spectrum that could still be ascribed to the actual point of adjustment itself. To later series of photographs, however, the spectrum of the point at 0.995 R was added. From the beginning I was aware of the fact that the reliability of measurements on photographs of this point should not be overestimated, for, quite close to the limb, the variations in some parts of the profiles are considerable, while, owing to scintillation and to unavoidable minute errors in adjusting the sun's image, it is in reality a small region round the point 0.995 R, that forms the observed spectrum, which, therefore, cannot be accurately ascribed to a definite point of the sun's disc. When, however, it became clear that measurements referring to this point could lend a strong support to the explanation of the origin of Fraunhofer lines, I decided to add to the observations at Potsdam the one referring to the point at 0.99 R. In a series, completed in this way, the profiles were determined for 8 points, of which the distances from the centre of the sun's disc are, in terms of its radius: 0.00; 0.60; 0.80; 0.90; 0.95; 0.98; 0.99 and 0.995. From the mutual location of these points the extent can be clearly seen to which the increase of the variations on approaching the limb has been taken into account.

Apart from a series of the Mg b triplet, which was photographed for me by G. F. W. Mulders at Mount Wilson, all the spectra, discussed in this thesis, were photographed by me at Utrecht and at Potsdam. The technique of exposure is radically different in the two places; the fact that, nevertheless, the results agree so satisfactorily speaks well for

the reliability of the measurements. I now proceed to the discussion of the two methods of observation separately.

§ 6. The method of observation at Utrecht.

The sun's image of the Heliophysical Institute at Utrecht *) had a diameter of about 12 cm. By a few simple manipulations, which move the second of the two coelostat-mirrors round two axes perpendicular to each other, the image can be located arbitrarily in the plane of the slit of the spectrograph. At its lower end the vertical spectrograph rests on a steel point; by moving it as a whole, therefore, the slit can be adjusted in any direction and in any position, that may be required, relatively to the sun's image. Its focal length is 4 m and the grating is ruled over a width of 8 cm with 568 lines to the mm. For further details the reader is referred to the description by W. H. Julius [25]).

In all centre-limb exposures the direction of the slit was at right angles to that of the sun's radius, along which the various photographs were taken, so that from each exposure the spectrum was obtained for a definite distance from the centre of the sun's disc. Owing to the curvature of the limb, however, the distance slit—limb is already in the point at 0.98 R no longer constant; as the slit is about 10 mm long, its middle is about 0.2 mm farther from the limb than its ends, or, in other words, if the middle of the slit is adjusted on 0.98 R, its ends will be adjusted on 0.984 R. For that reason the upper and lower strips of the spectrum were, as a rule, not used in determining the profiles.

The adjustment on the right points was achieved in the following way. The distances of the points from the limb of the sun's disc were marked on a mm scale provided with a sharp straight edge at its one end. This edge was placed accurately above the slit by making its shadow coincide with the latter, whereupon the sun's limb was adjusted on one of the marks. The scale was then shifted so as to leave the slit free, the sun's limb now coinciding with some arbitrary division of the scale, where it was kept during the exposure, by a compensating adjustment, if necessary. Owing to chromatic aberration of the objective, small adjusting errors may have occurred in some parts of the spectrum, as the adjusting was performed visually in the light of the sun's image.

This image was formed in such a way as to be perfectly sharp in

*) Since 1937 this institute is made a part of the observatory "Sonnenborgh" of the university.

the plane of the slit, this being indeed, for points near the limb, an essential requisite for receiving light in the spectrograph only from the right distance from the centre. Visually a region was then selected, that was not perturbed by spots or faculae. In this selection we were always successful, as all photographs were taken during the minimum of solar activity, and the exposures were then made along a radius in this region.

The slit-width was always in accordance with P. H. van Cittert's theory [26], prescribing in our case 0.03 mm at 4000 A and 0.06 mm at 8000 A. The accurate focus was determined by means of preliminary photographs of the solar spectrum in the spectral region concerned.

A platina step-reducer of Zeiss with 5 steps of 2 mm width each was placed on the slit; 1 cm above it the mm scale was applied and 2 cm above the slit a general reducer was placed, selected in such a way for each exposure from a set of reducers (homogeneously blackened photographic plates with transmissive powers ranging from 40 % to 80 %) that, taking the darkening towards the limb into account, one could expect all spectra to show, for the same time of exposure, about the same degree of blackening. The spectra from the point at 0.98 R were always, and those from the point at 0.95 R often, photographed without any auxiliary reducer. For that same time of exposure, the spectrum from the point at 0.995 R would have shown a too slight density; for that reason the exposures on this point were made 1 to 2 times as long. The auxiliary reducers were, all of them, tested as to their homogeneity and turned out to satisfy this condition to within 1 %. Finally, a colour filter was applied 10 cm above the slit to intercept spectral light of other orders and scattered light.

In order to ascertain whether any difference occurred in blackening in the direction of the slit, either from the slit-jaws not being exactly parallel or from any other cause, we photographed several times without step-reducer the spectrum of an unperturbed region in the central part of the sun's disc; without any exception the constancy of the blackening in the direction of the slit left nothing to be desired.

In the beginning we rather feared that, during an exposure on the limb, the scattering in the earth's atmosphere and in the auxiliary reducers might cause an appreciable fraction of the so much larger amount of light from the central parts of the sun's disc to enter the apparatus. This was also why we made these exposures with a tangential slit. In order to judge the amount of scattering, a thermo-element was placed successively on and immediately next to the image of the sun's disc and

the ratio between the intensities was determined. At a distance of 2 mm this ratio turned out to be already less than 0.001, as well for red as for blue light, so that entering of any light from parts of the sun more than 2 mm distant from the points of adjustment can be completely neglected. Moreover, these measurements were carried out expressly, when the atmosphere showed strong scattering or intense scintillation, whereas the centre-limb exposures were made on days with good visibility and preferably slight scintillation. An unfortunate complication in this connection is the fact that transparent air and weak scintillation practically never coincide. The degree of scintillation was judged from the amplitude of the wave-motion of the sun's edge and was expressed in a scale from 0 to 10; for the photographs, actually used, it varied from 3 to 7.

The exposures were made in the most luminous of the second order spectra of the grating, of which the dispersion amounts to 0.5 mm/A. Only the H- and the K line of Ca^+ were photographed in the first order. The plates used for the various wave-length regions are given in Table 1b. On a single plate, of which the height is 6 cm, there is room for four spectra, so that we had to distribute each series over two plates, which were either cut from one piece or were taken from one and the same box. The two plates were developed simultaneously. The plates used were always backed; if not originally so, they were backed with black paper stuck on with glycerine. The plates were developed during 7 minutes in metol-hydrochinon borax; after being fixed, they were bathed in a 2 % HCl-solution, until the gelatine had become completely transparent. The Ilford infra-red plates were hypersensitized with ammonia, the Agfa infra-rot plates with methylated alcohol.

Originally, the direction of the radius on which the successive points for the exposures were located, was determined for each series of photographs, because it might be that the centre-limb variations along, say, the sun's equator were different from those from the centre towards the sun's poles. G. Abetti and I. Castelli [27]) found, for example, small differences between the limb-spectra at the equator and at the poles. It appeared, however, from a comparison between series referring to points located quite differently with respect to the sun's disc, that these deviations were completely negligible compared with the centre-limb variations themselves, so that later on no further attention was paid to this question.

A survey of the centre-limb photographs, actually discussed, is given in Table 1 (p. 21 and 22).

The characteristic curves for the plates were determined from the spectra of the points at 0.00 R and 0.60 R and then checked by those of the points at 0.80, 0.90 and 0.95 R. The spectrum of the point at 0.98 R is less suitable for the determination of the characteristic curve, because, owing to the darkening towards the limb, the illumination of the slit is not homogeneous. In all series the characteristic curves of the two plates were so much alike, that we could work with one curve for both plates.

The registering of the spectra was carried out by means of a Moll-microphotometer. The maximum widths of the slits corresponded to 0.03 A on the plates for photographs of the second order spectrum. The transmission ratio between registrogram and plate was 50 or 7; the latter ratio only being used when, otherwise, the registered spectrum would leave insufficient room for the continuous background. This was the case with the Ca^+ lines and with the ultra-violet lines of Fe and Mg, with the exception of Fe 3859.9.

From four or five steps the intensity-profiles were determined, which always agreed within 5 % and as a rule still better. A preliminary determination of the run of the continuous background in the gaps made by the lines was obtained by drawing a straight line through points of the continuous spectrum lying at a great distance from the lines. This method fails, however, in the case of the H- and the K line; here a decided curvature occurs and the continuous background was interpolated according to the best fitting curve onwards from 100 A away from the centres of the H- and the K line; this was done as well for the intensity run itself as for that of log intensity, the latter approximating the linearity better, as appears from the run of the continuous background at a great distance. From the agreement between the two determinations, which never differed more than 1 %, it appeared that this interpolation is fairly unambiguous.

The intensity of the ghosts of the grating is in the first order spectrum 1.25 % and in the second order spectrum 5.1 %. As a rule, the ghosts lay outside the lines, so that to all intensities the correction according to the formula $i = (i_0 - g)\frac{100}{100 - g}$ could be applied [28, 29]. Here i_0 denotes the observed intensity, g the sum of the intensities of the ghosts and i the corrected intensity, all of them in percentages of the intensity

of the continuous background. In a few cases as, for example, in that of the D lines of Na, the ghosts lay in the wings and the measurements were then sufficiently accurate for applying the local correction to each measured point.

§ 7. The method of observation at Potsdam.

When I had completed the measurements at Utrecht, I was given the opportunity to go and work temporarily at the Institut für Sonnenphysik at Potsdam. This meant a very welcome occasion not only for checking the Utrecht results by an exposing-technique differing in so many respects from the one at Utrecht, but also for a more accurate investigation of the central parts of the Fraunhofer lines than, owing to the smaller resolving power, could be performed there. Paying special attention to the central intensities, the profiles of a number of lines, already measured at Utrecht, were again determined for the same distances from the centre of the sun's disc, and, besides, for the point at 0.99 R. It being of importance for the problem of central intensities to know the degree to which these are equal for the components of a multiplet [2, 3], the D lines of Na, two of the Mg b lines and six lines of the Fe multiplet a^3F_4—$y^3F_3^\circ$ were investigated, so that three more lines were added to the lines of this multiplet, measured at Utrecht. The line Fe 3969.3 was omitted, because it lies in the wing of the H line of Ca^+, and the line Mg 5167.3 because it is strongly disturbed at its very centre by the line Fe 5167.5. It was in my opinion superfluous to determine again the central intensities of the H- and the K line, as, owing to the great width of these lines, we may safely assume that, also at Utrecht, the measurements will have been free from the obliterating effect of the spectrograph. This is also evidenced by the agreement between the results of different investigators (K. Schwarzschild [5], M. Minnaert [30], A. D. Thackeray [31])). The central intensity of the line Ca 4226.7 was added to those measured at Potsdam, as the accurate measurements of this line by R. O. Redman [32] and A. D. Thackeray [31], referring to the centre of the sun's disc, were available for comparison. The ultra-violet and infra-red lines, measured at Utrecht gave rise to difficulties at Potsdam, in connection with the special exposing-technique, presently to be described; they were, therefore, omitted.

1. *Apparatus.* In the Institut für Sonnenphysik an intense objective of 60 cm diameter forms an image of the sun, of which the diameter is

13 cm. For the present investigation this image was thrown on the vertical plane of the slit of the monochromator, mounted by P. ten Bruggencate and H. von Klüber, and serving the purpose of enabling one to admit only light from a narrow wave-length region, thereby eliminating stray light and making accurate intensity-measurements possible. It has already been described elsewhere in detail [1, 33]). The image of the sun formed on the slit of the large spectrograph by the light, let through by the monochromator, has about twice the size of the original image, its diameter being 25 cm. The focal length of the horizontal spectrograph is 12 m; of the grating a width of 12 cm was used, ruled with 600 lines per mm. For further details the reader is referred to the description by E. Freundlich [34]) or to [1]).

2. *Exposures.* The centre-limb exposures were, all of them, made in the light of the second order spectrum with a dispersion of 1.5 mm/A, the monocromator being always inserted in the path of the rays. The preliminaries for the taking of a photograph consisted in the first place in selecting an unperturbed region at the distance to be investigated from the centre of the sun's disc. As the exposures were made only a short time before the maximum of solar activity, it was impossible to select all the points from centre to limb on one and the same radius and we were obliged to find for each point a new unperturbed region. A rotation of the sun's image is at Potsdam only possible by changing the azimuth of the coelostat-mirror, so that for points at the limb only part of the sun's circumference is available. The image of an unperturbed region was thrown on the first monochromator-slit and kept there steadily by careful compensating adjusting. This was achieved by keeping the image of a sharply defined sunspot on the cross-threads of a small auxiliary telescope, having in front of its eye-piece a little plate of glass of the colour of the wave-length region under investigation, and as the sun's image was focussed for that same region, chromatic aberrations of the objective were for the greater part eliminated. By forming a sharp image of the first monochromator-slit in the plane of the slit of the spectrograph, one is sure that the image of the sun, formed there, is in its turn also sharp.

For the points from 0.00 to 0.90 R, the slit was placed at right angles to a radius of the sun's disc, for points closer to the limb in the direction of a radius. Each of the limb-spectra was photographed twice. First, with the slit made so long that both the limb itself and the point at

0.95 R fell within its length. On these photographs the points at 0.95 and 0.98 R were measured. The second time, the spectra were photographed, while only slightly more than the part from the limb to 0.98 R fell on the slit, the latter now being illuminated over a length of 3 mm. On these photographs the limb-points at 0.98, 0.99 and 0.995 R were measured. No systematic difference was found between the line-profiles at 0.98 R, obtained from the first and the second procedure.

All centre-limb exposures were made in two ways. First, while the monochromator let through a wave-length region of about 30 A. From these photographs the intensity of the wings of the strong lines was determined in terms of the intensity of the continuous background; these photographs will henceforth be called "continuum-photographs". The second time, a wave-length region of only 3 to 4 A was let through. The photographs obtained in this way served for measuring the intensity of the lines close to and including their centres; they will henceforth be called "inner-photographs". In the latter case the monochromator had to be adjusted very carefully, in the first place to locate the Fraunhofer line, to be measured, exactly in the middle of the spectral region let through, and in the second place to cut off this region sharply at both ends. This adjustment was judged visually; a photographic determination of the right positions would have taken a very long time. For that same reason the ultra-violet and the infra-red lines were not photographed at Potsdam.

The photographic material used consisted of Agfa Isopan F or Isopan SS film in a Nettax Kleinbild (small picture) camera, which could be fastened to the spectrograph; each part, meant for a picture, was used for a spectrum, so that it was possible to photograph 36 spectra successively on one film. Some of these were spectra for standardizing, photographed by means of a small grating spectrograph with step-reducer, either immediately after the other photographs were taken or in between them. The Fraunhofer lines were obtained with different times of exposure, on the one hand, in order that the spectra should possess about the same density notwithstanding the darkening towards the limb, so that one and the same part of the characteristic curve could be used, and, on the other hand, because for the continuum-photographs a shorter time of exposure sufficed than for the inner-photographs. For this reason the standardizing spectra were photographed in series of different times of exposure, so that the profiles could be deduced from a characteristic curve, for which the times of exposure differed by less than a factor

2 from those for the solar spectra. We did not notice, for that matter, that the time of exposure ever influenced the shape of the characteristic curve in any way.

In order to eliminate too strong contrasts, the films were developed in Rodinal 1 : 40 at 18° C for 8 minutes, during which the bath was constantly rocked vigorously to and fro. They were then registered by means of a Zeiss photometer, of which the slits were adjusted in such a way that their widths corresponded to 0.02 A on the film, while their lengths corresponded to 8″ for the points at 0.00 to 0.95 R, down to 3″ for those at 0.99 and 0.995 R (see Fig. 2).

3. *Determination of the intensity-profiles of the inner part of the lines.* The possibility of admitting into the spectrograph a spectral region of only 3 to 4 A offers not only the advantage of eliminating any stray light from other wave lengths, but also that of getting rid of the ghosts. For the lines measured, the first ghost lies at least 2.5 A distant from the principal line; when only a region of 4 A is let through, therefore, the inner part of a strong Fraunhofer line is entirely free from ghosts and the only remaining correction to be applied is the one for the instrumental curve (this §, 5). A region of 4 A, however, is too narrow for locating the continuous background. This requires, therefore, the combining of the spectra photographed with narrow and with wide monochromator-slit, which was done in the following way, the same as that used by A. D. Thackeray [31]). To the intensity-profile obtained from the continuum-photograph the general correction for ghosts $i = (i_0 - g)\frac{100}{100-g}$ (see p. 11) was applied, where for g was taken the sum of the intensities of all disturbing ghosts, as determined from photographs made for that purpose. These photographs were of two kinds. In the first, the lines Kr 4320 and Kr 5570 emitted by a Kr discharge tube were photographed; on these we could measure the four nearer ghosts on both sides, and their aggregate intensities amounted to 3.5 % for 4320 A and to 4 % for 5570 A. The second method for determining directly the total intensity of the ghosts consists in measuring the central intensity of a narrow Fraunhofer line, located in a practically undisturbed part of the continuous spectrum, first, on a photograph covering a wave-length region of 30 A and, again, on one for which this region is restricted to a few A only. The surplus of light in the inner parts of the line on the first photograph relatively to that on the second photograph

is due to the disturbing ghosts, apart from scattered light, which in this connection can be safely neglected. The total intensity of the four nearer ghosts, obtained in this way for 5500 A, agreed fairly well with the one determined in the first manner. For the wings the value of g is less essential and their profile is, therefore, known sufficiently well from the continuum-photographs.

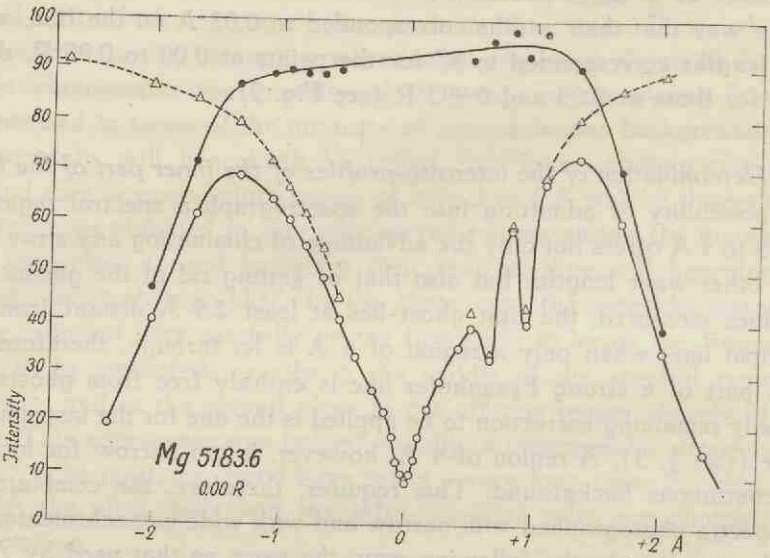

Fig. 1. — Determination of the inner part of the profile of a strong Fraunhofer line; exposure with narrow monochromator-slit in order to avoid scattered light and ghosts (first ghost at 3.5 A from principal line);
O intensity curve from photographs made with narrow monochromator-slit (inner-photograph);
△ intensity curve of the wings, relatively to the intensity 100 of the continuous background, from photographs made with wide monochromator-slit (continuum-photograph);
● continuous background belonging to O, deduced from O and △.

On the continuum- and the inner-photographs a number of points at the same distance $\Delta\lambda$ from the line-centre have been measured. Let r be the intensity in terms of the continuous spectrum in such a point, obtained from the continuum-photograph, and i the intensity in arbitrary units obtained from the inner-photograph; the intensity of the continuous background in the latter will then amount to $100\ i/r$. The line drawn fluently through the points determined in this way is then regarded to represent the continuous background (Fig. 1), while, finally, the

intensities of the inner parts of the line are determined relatively to this continuous background. When, later on, the central intensities are corrected for the instrumental curve, we start, as a matter of course, again from the inner-photographs.

The way in which the wave-length region is cut off by the monochromator did not always turn out to be perfectly sharp, and the run of the continuous background belonging to the inner-photograph was not always straight. This deviation from straightness can presumably be explained by the fact that the image of the first slit was not always centred perfectly on the slit of the spectrograph. In principle, however, this does not matter at all; the essential points are, that no light shall have passed the monochromator from wave lengths farther than about 2 A away from the centre of the line, and that the run of the continuous background be correctly determined by the values $100\, i/r$; both conditions were always satisfied.

4. *The definition of the sun's limb in the limb photographs.* From the fact that at Potsdam the limb spectra were photographed with a radial slit, in such a way, that the sun's limb is one of the bounding lines of the spectra, it is possible to determine its definition from each of these photographs, on which it is never sharp, owing to scattering, scintillation and guiding errors. In the narrow confused region the true position of the limb was estimated visually to within 0.1 mm. If, now, the distance of this estimated position from the perfectly sharp lower edge of the spectrum, determined by the end of the spectrograph-slit amounts to a cm, it is fairly easy to register the film by means of an accurately adjustable plate, on which it is clamped during the registering, in strips, at distances $(a - 0.625)$ mm, $(a - 1.25)$ mm etc. from the sharp edge of the spectrum, corresponding respectively to the points at 0.995 R, 0.99 R etc. In all series registrograms were made of a few continuum-photographs at the limb, in a region free from Fraunhofer lines, in a direction at right angles to the dispersion, from which the run of the intensity at the sun's limb was deduced. It was thereby possible a posteriori to locate accurately the registered strips in the spectrum and to find the error in the estimated position of the limb, which was defined in this connection by the equality of the areas S in Fig. 2. This error amounted at the most to 0.2 mm (about 1."5) and did not show any systematic character. Accidentaly, therefore, the way of judging the position of the limb on the film agrees practically with the definition given above.

The intensity-variations at the limb obtained are drawn, for the neighbourhood of λ 4100 and λ 5900, in Fig. 2, respectively from photographs of the violet Fe lines and of the D lines of Na. In photographs made on different days, the deviations at some fixed λ are insignificant. One can take this as an indication that guiding errors are the principal

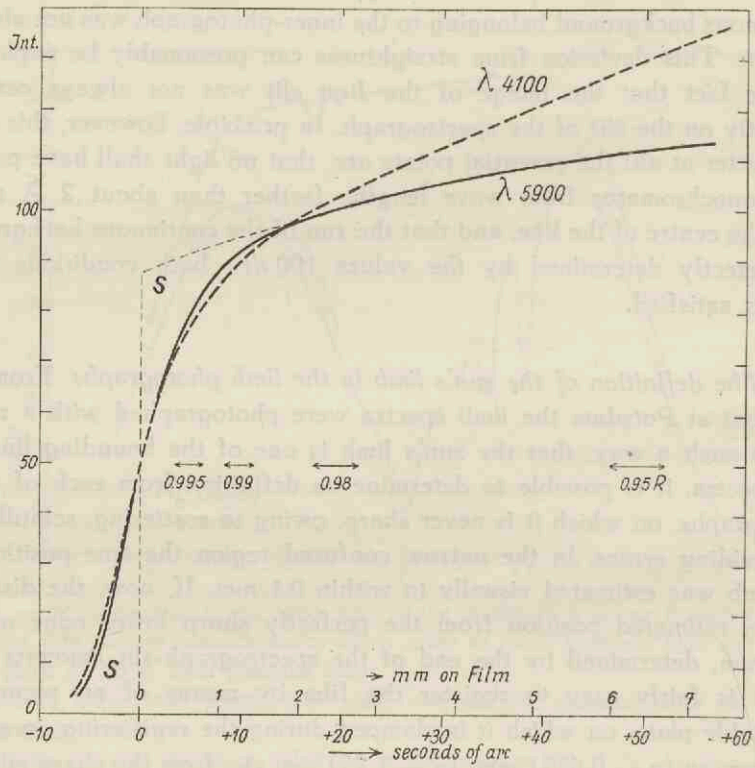

Fig. 2. — Intensity of the continuous background along a radius of the solar disc near the sun's limb; at λ 4100 from photographs of the Fe multiplet and at λ 5900 from the Na D doublet. The double arrows indicate the places used in registering the spectra, while their lengths correspond to the lengths of the photometer-slit. The abscissa of the sun's limb is fixed by the condition that the areas S shall be equal. In the figure only the areas referring to λ 5900 are drawn.

cause of the lack of sharpness, as for a few of these photographs the atmospheric conditions were decidedly different. On the inner-photographs, for which the times of exposure were 2 to 3 times as long as those for the continuum-photographs the definition is likely to be slightly worse. From Fig. 2 the extent can be judged to which the radiation

assigned to the measured points is in reality an integrated radiation from the small parts surrounding them. One must bear in mind, however, that, as the only consequence of this, the measurements at the extreme limb must be ascribed to points slightly different from those at 0.995 R etc. In comparing the observations with theory, this will always be taken into account.

5. *Correction of the central intensities for finite resolving power.* The instrumental curve of the grating spectrograph has been accurately determined from narrow Kr lines [1]). An elegant method for correcting observed line-profiles for its obliterating effect was developed by H. C. van de Hulst [35]), while P. Kremer [36]) designed an apparatus by means of which the necessary computations of this kind can be quickly performed. The two instrumental curves for λ 4320 and λ 5570, determined at Potsdam, were each reduced to λ 5000, and their mean was used in applying the correction to the observed central intensities, taking into account the change of the scale of abscissae proportional to wave length. Curves I and III in Fig. 3 represent this mean instrumental curve for λ 5000. It was sufficiently narrowed by operating on it with the following peak-function [35]), likewise referring to λ 5000:

Distance from centre of instrumental curve in mA	−150	−100	−75	−50	−25	0	+25	+50	+75	+100	+150
Normalized height of peak	−0.05	−0.04	−0.02	−0.07	−0.37	+2.06	−0.37	−0.03	−0.04	−0.05	−0.02

As appears from the above values of the heights of the peaks, the asymmetry of the instrumental curve has been taken duly into account. The factor β, by which the accidental errors are multiplied in the corrected profile, amounts in our case to 2.1. Curve II represents the instrumental curve, after the peak-function has operated on curve I, so that the corrected profile is the true profile obliterated by curve II. On comparing its width with the intensity-variation over a corresponding width in the inner part of a — corrected — Fraunhofer line, it appears that in this connection further correction is superflous; the principal effect is the suppression of the wings of the original instrumental curve I.

The correction by means of the peak-function could be applied to the spectra photographed with narrow monochromator-slit (see Fig. 1).

This has the advantage that the shape of the instrumental curve at distances larger than about 2 A from its centre becomes irrelevant. Its shape between 200 mA (that is as far as it was measured) and 2 A cannot be accurately taken into account. The peak-function,

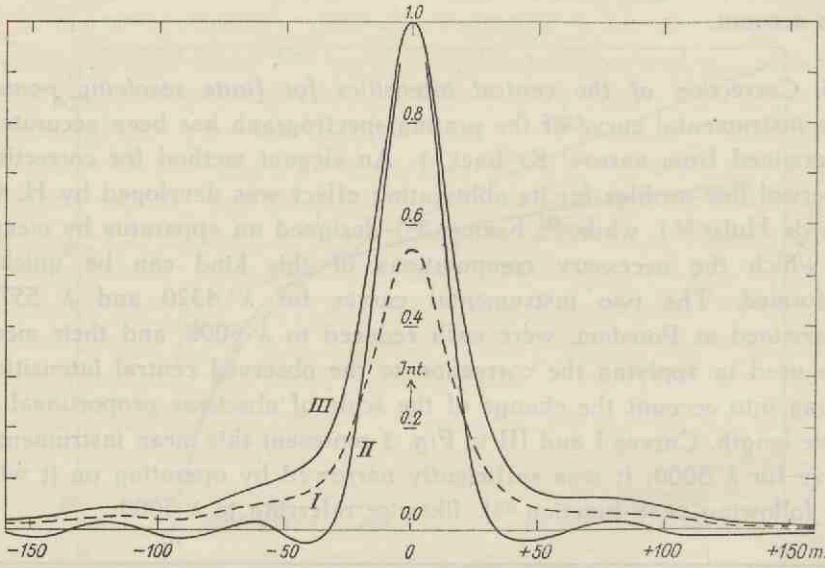

Fig. 3. — I: instrumental curve of the Potsdam grating spectrograph for λ 5000;
II: instrumental curve I transformed by the peak-function operation; I and II have equal areas;
III: instrumental curve obtained from I by multiplying its ordinates so that the top coincides with that of II.

however, applies partly an automatic correction for this part of the curve, as its total area has been computed on the assumption that its far wings are shaped in conformity to c/x^2, where c is determined from the average shape of the wings up to 200 mA (see [1]). These imperfections, however, have only a slight influence on the final value of the central intensity of a Fraunhofer line.

§ 8. Survey and points in common in the discussion of the complete observational material.

From the photographs, of which a survey is given in Table 1, 1266 profiles were deduced, distributed over the three places of observation as follows: Utrecht 857; Potsdam 358 and Mount Wilson 51. It was

unfeasible to determine the shape of all these profiles where they were disturbed by blends and, besides, this did not concern us. As it was our purpose to determine the variations of the profiles of the strong lines themselves, we measured in the first place, if at all possible, points, that could be considered to lie on the undisturbed profile. Only, where this turned out to be impossible, did we measure also, for lack of better,

Table 1a. **The Observed Lines** *)

Line		Transition	Lower E.P. **)	Observatory ***) and Number of Plate or Film
Fe	3815.9	$a\ ^3F_4 - y\ ^3D_3^\circ$	1.478	Ut. 15, 16, 44, 49, 50
	3820.4	$a\ ^5F_5 - y\ ^5D_4^\circ$	0.855	id.
	3859.9	$a\ ^5D_4 - z\ ^5D_4^\circ$	0.000	id.
	4005.3	$a\ ^3F_4 - y\ ^3F_3^\circ$	1.478	Po. 86, 87
	4045.8	4 4	1.478	Ut. 6, 7, 8, 9, 47, 48; Po. 78
	4063.6	3 3	1.551	Ut. 47, 48; Po. 80, 81
	4071.8	2 2	1.601	Ut. 47, 48; Po. 81, 82
	4132.1	2 3	1.601	Po. 82, 83
	4143.9	3 4	1.551	id.
Mg	3829.4	$3\ ^3P_0^\circ - 3\ ^3D_1$	2.697	Ut. 15, 16, 44, 49, 50
	3832.3	1 2, 1	2.700	id.
	3838.3	2	2.705	id.
	5167.3	$3\ ^3P_0^\circ - 4\ ^3S_1$	2.697	Ut. 58, 59; Mo. 51, 225, 226, 227
	5172.7	1 1	2.700	Ut. 58, 59; Mo. 51, 225, 226, 227; Po. 37, 59, 63, 64, 71
	5183.6	2 1	2.705	Ut. 58, 59; Mo. 51, 225, 226, 227; Po. 6, 8, 37, 45, 59, 64, 68, 71
Ca	4226.7	$4\ ^1S_0 - 4\ ^1P_1^\circ$	0.000	Ut. 12, 13, 41, 42; Po. 75, 76
Ca+	3933.7	$4\ ^2S_{1/2} - 4\ ^2P_{3/2}^\circ$	0.000	Ut. 21, 22, 45, 46, 53, 54
	3968.5	1/2 1/2	0.000	id.
	8498.1	$3\ ^2D_{3/2} - 4\ ^2P_{3/2}^\circ$	1.685	Ut. 25, 26, 57
	8542.1	5/2 3/2	1.693	id.
	8662.2	3/2 1/2	1.685	Ut. 19, 20, 25, 26. 57
Na	5890.0	$3\ ^2S_{1/2} - 3\ ^2P_{3/2}^\circ$	0.000	Ut. 23, 24, 29, 30, 39, 40; Po. 65, 66, 68
	5895.9	1/2 1/2	0.000	Ut. 23, 24, 29, 30, 39, 40; Po. 65, 66, 67

*) The notations and constants are taken from C. E. Moore [37]).

**) Excitation potential of the lower energy level in electron volts.

***) Ut.: Utrecht; Po.: Potsdam; Mo.: Mount Wilson.

points on the slightly disturbed profile, for, generally speaking, the slight disturbance by a blend will not seriously interfere with the centre-limb variation of a strong line. A point once having been chosen, its intensity was measured in all profiles of a series at the same distance from the centre of the line. This was, in its turn, determined from the mostly sharply defined top and from undisturbed points located, as much as possible, symmetrically around it.

Table 1b. **Details of the Exposures**

Plate Number	Plates used	Date of Exposures	Time of Exp. for each Spectrum	Lines, Points of Adjustment on the Solar Disc and (for Potsdam) Type of Photograph
Ut. 6; 7	I.s.r.	1935 Mar. 19	45 sec.	Fe 4045.8; 0.00—0.98 R
8; 9	„	21	20 „	id.
12; 13	„	May 29	8 „	Ca 4226.7; 0.00—0.98 R
15; 16	„	June 25	10 min.	Fe 3815.9, 3820.4, 3859.9 and Mg 3829.4, 3832.3, 3838.3; 0.00—0.98 R
19; 20	I.i.r.	July 12	20 „	Ca+ 8662.2; 0.00—0.98 R
21; 22	I.s.r.	Sept. 14	0.5—1 „	Ca+ 3933.7, 3968.5; 0.00—0.995 R
23; 24	I.r.p.p.	23	0.5 „	Na 5890.0, 5895.9; 0.00—0.995 R
25; 26	A.I.R.850	1936 May 17	10—15 „	Ca+ 8498.1, 8542.1, 8662.2; 0.00—0.995 R
29; 30	I.r.p.p.	19	1—1.5 „	Na 5890.0, 5895.9; 0.00—0.995 R
39; 40	„	Aug. 16; 17	30 sec.	Na 5890.0, 5895.9; 0.00—0.98 R
41; 42	I.s.r.	27	3.5—7 „	Ca 4226.7; 0.00—0.995 R
44	„	27	12—18 min.	Fe 3815.9, 3820.4, 3859.9 and Mg 3829.4, 3832.3, 3838.3; 0.995 R
45; 46	„	27	20 sec.	Ca+ 3933.7, 3968.5; 0.00—0.98 R
47; 48	„	28	7—10 „	Fe 4045.8, 4063.6, 4071.8; 0.00—0.995 R
49; 50	„	28	4 min.	Fe 3815.9, 3820.4, 3859.9 and Mg 3829.4, 3832.3, 3838.3; 0.00—0.98 R
53; 54	„	29	20—30 sec.	Ca+ 3933.7, 3968.5; 0.00—0.995 R
57	A.I.R.850	Oct. 5	10 min.	Ca+ 8498.1, 8542.1, 8662.2; 0.00, 0.80, 0.98 R
58; 59	I.r.p.p.	1937 May 26	1 „	Mg 5167.3, 5172.7, 5183.6; 0.00—0.995 R
Mo. 51	E.K. III F	1936 Oct. 5	4—16 „	Mg 5167.3, 5172.7, 5183.6; 0.00 R
225	„	1937 Dec. 15	20 „	Mg 5167.3, 5172.7, 5183.6; 0.90—0.995 R
226	„	15	15 „	id.
227	„	16	15—26 „	Mg 5167.3, 5172.7, 5183.6; 0.60, 0.80 R
Po. 6	A.S.G.R.	1938 June 5	40 sec.	Mg 5183.6, cont. 0.00 R
8	„	5	1.5 min.	Mg 5183.6, inn. 0.00 R
37	A.I. F	July 7	0.5—8 „	Mg 5172.7, 5183.6, cont. 0.99, 0.995 R
45	A.I.SS	15	0.2—2 „	Mg 5183.6, cont. 0.98—0.995 R, inn. 0.00—0.995 R
59	„	Aug. 2	0.2—2 „	Mg 5172.7, 5183.6, cont. 0.00—0.90 R
63	„	4	5—40 sec.	Mg 5172.7, inn. 0.00, 0.95—0.995 R
64	„	4	5—20 „	Mg 5172.7, 5183.6, cont. 0.00—0.995 R; Mg 5172.7, inn. 0.00—0.995 R
65	„	4	5—40 „	Na 5890.0, 5895.9, cont. 0.00, 0.95—0.995 R
66	„	4	8—40 „	Na 5890.0, 5895.9, cont. 0 60—0.90, 0.98—0.995 R
67	„	5	6—70 „	Na 5895.9, inn. 0.00—0 995 R
68	„	5	13—70 „	Na 5890.0, inn. 0.00—0.995 R
71	„	6	15—40 „	Mg 5172.7, inn. 0.98—0.995 R; Mg 5183.6, inn. 0.95—0.995 R
75	„	8	5—20 „	Ca 4226.7, cont. 0.00 R
76	„	8	8—120 „	Ca 4226.7, cont. 0.60—0.995 R, inn. 0.00—0.995 R
78	„	9	0.5—4 min.	Fe 4045.8, cont. and inn. 0.00—0.995 R
80	„	10	0.7—6 „	Fe 4063.6, inn. 0.00—0.995 R
81	„	10	0.5—1.5 „	Fe 4063.6, 4071.8, cont. 0.00—0.995 R
82	„	11	0.3—6 „	Fe 4071.8, inn. 0.00—0.995 R; Fe 4132.1, 4143.9, cont. 0.00—0.995 R
83	„	11	0.5—6 „	Fe 4132.1, 4143.9, inn. 0.00—0.995 R
86	„	Sept. 29	0.7—4 „	Fe 4005.3, cont. 0.00—0.90 R, inn. 0.00—0.90 R
87	„	30	1.5—4 „	Fe 4005.3, cont. 0.00—0.995 R

Explanation of the abbreviations: I.s.r.: Ilford special rapid; I.i.r.: Ilford infra red; I.r.p.p.: Ilford rapid process panchromatic; A.I.R. 850: Agfa Infrarot 850 hart; E.K. III F: Eastman Kodak III F; A.S.G.R.: Agfa Spectral Grün Rapid; A.I.F: Agfa Isopan F; A.I.SS: Agfa Isopan SS; cont.: continuum-photograph (see p. 14 and Fig. 1); inn.: inner-photograph (see p. 14 and Fig. 1).

It must be emphasized here that the centre-limb variations in a series are always more reliable than the intensities themselves. This is due to using, as far as possible, a homogeneous method in working out the data of a series. Yet, the separate series of one and the same line showed, not unfrequently, appreciable differences, of which one can form some idea by comparing the results, given in Chapter II with those of previous publications [15, 17]) and by comparing mutually the Utrecht-, Mount Wilson- and Potsdam measurements, which are always given separately in the Tables 2—20.

§ 9. Discussion of errors.

1. *Accidental errors.* The photographic method applied, and conform to which the characteristic curve is obtained from spectra taken via a standardized step-reducer, has already been frequently applied and it has turned out that the accidental errors thereby introduced in the relative intensities of the profiles may have values up to 5 %. A comparison of the measurements of the Utrecht-, Potsdam- and Mount Wilson material mutually (Tables 2—20) and with those of other investigators makes it likely that, also in the results communicated here, errors of this magnitude occur. The central intensities in the tables under the heading "Potsdam" are, each of them, the average of the values obtained from various spectra and films, of which the mutual differences amount at most to 3 %. The error, arising from the steepness of the slope of the inner wings of a few Fraunhofer lines, is apt to be rather considerable, because any small error in $\Delta\lambda$, the distance from the centre of the line, entails a large error in r. This error will, however, have no systematic influence on the centre-limb variation, though it will give rise to a certain spreading of the observed variation round the true one.

2. *Systematic errors.* a. *Stray light.* By scattering of light in the spectrograph the measured intensities may be subject to a systematic error. There was no fear of this at Utrecht — considering that there the step-reducer is applied on the slit of the spectrograph — provided only that the scattered light be spread evenly over the photographed spectrum, which, from check photographs, proved to be the case. At Potsdam the comparison of the photographs, in the taking of which wide and narrow spectral regions were let through by the monochromator, showed that stray light is not present to any appreciable amount. From the fact that

only light from a region of a few A was admitted, one could hardly expect anything else.

b. *Eberhard effect.* Another systematic error can arise from the Eberhard effect, especially in the central intensities and, therefore, also in their centre-limb variations, as the profiles of the lines at the limb are narrower than those at the centre. As in the theoretical interpretation of these intensities only the measurements at Posdam are used, we shall dwell for a moment on the influence, that this effect has on them. In order to reduce it to the utmost, the films were developed in diluted Rodinal and were rocked steadily to and fro during the process. From check measurements on very narrow Kr lines for determining the instrumental curve, the Eberhard effect, although present, appeared to be of little moment [1]) and since the profiles of the Fraunhofer lines cover a larger wave-length region and show a less steep density variation, the effect will be in this case still less appreciable and can safely be neglected. Moreover, in correcting the central intensities, the influence of the Eberhard effect on the determination of the instrumental curve is opposed to that influence on a Fraunhofer line, a too low central intensity being corrected with a too narrow instrumental curve.

This same effect may likewise influence the maxima in an intensity profile, arising from the occurrence of blends. Considering the remark made above, one may assume that here, too, the Eberhard effect is negligible.

c. *Finite resolving power.* It is chiefly in those parts of a profile, where the curvature in the run of the intensities is considerable, that the true intensities will deviate appreciably from the observed ones. The correction to the central intensities has already been dealt with in detail, and it follows from § 7, 5 and the present §, 1 that the corrected central intensities given are still liable to fairly large relative errors. The further points of the inner part of the lines were not corrected. The effect of the finite resolving power on maxima in the intensity-profile, due to blends, will likewise be appreciable, when such a maximum is rather sharp, and it will decrease its intensity. As regards the centre-limb variation, this influence is in sofar of importance, as the shape of the maximum for the centre of the sun's disc is different from that for the limb, that is, therefore, only in second approximation. That is why no correction was applied for this effect. It is an additional cause by which the equivalent widths come out to large (§ 10, 1).

d. *Blends.* The disturbing effect of blends is in many cases considerable

and to take them into account is no simple matter. It may very well be that, owing to their presence, the intensity of points that, to all appearances, are only slightly disturbed, is, nevertheless, appreciably too low. They do affect the centre-limb variations, because, in the first place, the measured centre-limb variation refers, strictly speaking, to points of slightly larger intensities and, in the second place, the blends themselves suffer also a centre-limb variation. Fortunately, however, both these factors have only a second order effect. The fact that this disturbance is small, in any case, appears clearly from a comparison between undisturbed points and points of practically the same intensity, that are decidedly disturbed by blends; the centre-limb variations are, practically speaking, identical, so that we have refrained from applying a correction in this connection.

In the wings, the relative influence of blends is more serious, so that they invalidate more in particular the determination of the c's (see § 10) and consequently that of the equivalent widths, these being partly deduced from the c's. If, owing to their influence, the determination of the c's is erroneous, their values will always come out too large, but just as well for the centre of the sun's disc as for the limb. From the c-determinations appeared clearly the by no means unappreciable amount of the errors, that may still arise from deducing the continuum from the background in the registrograms. These frequently turned out to be located erroneously to an amount of 2 to 3 %, too high as well as too low.

e. *Ghosts.* The error, remaining after the general correction for ghosts (see p. 11), can at the most amount to 1 or 2 %, and can, besides, have no influence on the centre-limb variations. Neither can ghosts affect appreciably the central intensities, owing to the precautions taken in making the inner-photographs (§ 7, 3).

f. *Correct adjustment on the points of the solar disc.* A small difference in the adjustment of the tangential slit of the spectrograph may have a considerable effect on the limb spectra, because on approaching the limb, the profiles vary strongly. As the error may amount to a few 0.1 mm, which at Utrecht means about 0.004 R and at Potsdam about 0.002 R, the only thing one can say is that the point at 0.995 R measured at Utrecht will lie between 0.991 R and 0.999 R, an a posteriori check being in this case impossible. The exposures with a radial slit at Potsdam are more favourable in this respect, as, here, a subsequent location on the film of the points near the limb is possible (§ 7, 4).

g. *Irradiation from neighbouring points of the sun's disc.* In con-

sideration of what was said in § 7, 4 the measurements referring to the points near the extreme limb cannot be simply ascribed to the apparent points of adjustment.

h. *Perturbed regions.* The attempts to obtain the spectrum of the unperturbed photosphere, have certainly not always been successful, especially as regards the photographs at Potsdam in 1938 which were taken shortly before the time of maximum solar activity. As, however, for each point adjusted a new unperturbed region was visually selected, any systematic influence on the centre-limb variation is, practically speaking, out of the question.

i. *The sun's altitude.* With the longer times of exposure the sun's altitude may change materially during the photographing of a complete centre-limb series. In order to eliminate any sytematic influence of this change, the photographs were made in arbitrary succession.

Summarising we can say that the errors, which do occur, have but a very slight systematic influence on the centre-limb variation, that, however, the location at 0.99 R and 0.995 R, ascribed to the points near the extreme limb, must be used with some caution.

CHAPTER II

OBSERVATIONAL RESULTS

§ 10. General remarks.

1. *The tables of the intensity-profiles.* The results of the measurements are collected in the Tables 2 to 20, where, in general, the lines are arranged according to increasing wave length. The tables give the relative intensity of the selected points of the profiles as a function of $\sin \vartheta = r/R$, the distance from the centre of the sun's disc in terms of its radius. The first column gives the distance, expressed in A-units, of the measured point from the centre of the line. Distances towards the violet have the suffix v, those towards the red the suffix r. When no v or r is added, it means that the average has been taken of the intensities towards the violet and towards the red side. This was only done, when, for all points concerned of the sun's disc, these values did not differ more than 2 %.

The intensities are given separately for the various places of observation, Utrecht, Potsdam and (for the Mg b lines) Mount Wilson.

When a measured point was disturbed by blends, its intensities are printed in italics. Slightly disturbed points, of which the centre-limb variations will not differ materially from undisturbed ones, have not been marked separately. The estimation as to the degree of the disturbance is naturally more or less arbitrary; criteria for the absence of a disturbance at a point are: equal intensities towards the violet and the red; the smooth run of the profile just at that part. If, however, a line is strongly disturbed by blends, these criteria fail.

To the intensities of the profiles, deduced from the Potsdam photographs, we have occasionally added the central intensities of blending lines, of which the wave length (after [38]) of their centres is printed at the bottom of the table. They had to be measured in order to be able to correct the profile completely for the effect of the finite resolving

power. Afterwards, applying van de Hulst's correction-method, it turned out that the intensities within these blends need not be known; their central intensities, however, having once been measured, have been retained in the tables; they have not been corrected by the instrumental curve. The row indicated by "corrected central intensitities" gives the central intensities of the principal lines, from which the effect of the instrumental curve of the Potsdam grating spectrograph has been eliminated.

The position of the neighbouring continuous spectrum was, where at all possible, checked and, if necessary, corrected by means of the straight lines of the $i_0 - i$ versus $i/\Delta\lambda^2$-graph, as explained by M. Minnaert [24]). He showed that the distribution of the light in the wings of a Fraunhofer line is, in many cases, rendered by the expression $i/i_0 = 1/(1 + c's)$, where s is the ratio between the scattering coefficient and the coefficient of continuous absorption, and c' a proportionality-factor. In the wings s varies as $1/\Delta\lambda^2$ (damping), so that there $i/i_0 = 1/(1 + c/\Delta\lambda^2)$, from which it follows that $i_0 - i = ci/\Delta\lambda^2$, the formula yielding the value for the constant c, characteristic for each definite profile, this quantity, therefore, being a direct measure for the depression at large distances from the centre of a line. Minnaert has not investigated the extent to which this relation is satisfied for profiles in the spectrum of points close to the sun's limb. The following considerations, however, make it clear that his method can always be applied with advantage. Starting from the fact that, owing to damping, the scattering and absorbing action of an atom varies in the far wings as $1/\Delta\lambda^2$, and that for slight depressions these actions are simply additive, one can write: $i_0 - i = ci_0/\Delta\lambda^2$. From this formula c is found graphically by plotting $i_0/\Delta\lambda^2$ against $i_0 - i$. The tangent in the point $i = i_0$ coincides with the one drawn according to Minnaert's method, as for $i \to i_0$ both expressions merge into each other. As it turns out from the observations, however, that the formula $i_0 - i = ci/\Delta\lambda^2$ remains valid for deeper depressions than $i_0 - i = ci_0/\Delta\lambda^2$, we have used preferably the former expression for the determination of the tangent line in $i = i_0$. The values for c, obtained therefrom, are printed in the last row.

The equivalent widths, given in mA, are partly obtained by planimetring the smoothed-out profile drawn through the undisturbed points measured. As this method may lead to large errors in the far wings [24]), their contributions to the equivalent widths w_a have been determined, from a certain definite $\Delta\lambda$ onwards, from the constants c by means of the

formula $w_a = \sqrt{c}\left(\frac{\pi}{2} - \text{arctg}\,\frac{\Delta\lambda}{\sqrt{c}}\right)$. Care was always taken that the $\Delta\lambda$ used in this computation should still lie on the straight part of the graph i versus $i/\Delta\lambda^2$ at about $i/i_0 = r = 0.90$. For a definite centre-limb series, the same value for $\Delta\lambda$ was used throughout. The directly measured parts of the equivalent widths may have come out systematically too large, owing to an insufficient correction for blending and for finite resolving power. Likewise, the computation of the contributions from the far wings to the equivalent widths by means of the above formula yields, mostly, larger values than direct measuring of the areas [24]). Owing to these factors, the values obtained for these widths will, in general, be perhaps larger than those of other investigators. This is, however, of only secondary importance for the centre-limb variation, that means for the mutual ratios between the equivalent widths at the various points of the sun's disc.

For those Fraunhofer lines, that have been measured at different observatories, the equivalent widths as well as the c's have been determined from their average profiles.

2. *The cross-section figures.* Though a few profiles for different values of r/R are drawn, belonging to the most characteristic and best determined lines, the centre-limb variations are not represented by means of line-profiles, but by so-called cross-section figures. These are drawn for all lines separately; although showing less detail, they give a better general idea than the tables. A curve in a cross-section figure represents the variation of the relative intensity at some definite distance $\Delta\lambda$ from the centre of a line as a function of $\cos\vartheta$. The use of this quantity offers the advantage that the curves are drawn out on approaching the sun's limb, thereby affording a better survey of the variations, which, precisely in the narrow part close to the limb, become considerable. The comparison of the observational results with theory will, later on, always be carried out with the help of these cross-section curves.

3. *The determination of the c's* (see also this §, 1). We may suffice here with the remark that, by giving figures in detail, referring to this subdivision of the investigation, due attention has been paid to the determination of the c's and to their centre-limb variation; this was done on account of the important conclusions to be drawn from them in the theoretical part.

§ 11. The lines Fe 3815.9, 3820.4, 3859.9 and Mg 3829.4, 3832.3 and 3838.3 (Tables 2 and 3).

These ultra-violet Fe- and Mg lines are seriously disturbed by blends; only from a few points, in which the profiles are clearly not too strongly disturbed, is it possible to determine the centre-limb variation. This

Table 2. **Fe 3815.9**

$\sin\vartheta = r/R$	0.00	0.60	0.80	0.90	0.95	0.98	0.995
Distance from Line Centre in A	Observed Intensities in per cent. of the adjacent Continuous Spectrum						
0	10.0	9.4	9.0	10.0	14.0	13.2	14.0
0.15	20.4	19.0	20.3	23.2	28.0	31.0	43.0
0.36 r	29.0	28.0	27.0	29.5	36.5	39.0	52.5
0.56 v	53.0	53.0	49.5	49.0	53.5	55.7	68.5
0.68 r	51.3	52.0	48.3	48.0	52.2	54.0	66.5
0.77 v	76.0	71.0	69.5	69.5	72.0	72.5	81.0
0.80 r	64.0	60.5	58.0	55.5	59.0	59.0	72.5
1.42 r	84.5	81.5	82.0	79.0	81.0	80.5	87.5
1.57 v	82.0	79.0	77.5	76.6	78.5	79.0	86.4
			Fe 3820.4				
0	9.7	6.6	7.8	8.0	11.0	12.5	12.5
0.15	15.5	14.3	14.7	16.0	22.0	23.8	29.5
0.27 r	20.7	20.0	20.4	22.0	32.5	33.5	41.0
0.46	30.5	29.5	29.5	31.2	37.2	42.0	51.5
0.59 r	39.7	37.2	36.3	37.0	45.0	46.2	56.0
0.62 v	42.3	39.7	40.0	39.0	45.0	48.0	60.0
0.99 r	62.5	59.0	58.0	56.0	59.8	61.7	71.5
1.08 v	56.0	51.5	50.5	48.0	52.0	54.7	68.5
1.54 v	78.5	77.5	77.5	75.0	76.5	78.0	87.5
			Fe 3859.9				
0	12.5	12.5	12.5	13.5	17.0	16.0	19.0
0.09	17.7	17.0	17.5	20.5	25.0	25.0	30.0
0.17	23.5	23.3	23.7	29.0	33.7	35.6	42.0
0.48	41.0	40.0	39.6	42.5	47.5	53.5	61.5
0.88 v	55.0	53.0	51.0	53.0	56.0	61.0	70.5

variation is very characteristic of moderate intensities: starting from the centre of the sun's disc, the intensity of the inner wings increases at first, to decrease again closer to the limb; the cross-section curves show a depression (Fig. 4 and 5), which is stronger for the Fe- than the Mg lines. The three Mg lines show these variations within the obser-

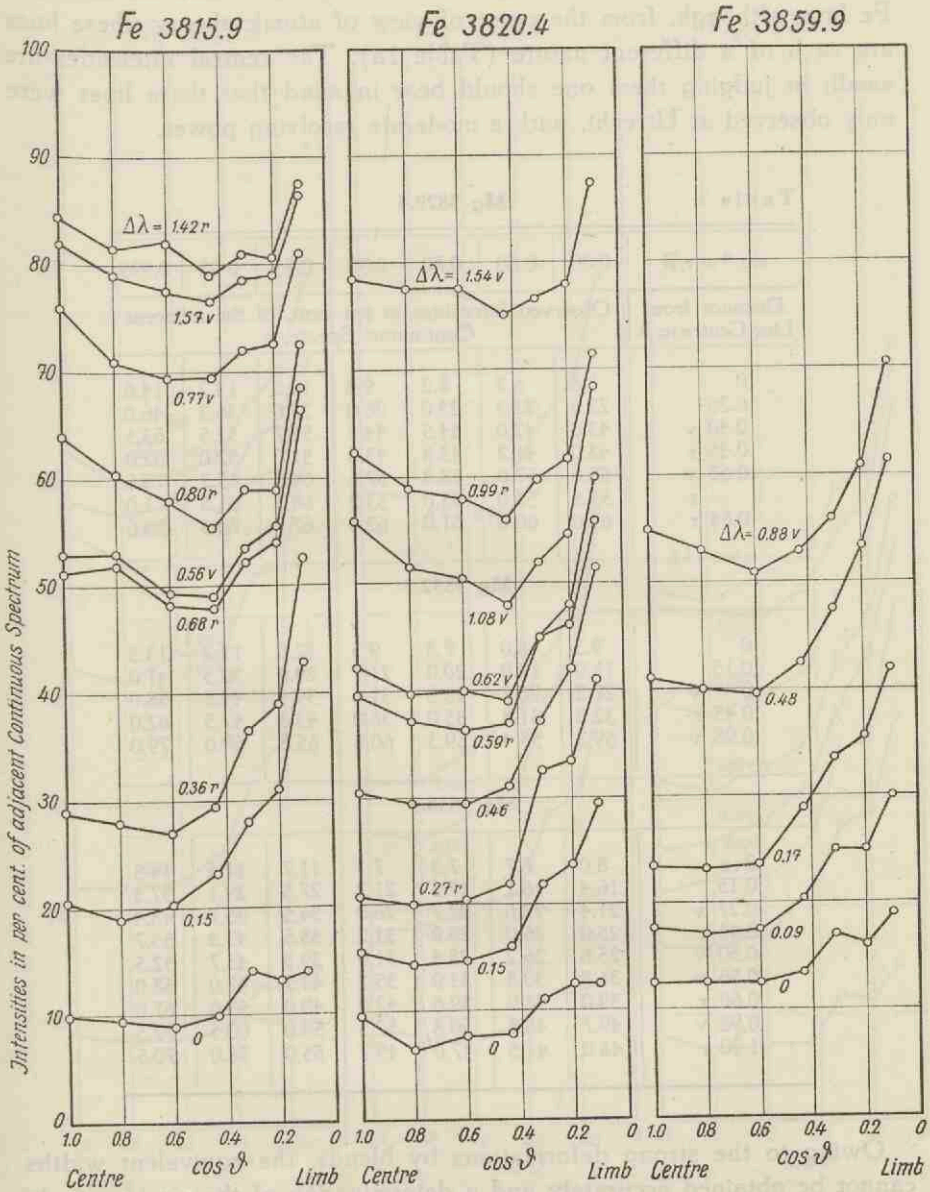

Fig. 4. — Centre-limb variations in the profiles of three ultra-violet Fe lines (parameter $\Delta\lambda$ = distance in A from centre of line).

vational errors to the same degree, and the same is true for the three Fe lines although, from the point of view of atomic theory, these lines are each of a different nature (Table 1a). The central intensities are small; in judging them one should bear in mind that these lines were only observed at Utrecht, with a moderate resolving power.

Table 3. **Mg 3829.4**

$\sin\vartheta = r/R$	0.00	0.60	0.80	0.90	0.95	0.98	0.995
Distance from Line Centre in A	Observed Intensities in per cent. of the adjacent Continuous Spectrum						
0	8.8	8.2	8.2	9.4	13.0	13.2	14.6
0.20	22.5	22.3	23.0	26.0	33.0	36.3	46.0
0.40 v	43.0	42.0	44.5	44.8	51.7	52.5	63.5
0.45 r	43.0	41.2	43.8	43.6	51.0	52.0	62.0
0.62 v	58.6	57.0	58.3	57.6	64.0	65.7	73.5
r	55.5	53.0	53.0	53.2	60.5	61.5	71.0
0.84 r	63.0	60.0	61.0	62.5	67.7	70.5	79.0
			Mg 3832.3				
0	9.3	8.0	7.8	9.3	12.0	12.2	13.3
0.15	18.0	18.0	20.0	21.7	29.0	30.5	41.0
0.37 v	27.2	26.7	28.8	31.6	39.5	44.8	58.0
0.45 r	32.0	31.8	35.0	38.0	43.3	47.5	62.0
0.96 v	59.3	58.4	59.3	60.5	65.8	69.0	79.0
			Mg 3838.3				
0	8.0	6.7	7.3	7.3	11.7	11.5	14.5
0.15	16.4	16.1	17.6	21.2	27.5	29.1	37.5
0.27 v	21.4	22.6	22.7	26.0	34.5	35.7	48.4
0.43 r	25.0	26.0	28.0	31.2	38.5	43.3	55.7
0.50 v	25.6	26.2	28.4	31.6	39.3	43.7	52.5
0.56 v	31.8	30.8	33.0	35.2	43.2	47.0	58.0
0.66 r	39.0	38.0	39.6	42.0	49.0	53.0	67.0
0.98 v	49.7	48.3	50.8	52.5	59.0	60.5	72.5
1.20 r	48.0	47.5	47.0	49.7	55.0	58.0	70.5

Owing to the strong deformations by blends, the equivalent widths cannot be obtained accurately and a determination of the c's is entirely out of the question.

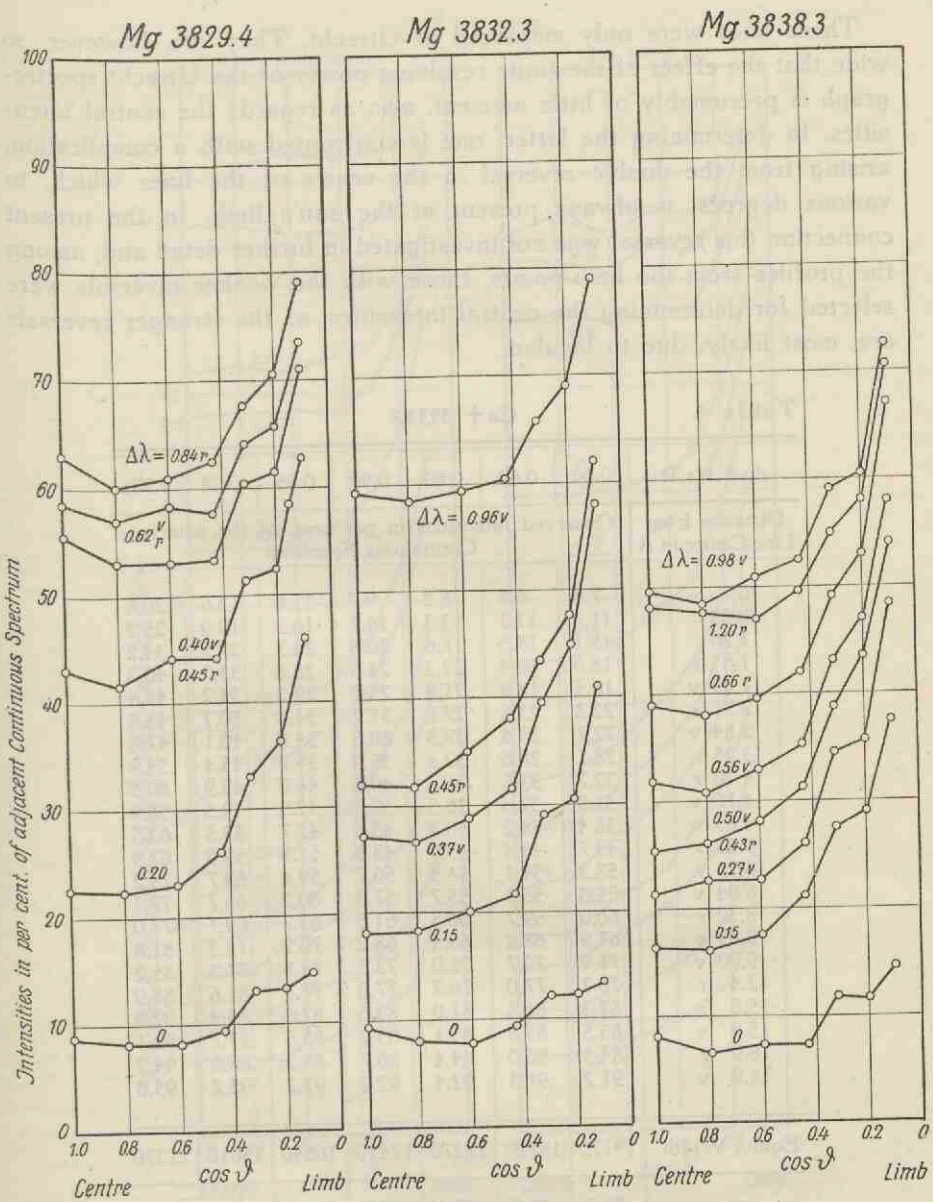

Fig. 5. — Centre-limb variations in the profiles of three ultra-violet Mg lines (parameter $\Delta\lambda$ = distance in A from centre of line).

§ 12. The H- and the K line of Ca^+ (Tables 4 and 5).

These lines were only measured at Utrecht. They are, however, so wide that the effect of the finite resolving power of the Utrecht spectrograph is presumably of little moment, also as regards the central intensities. In determining the latter, one is confronted with a complication, arising from the double reversal in the centre of the lines which, to various degrees, is always present at the sun's limb. In the present connection this reversal was not investigated in further detail and, among the profiles from the limb-points, those with the weaker reversals were selected for determining the central intensities, as the stronger reversals are, most likely, due to faculae.

Table 4. **Ca+ 3933.7**

$\sin\vartheta = r/R$	0.00	0.60	0.80	0.90	0.95	0.98	0.995
Distance from Line Centre in A	Observed Intensities in per cent. of the adjacent Continuous Spectrum						
0	7.4	6.8	8.2	9.7	11.6	13.6	20.8
0.63	11.3	11.1	13.3	14.7	16.9	19.9	25.2
1.26	15.1	15.5	18.6	20.8	24.3	27.7	34.2
1.83 r	18.0	18.4	22.2	24.6	28.8	33.7	40.3
1.89 v	18.5	18.9	21.9	25.2	29.2	34.2	41.4
2.71 r	22.8	23.8	27.6	31.2	34.8	40.2	48.9
2.84 v	22.7	23.8	27.3	30.6	34.6	40.1	47.8
3.28 r	28.1	28.6	32.4	35.9	39.7	45.4	54.9
4.10 r	32.7	33.6	36.5	40.6	44.0	49.9	60.5
4.16 v	31.9	32.6	36.5	39.3	42.9	49.5	58.9
4.85 v	38.4	38.2	40.8	43.6	47.7	53.5	63.5
5.55 r	43.7	44.4	45.9	48.9	51.8	59.0	67.9
6.75 r	53.3	54.1	54.5	56.7	59.4	64.7	74.2
6.94 v	55.3	55.3	55.7	57.3	60.2	66.7	77.1
8.32 r	60.0	59.7	60.5	61.5	63.7	69.1	78.0
8.89 v	67.9	68.2	68.4	68.2	70.2	75.3	81.8
9.90 v	71.9	72.7	72.0	73.5	74.3	77.3	85.2
12.4 r	76.2	77.0	76.2	77.3	77.1	81.6	88.9
15.6 r	82.3	81.8	81.0	83.6	82.5	85.4	92.9
15.8 v	85.8	85.8	85.1	85.2	85.5	87.7	92.1
16.9 r	84.5	86.0	84.4	86.7	86.2	87.8	94.2
18.9 v	91.2	91.3	92.4	92.2	92.2	93.2	95.0
Equiv. Width	19170	18720	18270	17410	16840	15010	11370
c	39.2	38.0	37.9	35.0	34.7	30.1	19.1

The equivalent widths, as far as the contribution from the wings is concerned, were determined from the violet half of the K line and from

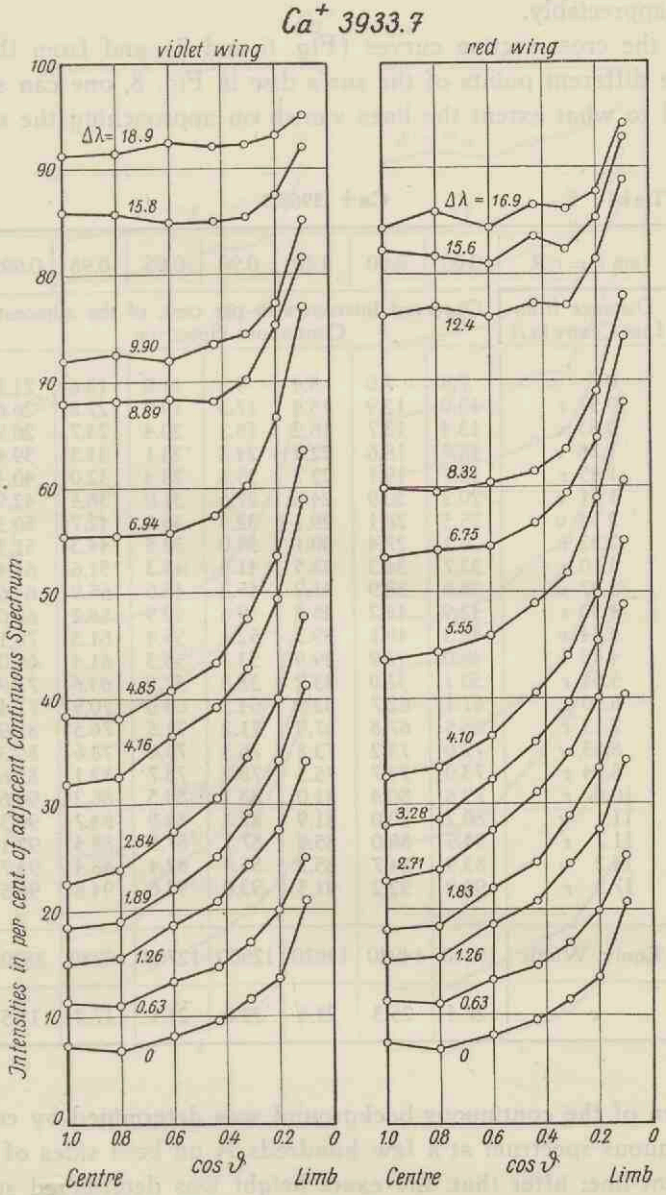

Fig. 6. — Centre-limb variations in the K line, Ca+ 3933.7 (parameter $\Delta\lambda$ = distance in A from centre of line).

the red half of the H line, because in the region between the lines they overlap appreciably.

From the cross-section curves (Fig. 6 and 7) and from the profiles for three different points of the sun's disc in Fig. 8, one can see clearly how and to what extent the lines vanish on approaching the sun's limb.

Table 5. **Ca+ 3968.5**

$\sin \vartheta = r/R$	0.00	0.60	0.80	0.90	0.95	0.98	0.995
Distance from Line Centre in A	Observed Intensities in per cent. of the adjacent Continuous Spectrum						
0	7.5	7.0	8.4	9.8	11.2	13.6	21.5
0.57 r	13.0	12.9	15.4	17.3	19.0	22.8	26.6
0.63 v	13.4	13.7	16.2	18.3	20.4	23.7	26.9
1.26 v	18.2	18.6	22.4	24.8	28.1	33.3	39.4
1.45 r	18.7	19.1	22.7	25.6	28.4	32.0	40.4
1.51 v	20.2	20.9	24.6	27.5	31.0	36.4	42.9
2.14 v	25.5	26.1	29.1	32.3	36.6	42.7	50.3
2.33 r	26.7	27.4	30.1	35.0	38.8	44.3	51.3
3.10 r	33.7	34.3	38.5	41.4	45.3	51.6	61.4
3.47 v	38.6	38.9	41.9	45.2	48.6	55.9	64.6
4.30 r	42.9	44.2	46.6	49.6	52.9	58.2	67.0
4.54 v	48.3	48.1	49.3	52.1	55.4	61.3	70.1
4.85 r	48.0	47.9	49.9	53.7	55.3	61.4	69.0
5.61 r	*50.1*	*51.0*	*53.2*	*55.8*	*57.9*	*63.6*	*71.9*
6.50 r	61.1	62.7	62.9	64.8	65.6	70.9	77.4
7.13 r	66.5	67.8	67.9	71.2	71.5	76.5	81.9
8.83 v	72.6	73.2	73.8	76.3	76.6	78.6	85.3
8.84 r	73.9	74.7	75.5	78.2	78.7	82.1	87.6
10.6 r	79.8	80.4	81.0	83.1	83.5	86.2	90.6
11.1 v	80.2	80.0	81.9	82.8	82.9	84.7	90.3
11.7 r	84.5	85.0	85.5	87.1	87.5	88.5	92.1
14.2 v	83.9	84.7	85.2	85.9	87.4	88.4	93.7
17.3 r	90.9	92.2	91.5	93.0	93.6	94.8	96.5
Equiv. Width	15240	14920	14620	12900	12760	10280	8820
c	26.4	25.3	24.4	22.0	21.1	17.2	11.5

The run of the continuous background was determined by connecting the continuous spectrum at a few hundreds A on both sides of the lines by a fluent line; after that, the exact height was determined still better by means of the $(i_0 - i)$ versus $i/\Delta\lambda^2$-graphs, which are shown completely in Fig. 9. For the centre of the sun's disc the connection remains linear down to relative intensities lower than 50 %, for the points near the limb the bend in the curves occurs already at higher intensities.

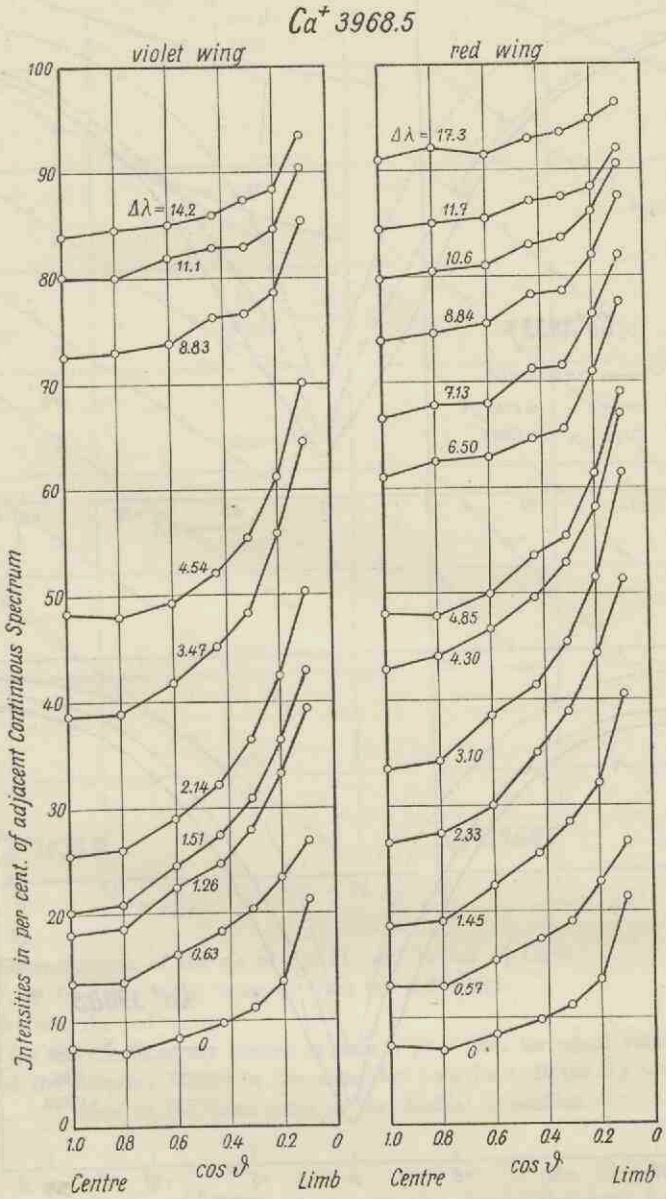

Fig. 7. — Centre-limb variations in the H line, Ca+ 3968.5 (parameter $\Delta\lambda$ = distance in A from centre of line).

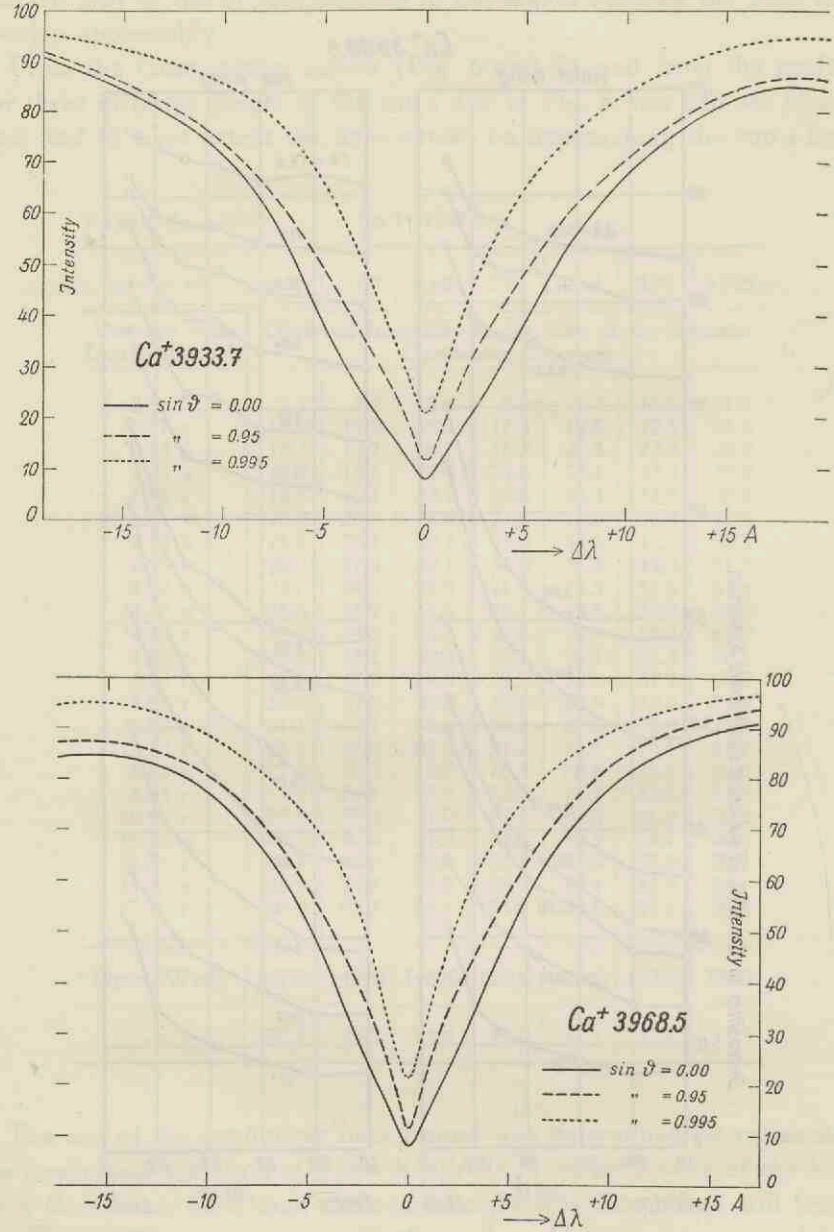

Fig. 8. — Profiles of the H line (lower fig.) and K line (upper fig.) of Ca+ in three different points of the solar disc.

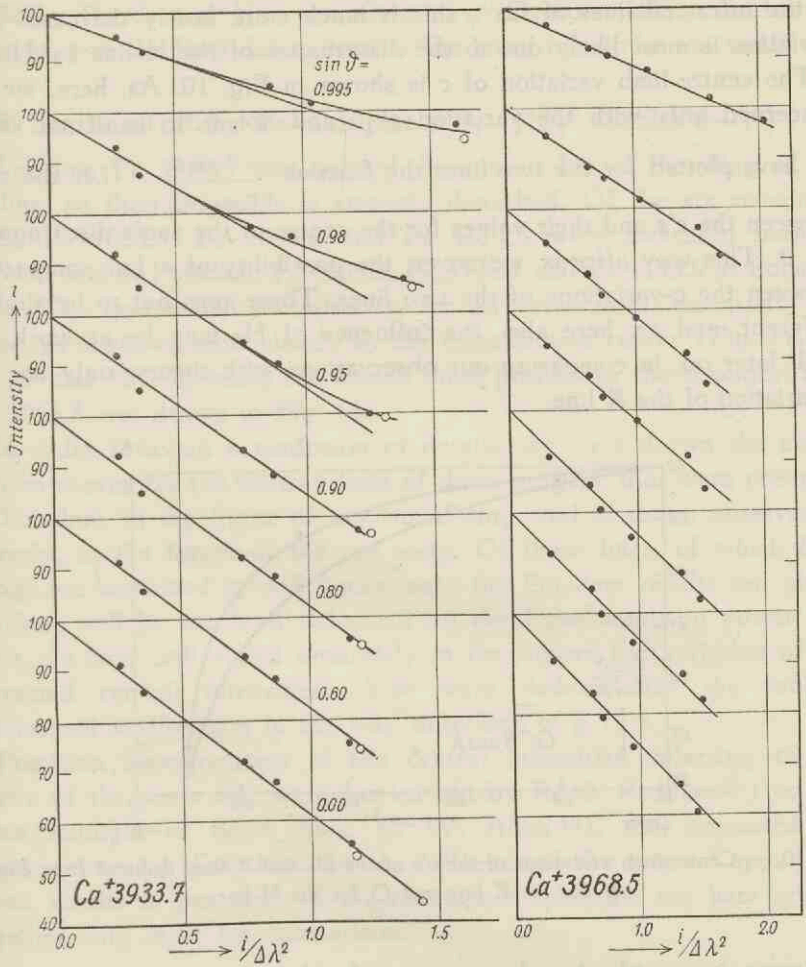

Fig. 9. — Determination of the c's of the H- and K line of Ca+.
Ca+ 3933.7: ● from the violet wing, ○ from the red wing;
Ca+ 3968.5: from the red wing.
The scales for the abscissae are chosen in such a way that, for equal values of sin ϑ, the slopes of the tangents would be the same for both lines, if the c's were to each other in the same ratio as the doublet intensities.

It is remarkable that the ratio between the c's of the two lines is not equal to the doublet-ratio (here, therefore, 1 : 2) but to 1 : 1.6. This is the more striking, as for other well-measurable multiplets, such as the D lines of Na, the two stronger lines of the Mg b triplet and those

of the infra-red lines of Ca^+, this is much more nearly the case. This deviation is most likely due to the disturbance of the H line by $H\epsilon$.

The centre-limb variation of c is shown in Fig. 10. As, here, we are concerned only with the variation of c and not with its actual value, we have plotted for the two lines the fraction $\frac{c \cos \vartheta}{c \cos \vartheta = 1}$ (i.e. the ratio between the c's and their values for the centre of the sun's disc) against $\cos \vartheta$. This way affords, moreover, the possibility of a fair comparison between the c-variations of the two lines. These turn out to be slightly different, and as, here also, the influence of $H\epsilon$ may be at work, we shall later on, in comparing our observations with theory, only use the c-variation of the K line.

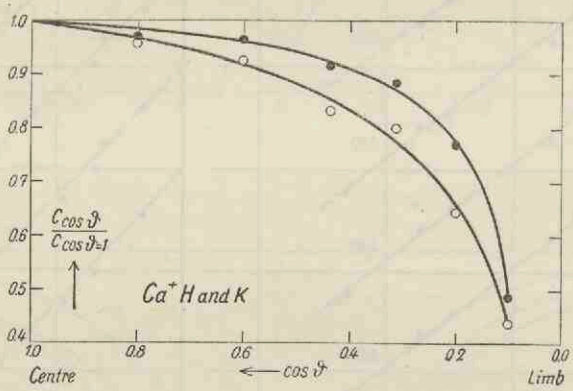

Fig. 10. — Centre-limb variations of the c's of the H- and K line, deduced from Fig. 9; ● for the K line and O for the H line.

Comparison with the observations of other investigators [18]) shows that, for the centre of the sun's disc, the profile and more in particular its central intensity, agrees satisfactorily with those obtained by K. Schwarzschild [5]), M. Minnaert [30]) and A. D. Thackeray [31]). The difference between our profiles for centre and limb is of the same nature as that found by Schwarzschild (more cannot be said about this, as Schwarzschild does not give the exact position of the point for his limb exposure). The centre-limb variation agrees fairly well with that determined by T. Royds and A. L. Narayan [12]), although they give appreciably larger relative intensities. In this connection attention may be drawn to a remark of D. S. Evans [19]), who found for the hydrogen lines deviations in the same sense between his own measurements and

those by Royds and Narayan. One may, therefore, safely assume the intensities of the lines determined by the latter two to be too small.

§ 13. Six lines of the Fe-multiplet a^3F_4—$y^3F_3^\circ$ (Tables 6—11).

The line Fe 3969.3 was omitted, because it lies in the wing of the H line, so that its profile is strongly disturbed. Of the six remaining lines, Fe 4045.8, Fe 4063.6 and Fe 4071.8 were measured both at Utrecht and at Potsdam, Fe 4005.3, Fe 4132.1 and Fe 4143.9 at Potsdam only. The centre-limb variation is, for all these lines, essentially the same, as is shown most clearly by the cross-section curves (Fig. 11, 12, 16, 17 and 18). Ignoring the blends three profiles of the strongest line, Fe 4045.8, are drawn in Fig. 14.

In order to avoid a confusion of details, we have drawn the cross-section curves for the central parts of those profiles, that were observed at Potsdam, in the figure of the violet wing, and of those, observed at Utrecht, in the figure of the red wing. Of those lines, of which both wings are combined in one figure, only the Potsdam results are given, as these will be the least deformed by the finite resolving power. To these we have still added separately in the figures the variation of the corrected central intensities; these were deduced for the profiles determined at Potsdam in the way described in § 7, 5.

Precision measurements of the central intensities, referring to the centre of the sun's disc were carried out by R. O. Redman [39]) on the three stronger of these lines; C. W. Allen [40]), too, corrected his measurements of these lines for the influence of the spectral apparatus. Their results in per cent. of the continuous spectrum are here added, together with mine for comparison.

	Fe 4045.8	Fe 4063.6	Fe 4071.8
Allen	3	3	3
Redman	2.1	1.9	2.2
this thesis	2.5	4.9	4.4

The lines Fe 4005.3 and Fe 4132.1 are so seriously disturbed by blends, that their equivalent widths are unreliable, while in their wings the blending is such that the c's cannot be determined; the c's of Fe 4143.9 are for that same reason unreliable. The graph from which they are deduced is given in full for the line Fe 4045.8 in Fig. 13. The ratios

between the c's of the best measurable four lines do not agree with the theoretical multiplet ratios, neither do they agree with the ratios following from R. B. and A. S. King's [41]) laboratory experiments after these had been recomputed for 6000° (see also [42])). It is difficult to come to a decision as to the cause of this difference, although the c-determinations for the lines Fe 4045.8, Fe 4063.6 and Fe 4071.8 would appear to be too accurate to afford an explanation for such a large discrepancy.

Table 6. **Fe 4005.3** [1])

$\sin\vartheta = r/R$	0.00		0.60		0.80		0.90		0.95		0.98		0.99		0.995	
Monochromator	narrow	wide	narrow	wide	narrow	wide	narrow	wide	narrow	wide	narrow	wide	narrow	wide	narrow	wide
Corrected Central Intensities	4.8		4.4		4.1		4.3									
Distance from Line Centre in A	Observed Intensities in per cent. of the adjacent Continuous Spectrum															
0	8.2		8.0		8.2		8.5									
0.034	10.8		10.8		10.6		10.4									
0.069	17.7	18.0	17.7	16.0	18.8	20.8	19.8	23.9		26.9		30.5		31.9		36.3
0.10 v	24.3		24.3		24.8		27.1									
r	*22.5*		*22.5*		*23.3*		*24.6*									
0.13 r [2])	*21.9*	*21.5*	*23.1*	*22.3*	*24.3*	—	*24.0*	—		*29.8*		*35.3*		*39.1*		*42.5*
0.14 v	28.0	27.5	27.6	27.6	27.2	26.8	29.3	28.3		34.4		39.0		43.1		45.0
0.17 r	36.9		36.3		34.2		36.7									
0.18 v [3])	*23.2*		*23.9*		*23.7*		*27.1*									
0.21 v		*29.5*		*28.5*		*29.2*		*30.7*		*35.4*		*39.0*		*45.1*		*46.0*
r		37.5		34.3		35.6		36.6		38.7		41.4		48.8		48.5
0.22 v	*31.2*		*29.3*		*28.4*		*30.1*									
0.23 r [4])	*35.2*		*34.0*		*33.6*		*35.6*									
0.27 v [5])	*20.0*		*21.6*		*23.0*		*25.4*									
r	57.0		55.6		54.7		53.6									
0.29 v	—		*22.3*		*23.5*		*28.5*									
0.34 v [6])	*18.6*		*19.9*		*20.7*		*23.2*									
r	74.0	75.0	71.7	70.3	72.2	69.7	69.7	66.8		69.0		70.0		75.8		75.3
0.45 v	*44.6*		*42.3*		*46.0*		*41.5*									
0.46 r [7])	*35.9*		*35.6*		*36.5*		*37.0*									
0.52 v	79.2		76.4		81.3		79.5									
r	*64.6*		*62.5*		*61.5*		*61.2*									
0.59 v		86.0		86.2		84.7		83.2		84.0		84.2		87.8		88.0
0.62 r		92.0		91.3		90.1		87.8		89.4		88.2		91.9		90.2
0.76 v		99.9		97.8		97.0		96.1		96.5		95.4		98.4		98.6
Equiv. Width [8])	482		507		512		539		503		504		439		425	

[1]) The only line for which at Potsdam, all points were not observed with narrow slit of monochromator.

[2]) Centre of 4005.390.

[3]) „ „ 4005.074.

[4]) „ „ Fe 4005.484.

[5]) „ „ „ 4004.986.

[6]) Centre of 4004.919.

[7]) „ „ V^+ 4005.712.

[8]) Values unreliable.

Besides, we are here concerned only with the line Fe 4045.8, the best determined one, as the observed ratios between the c's (strongest line : other line) are larger than the theoretical ones and the blending of Fe 4063.6 and Fe 4071.8 would affect these values in exactly the opposite sense. Nevertheless, the centre-limb variation of the c-values will presumably be about the same as for the undisturbed wings. This is confirmed by Fig. 15, which shows the centre-limb variation of $\frac{c_{\cos\vartheta}}{c_{\cos\vartheta=1}}$ for the four lines; all of them show the remarkable increase of the wings at $\cos\vartheta = 0.3$.

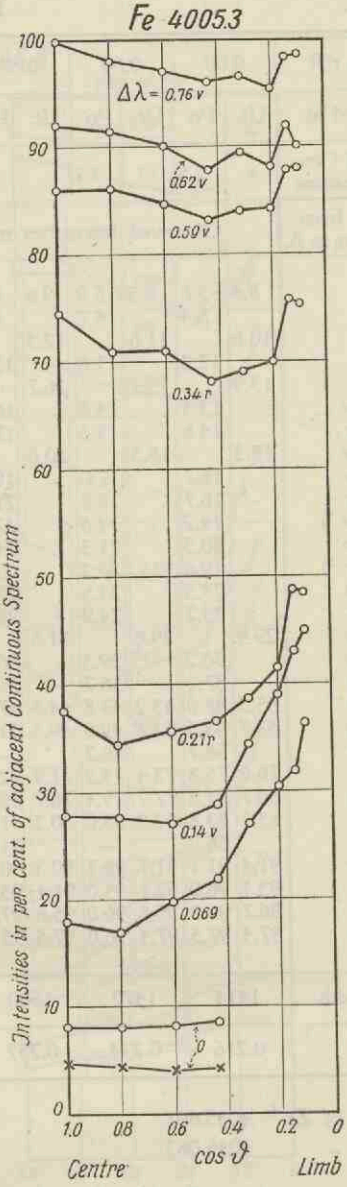

Fig. 11. — Centre-limb variations in the line Fe 4005.3 (parameter $\Delta\lambda$ = distance in A from centre of line); × corrected central intensities.

Table 7. **Fe 4045.8**

$\sin\vartheta = r/R$	0.00		0.60		0.80		0.90		0.95		0.98		0.99		0.995	
Observed at	Ut.	Po.	Ut.	Po.	Ut.	Po.	Ut.	Po.	Ut.	Po.	Ut.	Po.	Ut.	Po.	Ut.	Po.
Corrected Central Intensities		2.5		3.1		2.9		3.7		4.4		5.8		6.2		7.2
Distance from Line Centre in A	Observed Intensities in per cent. of the adjacent Continuous Spectrum															
0	8.4	5.6	9.3	5.9	9.6	6.9	10.7	6.7	11.8	7.6	12.5	9.0		9.9	12.9	10.8
0.034		8.4		8.2		8.5		8.2		9.8		10.5		12.0		13.0
0.042	10.6		11.6		12.3		13.7		15.8		16.4				16.9	
0.069		12.2		11.8		13.8		14.5		15.2		17.4		18.5		19.5
0.085	13.9		15.2		16.7		18.8		21.1		23.3				24.8	
0.10 v		13.4		14.8		16.6		19.3		21.0		23.5		24.7		27.0
r		14.6		15.3		17.6		20.0		20.0		24.2		26.8		28.3
0.13 v	17.3		18.3		20.0		23.2		26.2		29.6				31.6	
0.14 v		16.7		17.0		19.2		22.2		24.4		27.4		30.6		33.5
r		16.7		18.2		21.3		23.8		24.7		28.8		31.5		34.0
0.20 v [1]		*14.2*		*14.6*		*17.5*		*19.9*		*21.7*		*24.4*		*26.2*		*28.5*
r		20.3		21.3		24.7		27.8		28.0		33.8		37.4		40.0
0.24 r [2]		*19.6*		*20.2*		*23.5*		*24.7*		*25.2*		*30.6*		*33.2*		*34.8*
0.28 v		23.5		23.5		27.0		30.0		32.8		36.2		39.7		43.5
r		25.2		24.9		26.7		28.4		28.2		34.4		38.1		40.0
0.30 v	29.9		29.6		31.6		34.8		39.0		44.0				50.3	
0.34 v		*30.2*		*29.5*		*30.7*		*33.3*		*35.5*		*39.3*		*43.4*		*48.2*
r		37.2		36.7		39.0		40.4		39.7		46.9		50.8		53.9
0.42 r	45.3	48 0	43.2	43.8	44.3	47.0	46.3	47.4	51.2	45.5	55.6	52.4		55.6	64.2	61.4
0.55 v	*53.7*	*53.5*	*51.8*	*49.0*	*49.5*	*51.2*	*52.1*	*50.8*	*56.0*	*50.2*	*60.3*	*55.1*		*59.4*	*68.8*	*63.5*
r		58.7		56.2		—		54.1		54.3		60.0		64.4		66.1
0.84 r	76.0	75.8	73.4	75.2	71.9	72.8	71.3	72.1	72.2	70.1	74.4	71.1		73.6	80.7	75.6
0.95 v	80.7	81.2	77.7	79.4	76.7	80.0	75.9	77.8	76.7	74.6	77.7	76.5		78.6	85.2	81.1
1.04 r	83.1	83.8	82.2	85.0	80.2	81.9	79.0	80.4	79.7	78.4	80.6	82.0		83.4	86.5	83.8
1.30 r		86.9		—		81.9		80.4		80.0		82.5		81.8		84.5
1.52 v	91.4	91.1	91.7	90.7	90.3	90.2	89.4	88.2	88.9	89.2	88.9	88.1		88.9	91.8	88.5
1.71 r	93.1	96.0	92.1	95.0	91.1	93.0	90.8	91.0	91.1	90.2	90.4	93.5		92.2	94.8	90.7
2.45 r	96.7	96.0	95.8	96.0	95.6	97.2	95.9	95.8	95.3	95.5	95.1	98.0		96.6	97.4	95.3
2.71 v	97.4	97.5	97.4	96.0	97.5	95.3	98.5	99.2	99.0	95.5	99.1	95.7		—	100	96.0
Equiv. Width	1414		1472		1500		1532		1512		1406		1336		1196	
c	0.216		0.234		0.257		0.277		0.285		0.258		0.251		0.208	

[1]) Centre of Zr^+ 4045.601.
[2]) „ „ 4046.083.

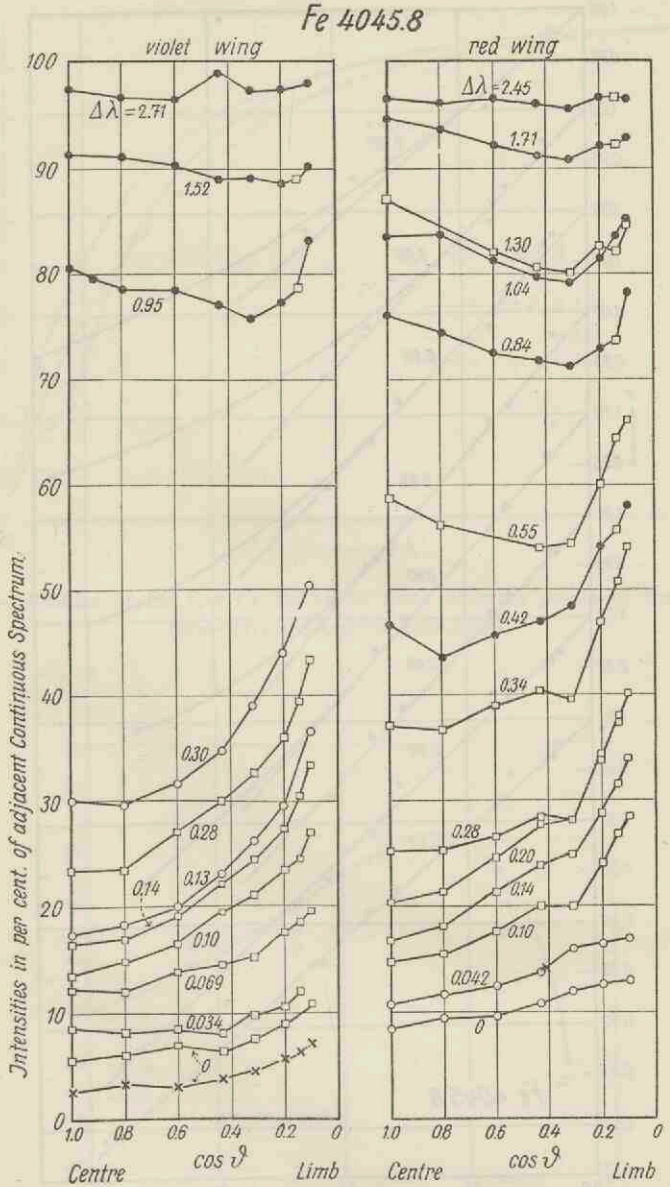

Fig. 12. — Centre-limb variations in the line Fe 4045.8; ○ Utrecht; □ Potsdam; ● mean; × corrected central intensities (parameter $\Delta\lambda$ = distance in A from centre of line).

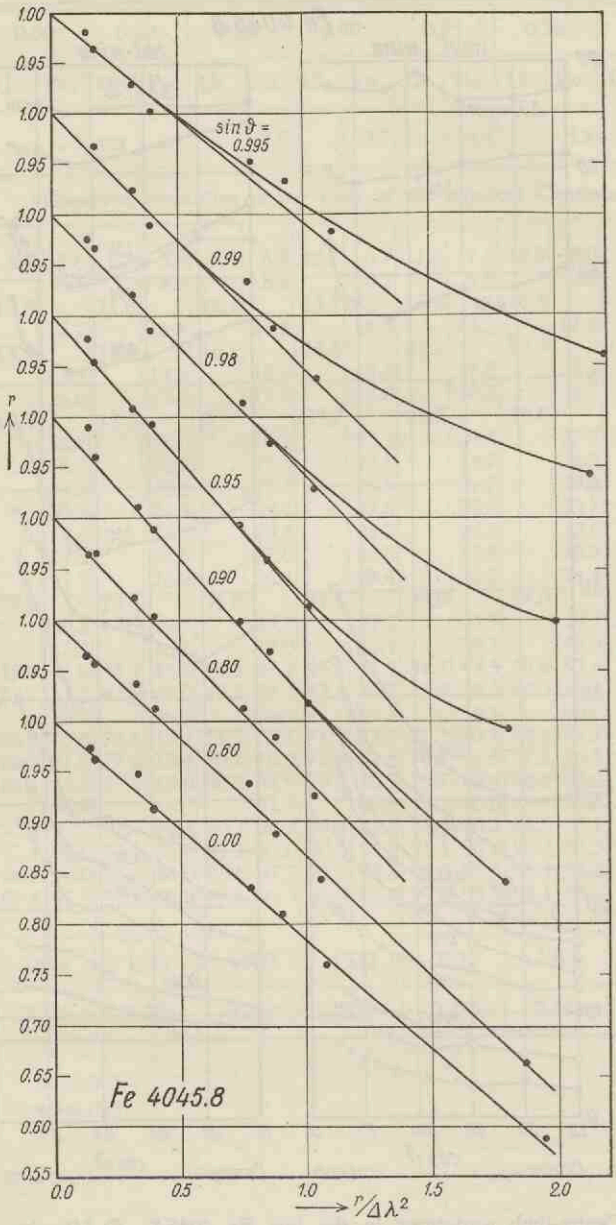

Fig. 13. — Determination of the c's of the line Fe 4045.8.

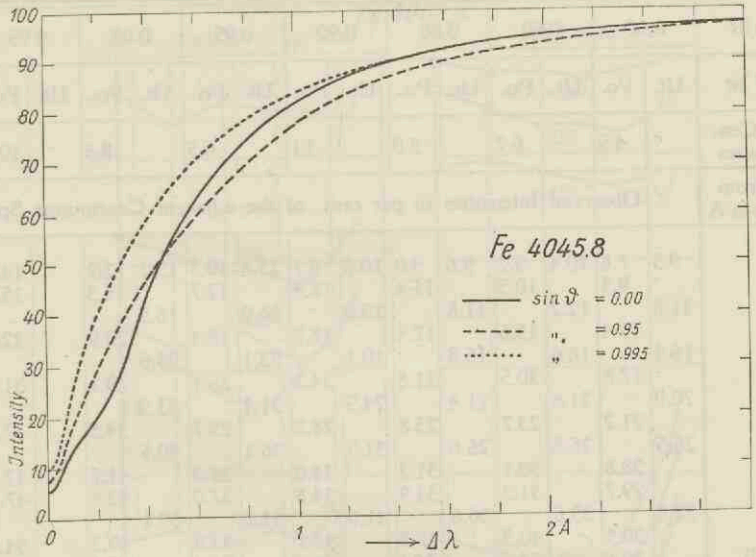

Fig. 14. — Profiles of the line Fe 4045.8 in three different points of the solar disc (non-corrected central intensities).

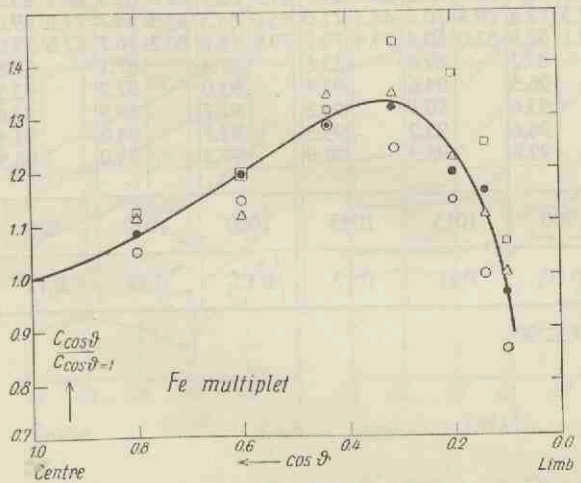

Fig. 15. — Centre-limb variations of the c's of four lines of the Fe multiplet a^3F_4—$y^3F_3^0$; ● Fe 4045.8; ○ Fe 4063.6; □ Fe 4071.8; △ Fe 4143.9.

Table 8. **Fe 4063.6**

$\sin\vartheta = r/R$	0.00		0.60		0.80		0.90		0.95		0.98		0.99		9.995	
Observed at	Ut.	Po.	Ut.	Po.	Ut.	Po.	Ut.	Po.	Ut.	Po.	Ut.	Po.	Ut.	Po.	Ut.	Po.
Corrected Central Intensities		4.9		6.2		5.0		3.1		6.5		8.4		10.8		9.4
Distance from Line Centre in A	Observed Intensities in per cent. of the adjacent Continuous Spectrum															
0	9.5	7.8	10.4	9.2	9.6	9.0	10.8	8.1	13.4	10.3	13.1	12.2		14.3	13.7	13.6
0.034		9.3		10.5		11.4		12.4		12.7		14.3		15.9		15.9
0.042	11.8		12.2		11.8		13.0		16.0		16.5				17.8	
0.069		13.4		15.6		17.4		18.7		18.4		20.9		22.6		24.6
0.085	16.4		16.6		16.8		19.1		23.1		25.6				27.1	
0.10		17.8		20.5		21.8		24.3		25.1		29.1		31.1		33.8
0.13	20.9		21.6		21.4		24.9		31.4		33.9				38.2	
0.14		21.2		23.7		25.8		28.2		29.7		34.5		37.7		41.0
0.17 r	26.5		26.6		26.6		31.3		36.1		40.5				47.7	
0.21 v		28.8		30.1		31.2		34.0		35.3		41.7		47.1		49.3
r		29.7		31.3		33.9		34.8		37.0		42.6		47.1		50.0
0.25 r	37.8		35.6		36.6		41.0		44.1		50.1				57.4	
0.27 r		39.5		40.3		42.2		43.1		43.8		49.3		54.0		56.1
0.31 v [1]		*20.6*		*22.3*		*24.3*		*26.4*		*26.4*		*30.2*		*32.7*		*35.6*
0.34 v		*28.5*		*30.6*		*31.1*		*33.6*		*35.6*		*38.4*		*39.9*		*43.9*
r		47.2		48.5		49.8		50.2		49.7		55.4		59.6		62.2
0.40 v		53.8		55.0		53.7		54.8		53.8		57.0		61.6		62.0
r	54.2	53.3	51.5	53.5	48.4	52.8	50.1	51.8	54.4	53.4	60.8	58.5		62.0	65.6	65.8
0.51 v	71.5		70.5		67.3		67.2		70.4		72.6				77.6	
0.55 v		74.5		72.4		74.7		72.0		71.1		72.2		75.0		76.4
r	*66.7*	*66.0*	*62.0*	*67.0*	*60.0*	*64.7*	*61.9*	*62.9*	*62.0*	*62.5*	*66.7*	*65.5*		*67.7*	*71.7*	*73.5*
0.70 r	*71.5*	*72.8*	*70.5*	*70.5*	*67.3*	*71.0*	*65.0*	*68.5*	*67.3*	*69.7*	*71.6*	*69.6*		*70.6*	*75.4*	*74.8*
0.74 v	83.1	82.9	82.0	80.4	79.4	79.2	79.6	78.8	80.2	76.7	82.6	79.0		83.1	85.5	82.7
1.02 r		89.2		89.6		83.6		87.4		87.1		87.8		85.5		88.5
1.23 r		96.5		94.6		92.8		93.0		92.2		93.5		94.5		95.4
1.40 v		*93.6*		*90.9*		*92.8*		*92.7*		*89.9*		*91.6*		*90.7*		*91.8*
2.26 v		96.6		93.2		95.5		94.7		94.6		94.4		93.8		95.1
r		99.0		98.3		97.9		97.3		98.0		98.5		98.8		99.1
Equiv. Width	990		1015		1045		1060		1040		970		895		825	
c	0.10_5		0.11		0.12		0.13_5		0.13		0.12		0.10_5		0.09	

[1]) Centre of Fe 4063.290.

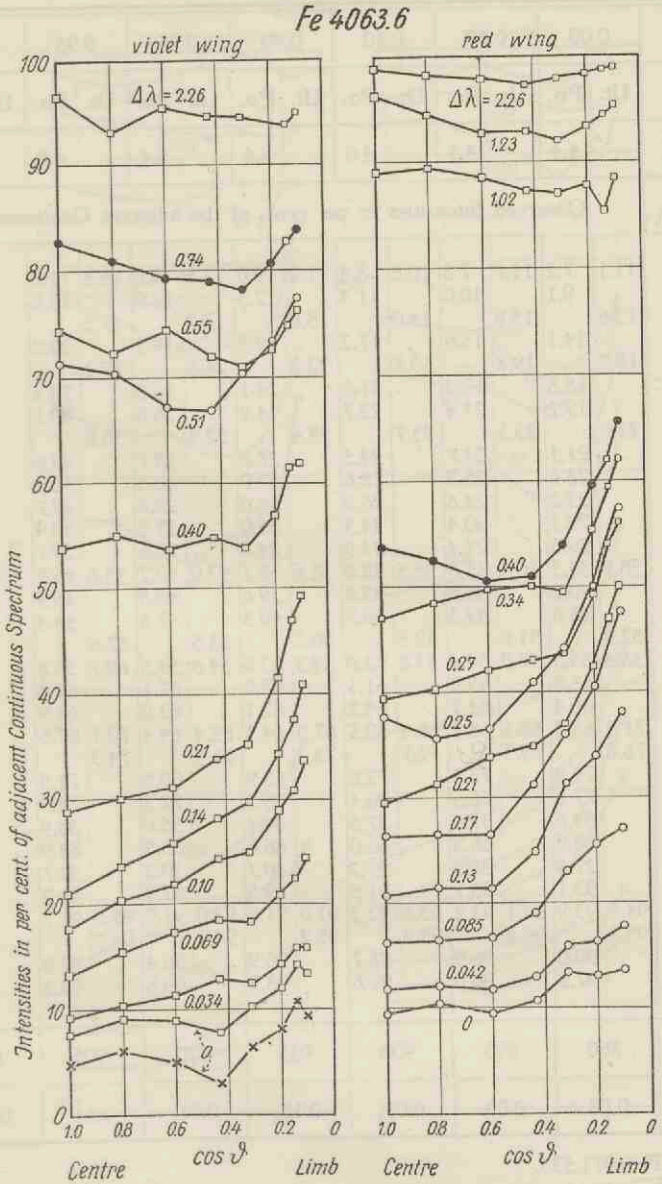

Fig. 16. — Centre-limb variations in the line Fe 4063.6; ○ Utrecht; □ Potsdam; ● mean; × corrected central intensities (parameter $\Delta\lambda$ = distance in A from centre of line).

Table 9. **Fe 4071.8**

$\sin\vartheta = r/R$	0.00		0.60		0.80		0.90		0.95		0.98		0.99		0.995	
Observed at	Ut.	Po.	Ut.	Po.	Ut.	Po.	Ut.	Po.	Ut.	Po.	Ut.	Po.	Ut.	Po.	Ut.	Po.
Corrected Central Intensities		4.4		4.3		4.6		5.6		6.4		6.8		8.3		8.2
Distance from Line Centre in A	Observed Intensities in per cent. of the adjacent Continuous Spectrum															
0	11.1	7.2	11.7	7.8	10.6	8.4	11.9	9.0	13.8	9.6	14.4	11.0		12.5	16.0	12.9
0.034		9.1		10.0		11.3		12.3		12.0		13.6		15.4		15.9
0.042	13.6		13.9		14.0		15.0		17.2		17.5				20.3	
0.068		14.1		15.9		17.2		19.1		19.5		22.2	22.9			25.1
0.085	18.2		19.8		19.8		22.2		24.6		27.2				31.3	
0.10 v		18.8		19.3		21.6		24.1		26.0		29.4	32.5			35.2
r		19.2		21.4		22.7		24.9		26.0		30.5	34.8			36.4
0.13 r	23.8		25.5		25.7		28.4		32.4		36.0				43.3	
0.14 v		*21.1*		*21.7*		*24.5*		*27.0*		*28.7*		*33.0*	*36.8*			*39.3*
r		23.6		25.3		28.6		30.0		30.4		35.7	41.2			43.2
0.17 v		*23.2*		*24.6*		*26.0*		*28.0*		*29.8*		*33.7*	*38.6*			*42.0*
r		29.3		30.4		34.5		34.0		35.2		40.9	45.7			50.2
0.21 v [1]		*20.5*		*21.4*		*24.9*		*24.8*		*26.6*		*29.7*	*33.2*			*36.4*
r	36.8	34.3	36.5	35.8	36.5	38.8	38.6	38.8	43.0	40.2	48.6	45.9	51.0		56.0	54.9
0.27 v		*40.2*		*36.8*		*35.8*		*39.6*		*40.8*		*45.4*	*49.2*			*53.8*
r		48.6		49.3		50.7		49.3		47.8		54.4	59.6			63.4
0.30 r	52.0		51.6		49.8		50.2		53.5		57.6				66.6	
0.34 v	*58.4*	*55.5*	*57.0*	*54.4*	*53.8*	*52.0*	*54.3*	*53.6*	*54.6*	*54.5*	*60.7*	*55.8*	*61.8*		*69.2*	*65.7*
r		58.8		59.9		61.1		57.9		57.1		62.8	68.3			71.6
0.42 v		66.4		64.2		64.2		62.1		62.0		64.9	68.8			72.1
r	71.3	68.3	69.1	68.2	66.4	69.5	67.5	64.5	68.4	64.4	70.1	67.6	70.5		77.0	75.4
0.51 v	76.6		75.3		72.7		73.2		71.5		74.3				83.8	
r		74.9		73.8		73.6		68.9		69.5		71.3	72.2			76.5
0.55 v		77.8		76.5		76.4		73.3		72.8		74.3	75.6			80.8
0.76 r [2]		*34.6*		*35.6*		*37.6*		*34.1*		*36.0*		*38.9*	*39.4*			*42.8*
0.79 v		88.0		86.5		86.0		86.6		83.9		84.9	87.5			87.7
0.97 v [3]		*27.8*		*28.5*		*29.2*		*30.1*		*30.2*		*31.7*	*34.6*			*38.2*
1.03 r		93.1		93.7		91.5		89.5		87.9		90.2	90.0			93.8
1.23 v	94.8	93.9	94.1	93.2	93.6	92.2	92.0	91.9	93.0	91.9	92.0	91.7	92.2		93.6	91.9
1.27 r	95.2		96.3		95.2		95.2		94.1		94.2				94.7	
1.58 r		99.0		96.9		98.7		96.9		96.4		97.9	99.9			97.7
1.92 v		97.9		96.9		97.6		98.9		99.6		99.3	97.4			97.7
Equiv. Width	860		890		900		935		970		905		825		710	
c	0.08		0.09		0.09_5		0.10_5		0.11_5		0.11		0.10		0.08_5	

[1]) Centre of VFe 4071.538.
[2]) „ „ $\overline{\text{Fe}}$ 4072.514.
[3]) „ „ Fe 4070.779.

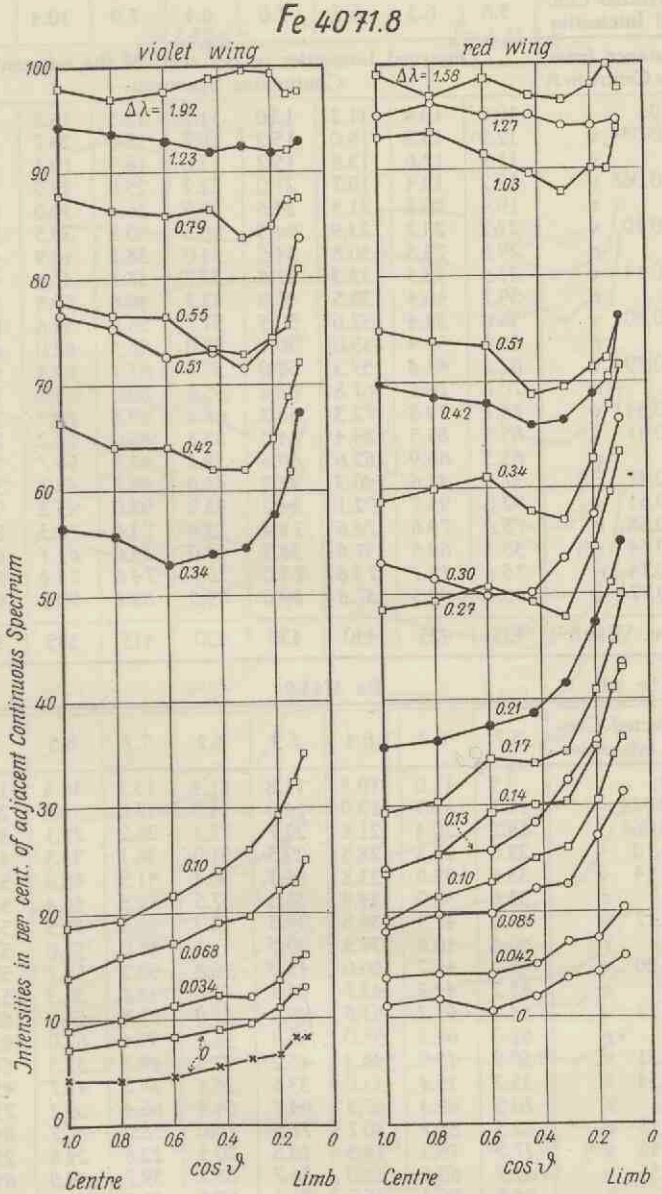

Fig. 17. — Centre-limb variations in the line Fe 4071.8; ○ Utrecht; □ Potsdam; ● mean; × corrected central intensities (parameter $\Delta\lambda$ = distance in A from centre of line).

Table 10. **Fe 4132.1**

$\sin\vartheta = r/R$	0.00	0.60	0.80	0.90	0.95	0.98	0.99	0.995
Corrected Central Intensities	5.6	6.3	6.5	7.0	6.4	7.9	10.4	11.3
Distance from Line Centre in A	Observed Intensities in per cent. of the adjacent Continuous Spectrum							
0	10.0	10.9	11.2	12.0	11.7	13.5	15.8	16.5
0.034 v	12.9	15.8	15.0	15.2	16.7	18.0	20.7	20.2
r	11.4	12.6	13.8	15.2	15.0	16.9	19.1	18.8
0.068 v	17.2	19.4	19.7	21.0	22.2	25.6	29.0	30.4
r	19.4	20.8	21.5	24.6	25.5	26.4	30.0	28.7
0.10 v	*21.2*	*23.2*	*23.9*	*24.5*	*26.6*	*30.8*	*33.5*	*36.2*
r	29.2	29.8	30.8	34.5	34.0	38.1	40.9	42.8
0.14 v	*31.5*	*33.5*	*32.3*	*31.6*	*33.7*	*37.7*	*41.4*	*44.3*
r	39.2	40.4	39.5	40.9	43.2	46.6	50.5	52.8
0.20 v	56.0	54.4	52.6	50.5	51.7	55.9	58.6	62.9
r	56.0	56.4	55.0	56.1	55.0	58.5	62 0	66.3
0.29 v	*61.2*	*61.4*	*59.3*	*58.0*	*59.3*	*61.1*	*65.8*	*66.3*
r	70.6	70.5	67.8	67.6	65.6	69.0	74.6	74.7
0.34 v	*76.1*	*74.8*	*72.3*	*68.2*	*68.8*	*69.8*	*74.9*	*74.1*
0.41 v	85.5	85.3	84.4	84.0	83.8	85.0	84.2	85.0
r	*65.3*	*66.9*	*62.6*	*60.5*	*59.2*	*62.7*	*66.7*	*70.2*
0.47 r [1])	*37.5*	*41.6*	*40.3*	*42.2*	*42.0*	*46.7*	*48.7*	*52.9*
0.51 v	92.0	93.7	92.1	94.2	93.9	92.6	95.2	92.2
0.58 r	*78.0*	*79.6*	*74.6*	*74.4*	*73.0*	*73.6*	*78.5*	*79.5*
0.64 r [2])	*58.1*	*60.5*	*57.6*	*58.3*	*58.0*	*59.6*	*61.1*	*63.0*
0.74 r	*75.8*	*77.1*	*73.8*	*73.0*	*70.7*	*74.6*	*75.4*	*79.5*
0.77 v	*90.3*	*90.5*	*87.6*	*89.0*	*89.0*	*88.8*	*90.1*	*90.3*
Equiv. Width [3])	435	425	440	430	430	415	385	380

Table 11. **Fe 4143.9**

Corrected Central Intensities	5.7	6.9	6.4	6.9	6.2	7.7	8.5	9.2
0	9.5	11.0	10.8	11.8	11.4	13.3	14.4	15.8
0.034	11.8	13.5	13.9	14.0	14.9	17.0	18.8	20.3
0.068	19.2	20.4	21.8	22.7	23.1	26.2	29.1	31.8
0.10	25.6	27.3	28.5	29.5	31.0	36.1	38.8	44.5
0.14 v	33.6	33.9	33.8	35.1	36.4	41.9	46.0	51.1
r	33.6	34.9	34.9	36.5	37.5	42.4	46.4	53.2
0.17 v	42.0	41.3	39.8	39.5	42.3	46.5	50.5	56.4
r	40.4	40.8	39.4	39.5	41.1	46.0	51.0	57.1
0.20 v	48.2	47.2	46.0	45.0	46.8	50.2	54.7	59.9
r	*42.2*	*44.2*	*42.7*	*43.1*	*43.6*	*48.7*	*51.3*	*58.6*
0.27 v	*54.3*	*53.2*	*51.6*	*49.2*	*51.0*	*53.5*	*58.0*	*62.3*
r	62.0	61.2	58.0	56.3	56.4	59.4	63.0	69.8
0.31 v	*50.9*	*48.9*	*48.3*	*45.2*	*47.5*	*49.3*	*52.5*	*57.8*
0.34 v	*35.2*	*35.4*	*35.0*	*33.6*	*36.6*	*37.8*	*41.7*	*45.0*
r	70.5	69.3	67.3	64.7	64.4	66.4	69.2	73.0
0.45 r	82.5	81.7	80.7	77.5	76.0	78.0	77.7	84.0
0.46 v [4])	*17.1*	*18.3*	*19.5*	*18.8*	*20.5*	*22.6*	*24.8*	*29.3*
0.55 v	*61.9*	*60.5*	*58.0*	*56.7*	*58.1*	*59.7*	*63.0*	*69.8*
r	86.6	86.4	85.5	81.1	80.6	81.7	82.8	87.0
0.68 v	*82.0*	*79.4*	*79.0*	*76.0*	*76.1*	*77.2*	*80.4*	*83.5*
0.75 r	*92.1*	*87.0*	*90.5*	*85.2*	*84.8*	*86.0*	*86.6*	*89.9*
1.03 r	*93.5*	*92.2*	*92.2*	*86.5*	*86.9*	*88.4*	*89.0*	*97.7*
Equiv. Width	515	515	520	550	565	530	505	435
c [3])	0.04_5	0.05	0.05	0.06	0.06	0.05_5	0.05	0.04_5

[1]) Centre of 4132.540.
[2]) „ „ 4132.713.
[3]) Values unreliable.
[4]) Centre of Fe 4143.418.

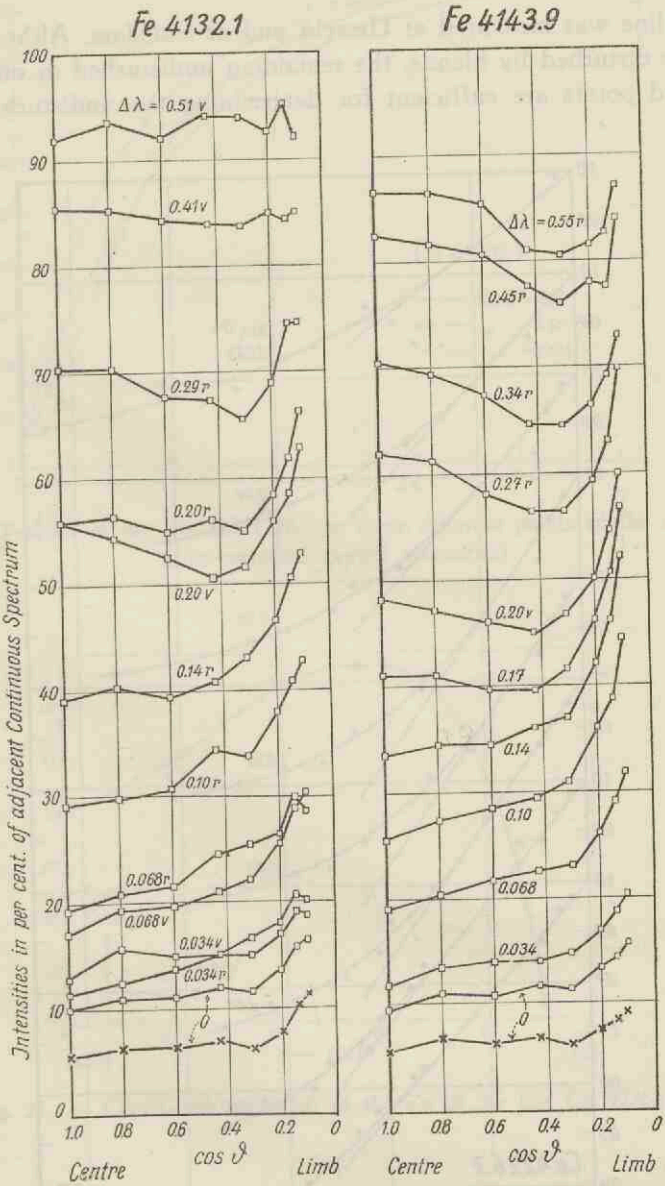

Fig. 18. — Centre-limb variations in the lines Fe 4132.1 and 4143.9; × corrected central intensities (parameter $\Delta\lambda$ = distance in A from centre of line).

§ 14. The line Ca 4226.7 (Table 12).

This line was measured at Utrecht and at Potsdam. Although rather strongly disturbed by blends, the remaining undisturbed or only slightly disturbed points are sufficient for determining the undisturbed profile.

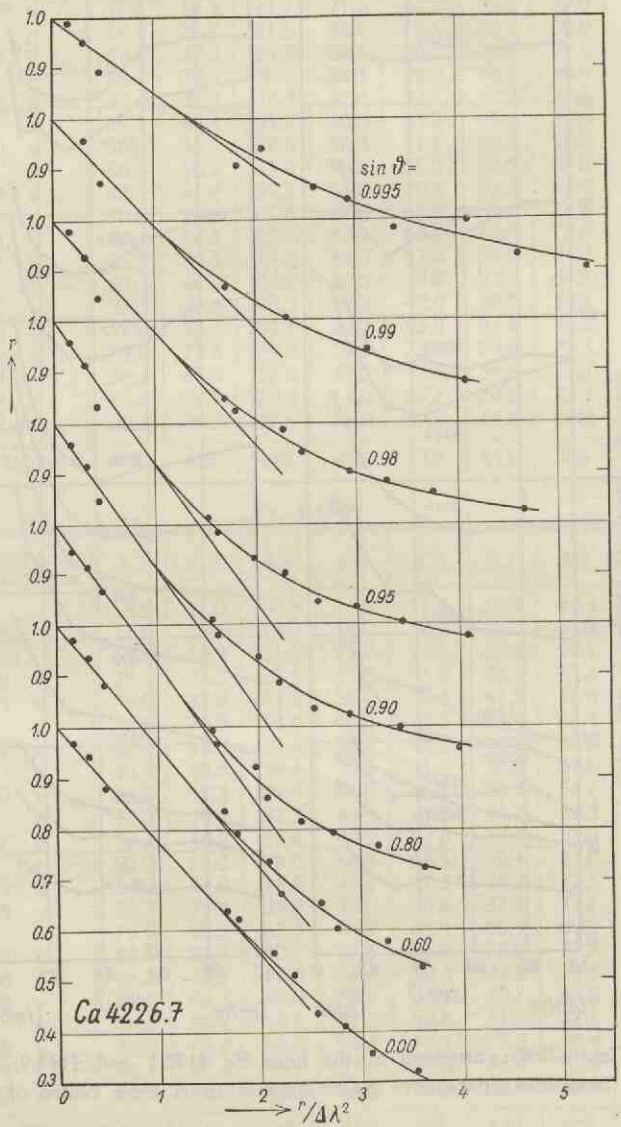

Fig. 19. — Determination of the c's of the line Ca 4226.7.

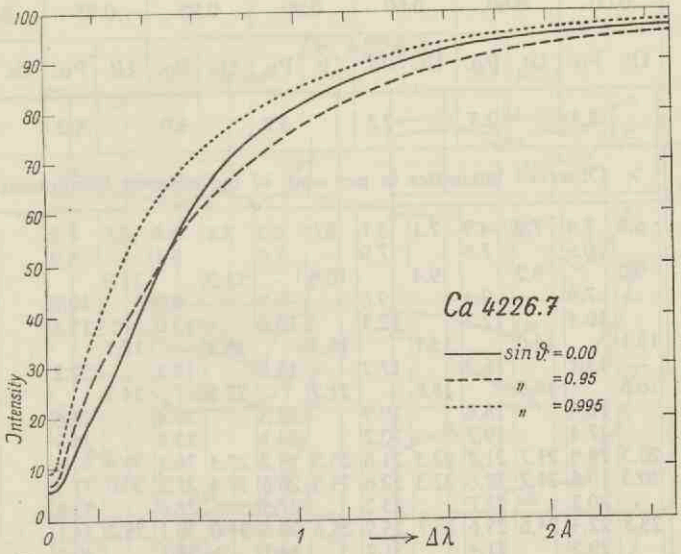

Fig. 20. — Profiles of the line Ca 4226.7 in three different points of the solar disc (non-corrected central intensities).

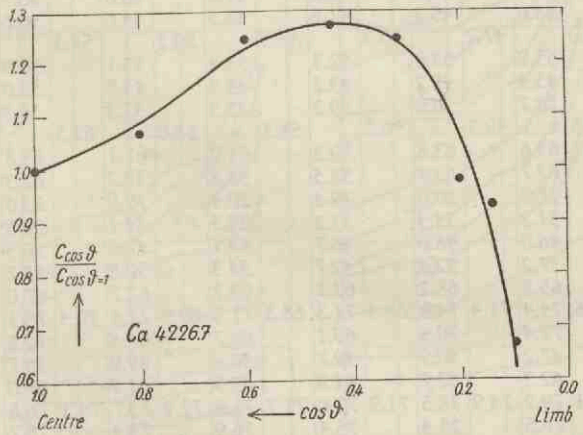

Fig. 21. — Centre-limb variation of the c's of the line Ca 4226.7.

As appears from the cross-section curves (Fig. 22) and a few profiles (Fig. 20) the centre-limb variations are very similar to those of the Fe multiplet and show likewise an increase of the wings for points lying excentrically on the sun's disc.

Table 12. **Ca 4226.7**

$\sin\vartheta = r/R$	0.00		0.60		0.80		0.90		0.95		0.98		0.99		0.995	
Observed at	Ut.	Po.	Ut.	Po.	Ut.	Po.	Ut.	Po.	Ut.	Po.	Ut.	Po.	Ut.	Po.	Ut.	Po.
Corrected Central Intensities		3.3		2.3		2.8		3.2		4.0		4.2		5.9		6.3
Distance from Line Centre in A	Observed Intensities in per cent. of the adjacent Continuous Spectrum															
0	6.8	5.4	7.0	4.9	7.1	5.7	8.0	6.2	8.1	6.8	8.6	7.2		8.4	10.3	9.3
0.034		6.5		7.5		7.9		7.6		8.1		8.9		8.9		10.3
0.042	9.0		9.2		9.4		10.9		11.3		11.9				14.3	
0.051		7.9		9.4		9.6		9.9		9.9		10.7		10.3		12.8
0.068		10.4		12.2		12.3		13.6		13.0		13.8		13.5		15.7
0.084	13.1		14.0		14.1		16.3		16.8		18.7				20.6	
0.10		14.1		16.2		17.2		18.8		19.2		21.2		21.6		24.4
0.13	16.8		18.0		18.6		21.2		22.5		24.5				29.0	
0.14 v		16.9		18.6		19.9		23.3		23.4		26.6		28.0		30.3
r		17.4		19.7		20.2		23.3		23.8		26.9		28.0		30.7
0.17 v	20.3	18.9	21.7	21.2	22.3	21.6	25.5	25.2	27.4	26.2	30.6	30.4		32.3	37.6	35.1
r	20.3	19.8	21.7	22.6	22.3	22.6	25.5	26.6	27.4	27.2	30.6	31.3		32.3	37.6	34.8
0.21 v		20.2		22.7		23.2		27.5		28.0		33.8		34.8		38.7
r	23.8	22.4	24.6	25.6	25.7	25.9	28.8	29.6	31.0	30.1	35.2	34.1		36.3	42.2	39.5
0.27 r		29.2		31.4		31.7		34.7		35.1		40.5		42.7		47.4
0.30 r	32.1		32.4		32.5		35.7		37.5		42.5				50.3	
0.31 v [1]		*18.2*		*20.2*		*21.0*		*24.8*		*24.6*		*29.9*		*32.2*		*35.0*
0.34 v		*26.5*		*27.4*		*28.4*		*31.2*		*32.5*		*37.5*		*40.6*		*43.9*
r		36.0		38.0		36.8		39.9		40.5		46.1		48.2		52.9
0.38 r	40.8		40.0		39.9		42.2		43.5		48.8				59.7	
0.41 v		*35.6*		*39.8*		*38.0*		*41.0*		*40.8*		*46.7*		*48.8*		*54.6*
r		43.6		45.2		41.6		43.5		44.6		50.6		54.1		58.3
0.47 v	51.0		47.2		46.2		48.5		50.2		54.3				63.9	
0.51 v		55.2		53.8		52.3		53.4		53.1		58.9		60.4		66.5
r		*45.4*		*48.2*		*43.2*		*45.3*		*45.7*		*52.0*		*54.7*		*60.2*
0.58 r [2]		*28.7*		*30.0*		*29.2*		*32.3*		*33.3*		*38.3*		*41.5*		*45.1*
0.59 v	62.3		59.2		56.7		58.1		58.6		62.5				74.2	
0.62 v		63.6		63.8		59.3		61.0		61.1		64.8		66.5		70.9
0.68 v		*62.7*		*62.8*		*58.5*		*58.8*		*59.2*		*62.3*		*64.8*		*67.0*
0.70 r [3]		*17.7*		*20.0*		*19.4*		*20.4*		*19.9*		*23.0*		*25.3*		*28.8*
0.78 v [4]		*31.2*		*33.3*		*33.2*		*35.5*		*34.1*		*38.8*		*40.3*		*44.3*
0.79 r		*46.0*		*48.0*		*46.7*		*48.1*		*47.6*		*50.5*		*55.9*		*59.1*
0.82 v		*57.2*		*52.8*		*52.7*		*54.3*		*50.8*		*55.7*		*57.6*		*62.2*
0.86 r		65.8		68.2		62.1		63.2		62.7		67.0		69.3		73.6
0.91 v	74.6	74.4	71.4	74.9	68.4	71.3	68.3	71.9	69.5	71.4	70.4	75.1		75.5	80.3	79.1
0.94 r		*71.4*		*70.4*		*69.1*		*66.7*		*66.8*		*70.8*		*72.8*		*78.5*
1.02 v [5]		*47.2*		*50.9*		*49.7*		*50.9*		*49.9*		*55.7*		*56.1*		*61.2*
r [6]		*62.3*		*62.7*		*64.9*		*63.9*		*61.9*		*69.0*		*71.0*		*79.9*
1.10 r	77.4	79.2	74.9	78.5	71.9	77.0	71.7	75.4	72.2	73.7	74.1	76.8		78.9	83.4	83.5
1.13 v		78.5		78.4		75.4		76.9		73.4		78.7		78.9		82.8
1.20 r [7]		*53.4*		*53.4*		*56.1*		*54.9*		*55.1*		*58.3*		*64.9*		*66.5*
1.28 v [8]		*26.2*		*26.8*		*29.5*		*30.2*		*29.3*		*33.0*		*35.8*		*39.1*
1.37 r		88.1		88.0		86.9		84.7		83.2		84.5		87.3		89.4
1.71 v	92.1	92.9	89.2	91.5	87.7	91.2	88.9	92.1	89.3	89.5	88.2	92.9		93.1	95.2	93.0
r		95.4		96.3		95.4		93.8		92.6		94.9		94.7		96.5
1.77 r	93.6		91.3		88.9		89.8		90.4		90.8				94.2	
2.41 r	97.0		97.3		94.6		95.9		95.6		97.7				99.3	
Equiv. Width	1430		1440		1540		1525		1530		1400		1280		1155	
c	0.22_5		0.24		0.28		0.28_5		0.28		0.22		0.21		0.15	

[1]) Centre of Fe 4226.433. [4]) Centre of Fe 4225.964. [7]) Centre of 4227.946.
[2]) Blend —Ti^+ 4227.317. [5]) „ „ Fe 4225.717. [8]) „ „ Fe 4225.463.
[3]) Centre of Fe 4227.442. [6]) „ „ Ce^+Zr 4227.760.

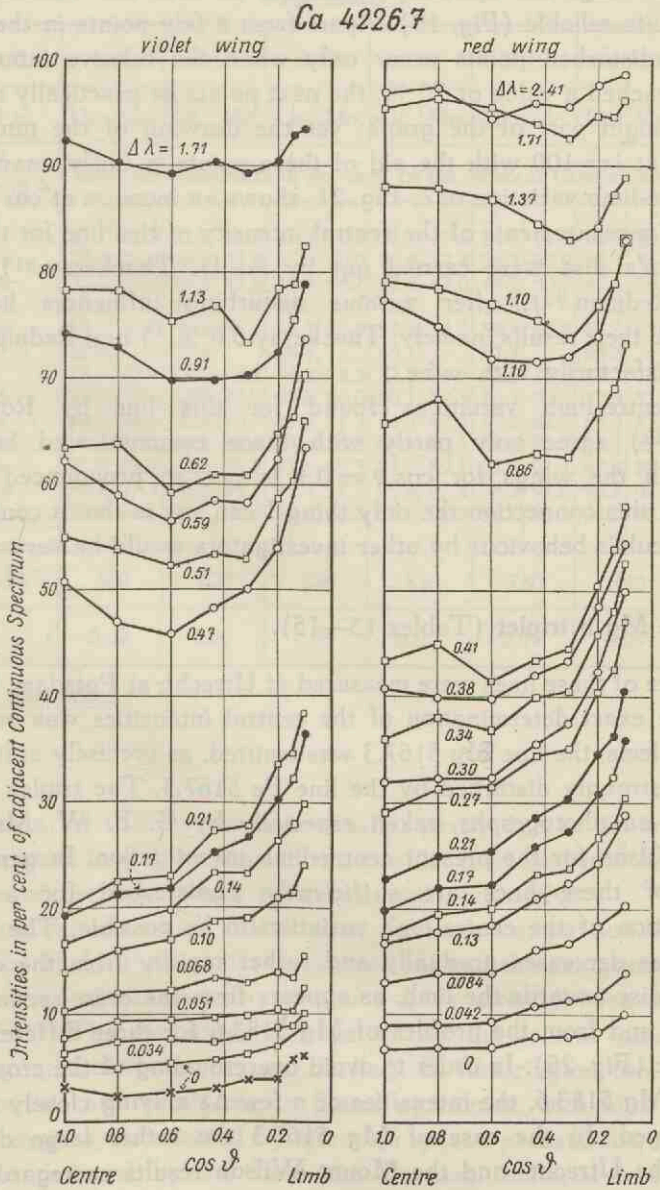

Fig. 22. — Centre-limb variations in the line Ca 4226.7; ○ Utrecht; □ Potsdam; ● mean; × corrected central intensities (parameter $\Delta\lambda$ = distance in A from centre of line).

The far wings are seriously disturbed, so that the c-determinations are not quite reliable (Fig. 19). Apart from a few points in the extreme wings, undisturbed points occur only when the relative intensity has already reached a value of 70 %, the next points lie practically no longer in the straight part of the graph; yet the drawing of the tangent line in the point $i = 100$ with the aid of these points is fairly unambiguous. The centre-limb variation of c, Fig. 21, shows an increase at $\cos \vartheta = 0.4$.

Careful measurements of the central intensity of this line for the centre of the sun's disc were carried out by A. D. Thackeray [31]) and by R. O. Redman [32]), after various disturbing influences had been eliminated; their results, namely: Thackeray 3.6 % *) and Redman 2.0 %, agree satisfactorily with mine.

The centre-limb variations found for this line by Royds and Narayan [12]) agree only partly with those communicated here. The increase in the wings for $\cos \vartheta = 0.4$ is not so pronounced in their results. In this connection the only thing I can say is that a confirmation of this peculair behaviour by other investigators would be very welcome.

§ 15. The Mg b triplet (Tables 13—15).

All three of these lines were measured at Utrecht; at Potsdam, however, where the exact determination of the central intensities was one of the chief problems, the line Mg 5167.3 was omitted, as precisely at its central part it is strongly disturbed by the line Fe 5167.5. The triplet was also measured on photographs, taken especially by G. F. W. Mulders at Mount Wilson for the present centre-limb investigation. In general, the profiles of these lines are sufficiently undisturbed for a reliable determination of the centre-limb variation to be possible. The intensity of the lines decreases gradually and rather rapidly from the centre of the sun's disc towards the limb, as appears from the cross-section curves (Fig. 23) and from the profiles of Mg 5183.6 for three different points of the disc (Fig. 25). In order to avoid overcrowding of the cross-section figure of Mg 5183.6, the intensities of a few $\Delta\lambda$'s, lying closely together, are averaged. In the case of Mg 5167.3 the rather large difference between the Utrecht- and the Mount Wilson results as regards the r's

*) The value found by Thackeray is not yet corrected for the instrumental curve; according to him this correction amounts to 0.5 %. In this connection, one should read Redman's article, from which one can form some idea of the uncertainties interfering with the determination of central intensities.

Table 13. **Mg 5167.3**

$\sin \vartheta = r/R$	0.00		0.60		0.80		0.90		0.95		0.98		0.995	
Observed at	Ut.	Mo.	Ut.	Mo.	Ut.	Mo.	Ut.	Mo.	Ut.	Mo.	Ut.	Mo.	Ut.	Mo.
Distance from Line Centre in A	Observed Intensities in per cent. of the adjacent Continuous Spectrum													
0	21.1	12.0	23.0	16.3	21.5	16.6	22.8	18.0	24.5	19.4	21.7	20.5	25.7	23.7
0.084 v	23.9	24.6	28.3	28.5	25.0	30.0	26.6	32.7	28.7	33.9	25.4	35.7	29.2	37.6
0.17 v	35.8	35.5	39.5	42.6	39.4	44.7	42.2	47.0	44.2	50.7	42.6	55.0	47.9	60.4
0.21 v	40.4		38.7		40.0		40.0		42.8		50.4		49.6	
0.29 v	51.9	52.0	55.2	55.3	55.3	56.2	57.1	58.7	59.4	60.8	63.9	68.3	68.9	71.9
0.34 r	*58.6*		*57.6*		*58.4*		*60.1*		*61.4*		*65.8*		*71.4*	
0.48	74.1	72.4	74.7	73.4	74.2	73.3	73.5	74.3	74.5	75.3	77.3	78.3	83.6	81.9
0.59 v	80.6	80.1	82.6	79.6	80.8	80.0	80.1	80.3	80.7	81.0	82.8	81.6	87.7	85.0
0.67 r	83.6	80.8	85.3	79.7	85.0	81.2	84.2	82.2	83.9	82 9	85.5	82.6	90.3	85.3
0.80 v	89.2	87.0	89.6	87.3	88.6	86.3	88.9	87.5	88.6	87.4	88.4	87.3	92.3	90.7
1.04 r	91.9	89.8	92.8	88.2	91.6	89.3	91.3	89.7	92.2	91.1	92.2	89.9	94.5	90.2
1.55 v	96.1	97.4	96.3	98.1	96.4	97.8	95.4	97.4	96.3	97.6	96.8	97.4	96.7	97.5
2.56 r	98.0	98.1	97.8	97.9	98.9	98.8	99.0	98.8	98.1	98.8	98.7	98.5	99.3	99.0
Equiv. Width [1]	860		820		830		810		780		740		640	
c [1]	0.09		0.09		0.09		0.09		0.09		0.09		0.06_5	

[1]) Values unreliable.

of the curves for 0.084 v, is, undoubtedly, partly due to the small error in $\Delta\lambda$, discussed in § 9, because in this profile, disturbed into asymmetry, the centre of the line cannot be determined accurately.

The observations which call first of all for a comparison with mine are those by H. H. Plaskett [8]); the agreement and the deviations between the two series of centre-limb variations have already been mentioned elsewhere [17]). The deviations concern chiefly the central intensities on the photographs of the points near the limb. E. Cherrington, too, measured these lines [10]); his results are in better agreement with mine [17]). The central intensities, determined by him with special precautions, are larger than those deduced by me from the Potsdam material and show a slightly stronger increase towards the limb, as far as this can be concluded from the two points on the sun's disc selected by him. Cherrington's measurements, as well as mine, make it likely, that the central intensities of the various lines of the triplet are nearly equal; this was also found by M. Minnaert and G. F. W. Mulders [43]) and C. W. Allen [40]).

Table 14. **Mg 5172.7**

$\sin\vartheta = r/R$	0.00			0.60			0.80			0.90		
Observed at	Ut.	Mo.	Po.	Ut.	Mo.	Po.	Ut.	Mo.	Po.	Ut.	Mo.	Po.
Corrected Central Intensities			5.5			5.5			6.9			8.6
Distance from Line Centre in A	Observed Intensities in per cent. of the adjacent Continuous Spectrum											
0	18.0	11.7	9.3	19.6	14.4	9.6	19.1	14.7	10.9	19.4	15.8	12.6
0.034			11.4			11.2			12.6			14.1
0.068			16.1			16.5			18.2			18.5
0.084	23.7	19.3		25.7	24.6		25.6	25.2		26.8	26.0	
0.10			21.9			23.2			25.5			25.3
0.14			25.8			27.6			30.7			30.4
0.17	32.3	27.5		34.4	34.1		35.5	37.2		38.2	39.2	
0.20			31.8			33.6			36.6			38.6
0.27 v			36.8			40.5			41.3			43.6
r			37.0			39.1			40.9			44.8
0.29 v	41.2	35.4		43.9	43.3		45.7	45.2		47.5	46.0	
r	42.0	35.4		43.9	43.3		46.0	45.2		48.1	46.0	
0.34 v			41.7			43.0			46.0			47.5
r			41.9			44.2			46.1			49.8
0.40 v			46.9			48.3			50.6			52.7
r			48.0			48.6			50.4			53.6
0.42 v	49.3	45.7		51.7	50.6		52.0	53.1		55.0	53.6	
r	50.6	45.7		52.0	50.6		53.3	53.1		55.9	53.6	
0.54 v			58.4			59.0			58.1			60.6
r			59.1			59.1			59.0			62.1
0.59 v	61.8	57.4		62.1	61.3		62.8	63.3		63.9	62.0	
r	62.8	57.6		62.7	61.9		63.8	63.7		64.7	64.1	
0.67 v			67.7			67.2			67.8			68.4
r			68.5			67.3			67.5			69.6
0.75 v	72.5	68.7		71.8	69.2		70.6	70.7		71.6	70.3	
r	73.0	68.7		72.2	69.2		72.9	70.7		72.0	70.3	
0.88 v			*74.1*			*73.8*			*73.0*			*74.0*
r			78.4			78.0			76.0			76.4
1.35 r			88.3			87.6			88.4			88.7
1.47 v	89.3	89.1	90.4	91.0	89.7	89.5	88.3	89.8	89.7	87.7	88.3	89.2
r	90.9	89.1		90.1	89.7		90.1	89.8		89.4	88.3	
2.02 r			95.1			95.3			96.2			95.2
2.09 r	95.5	95.4		94.5	95.9		96.0	95.9		95.6	95.2	
2.70 v	97.5	93.5	96.8	95.2	95.2	96.3	97.7	94.8	96.5	96.7	94.5	96.5
2.88 r	98.1	97.3	98.4	98.2	98.6	97.7	98.0	98.8	97.8	97.4	98.0	97.8
Equiv. Width	1405			1375			1375			1375		
c	0.23_6			0.24			0.24			0.25		

Table 14 (continued). **Mg 5172.7**

$\sin\vartheta = r/R$	0.95			0.98			0.99			0.99_5		
Observed at	Ut.	Mo.	Po.	Ut.	Mo.	Po.	Ut.	Mo.	Po.	Ut.	Mo.	Po.
Corrected Central Intensities			7.7			8.0			9.5			12.0
Distance from Line Centre in A	Observed Intensities in per cent. of the adjacent Continuous Spectrum											
0	21.1	17.0	12.6	18.4	18.9	13.3			14.4	22.4	21.5	16.4
0.034			14.3			15.2			16.2			17.1
0.068			19.3			20.8			20.6			22.3
0.084	28.6	27.6		28.2	28.2					30.9	33.0	
0.10			28.1			29.2			30.9			30.3
0.14			35.4			38.8			40.8			42.0
0.17	40.4	41.6		44.2	46.4					49.1	51.7	
0.20			43.0			47.5			51.7			54.4
0.27 v			47.6			52.3			58.2			61.2
r			47.2			51.9			57.5			60.7
0.29 v	50.8	50.5		56.3	54.4					62.4	62.4	
r	51.7	50.5		55.8	56.8					62.4	62.4	
0.34 v			51.5			56.4			62.5			65.3
r			52.1			56.1			62.2			64.5
0.40 v			55.2			60.0			64.8			68.1
r			55.9			59.9			64.2			67.9
0.42 v	58.9	57.6		60.4	63.1					69.4	68.7	
r	58.5	57.6		62.6	63.1					69.8	68.7	
0.54 v			63.1			66.9			71.6			73.1
r			63.6			67.4			71.5			75.0
0.59 v	66.9	65.0		70.2	68.2					76.5	74.8	
r	67.1	65.6		70.3	69.1					76.6	74.5	
0.67 v			69.1			72.0			76.5			77.7
r			69.5			72.8			76.7			78.8
0.75 v	71.2	72.0		76.6	74.6					80.6	79.6	
r	70.7	72.0		75.8	74.6					81.6	80.6	
0.88 v			*75.0*			*76.5*			*80.2*			*81.8*
r			75.0			78.8			82.4			83.6
1.35 r			87.0			88.3			91.0			91.8
1.47 v	87.9	89.2	89.3	89.1	90.4	88.9			91.6	90.7	92.1	92.7
r	89.9	89.2		90.1	90.4					92.0	92.1	
2.02 r			94.5			94.5			97.0			97.9
2.09 r	95.7	95.0		95.5	95.2					96.5	94.5	
2.70 v	97.5	94.7	95.7	97.0	95.4	96.4			96.7	98.4	96.6	97.4
2.88 r	97.8	97.6	96.6	97.5	98.1	96.4			97.4	98.8	99.0	97.5
Equiv. Width	1355			1245			1070			1000		
c	0.26			0.23_5			0.18			0.16_5		

Table 15. **Mg 5183.6**

$\sin\vartheta = r/R$	0.00			0.60			0.80			0.90		
Observed at	Ut.	Mo.	Po.	Ut.	Mo.	Po.	Ut.	Mo.	Po.	Ut.	Mo.	Po.
Corrected Central Intensities			5.9			6.1			7.6			7.6
Distance from Line Centre in A	Observed Intensities in per cent. of the adjacent Continuous Spectrum											
0	15.7	10.7	9.1	17.7	12.2	9.9	18.0	12.8	10.9	17.9	13.8	11.5
0.034			10.3			11.2			11.9			12.9
0.050			11.6			13.0			14.3			15.0
0.067			14.6			15.5			16.5			17.7
0.084	21.4	17.3	17.0	24.0	21.6	18.4	24.2	22.2	19.6	25.6	24.0	20.0
0.10			19.8			21.4			21.8			24.5
0.13			22.9			24.9			27.0			30.8
0.17	29.4	25.7		33.6	31.4		33.6	33.8		37.0	36.2	
0.20			29.8			30.3			33.3			37.0
0.27			31.1			34.2			36.6			41.0
0.29	37.9	32.3		41.2	38.4		41.7	40.4		45.8	43.3	
0.34			34.1			36.8			40.6			44.2
0.41 v	43.5	37.4	40.4	46.7	43.8	42.6	48.9	46.5	44.1	51.1	49.6	47.5
r	44.8	39.4	40.4	48.0	43.8	42.6	49.3	47.8	44.1	52.6	49.2	47.5
0.54 v			47.5			50.5			51.0			54.0
0.62 v	56.0	51.0		57.7	54.9		58.8	57.0		60.1	58.7	
0.68 v			56.6			58.4			58.4			60.5
0.81			64.6			65.0			64.8			66.0
0.83 v	65.3	63.4		66.5	64.0		66.7	66.1		67.1	67.3	
0.94 v			69.2			69.3			70.3			71.0
1.08 v	75.8	74.6	74.7	75.4	73.4	75.2	75.2	75.0	75.2	75.1	76.5	76.0
r			74.7			75.2			75.2			76.0
1.35			83.8			83.7			82.7			83.5
1.45 v	84.4	84.6		85.2	83.6		83.7	84.1		83.6	84.5	
r	85.5	85.9		86.5	83.8		84.2	85.0		84.6	84.5	
1.62 r			88.4			88.6			87.6			88.0
1.90 r	91.0	91.1	91.5	91.4	89.8	91.1	90.9	90.4	91.6	91.0	90.8	91.5
2.02			92.5			92.4			92.1			92.5
2.58 r	94.8	94.3	95.0	95.3	93.2	94.5	95.0	94.8	95.0	95.2	93.9	95.0
2.70 v			94.0			94.0			94.5			95.0
2.90 v	95.7	96.1		94.5	94.7		94.2	95.7		94.7	96.4	
Equiv. Width	1770			1750			1710			1660		
c	0.37			0.38			0.37_5			0.37_5		

Table 15 (continued). **Mg 5183.6**

$\sin\vartheta = r/R$	0.95			0.98			0,99			0.995		
Observed at	Ut.	Mo.	Po.	Ut.	Mo.	Po.	Ut.	Mo.	Po.	Ut.	Mo.	Po.
Corrected Central Intensities			6.9			7.9			10.4			12.9
Distance from Line Centre in A	Observed Intensities in per cent. of the adjacent Continuous Spectrum											
0	19.4	16.2	11.1	19.0	17.8	12.6			14.8	22.2	22.4	16.8
0.034			12.6			14.1			16.4			17.6
0.050			14.6			16.0			17.9			18.6
0.067			17.2			19.1			20.2			20.6
0.084	27.9	24.7	21.2	26.9	26.6	22.0			23.0	28.4	27.8	23.5
0.10			24.7			27.2			27.3			28.6
0.13			32.6			36.2			37.9			39.7
0.17	40.7	38.0		42.2	43.7					45.2	49.8	
0.20			40.2			46.2			50.3			53.3
0.27			44.9			51.3			55.9			60.3
0.29	50.1	47.2		53.9	53.6					60.8	59.3	
0.34			49.0			55.3			60.1			63.8
0.41 v	55.2	52.6	52.3	59.2	58.8	57.8			63.1	68.3	64.3	66.8
r	56.6	52.9	52.3	60.2	59.0	57.8			63.1	67.5	65.1	66.8
0.54 v			58.1			64.3			68.7			71.9
0.62 v	63.0	61.2		66.7	66.4					74.6	72.7	
0.68 v			63.1			69.3			72.7			75.4
0.81			68.7			73.4			76.8			79.4
0.83 v	69.3	69.1		72.7	73.0					78.7	77.9	
0.94 v			73.2			76.9			80.3			82.5
1.08 v	76.2	77.1	77.3	80.0	79.9	79.9			83.3	83.6	84.7	85.5
r			77.3			79.9			83.3			85.5
1.35			83.8			85.4			87.9			89.4
1.45 v	84.8	84.8		85.1	87.5					88.5	89.7	
r	86.2	85.6		86.2	86.7					89.0	90.4	
1.62 r			88.4			88.9			90.9			92.5
1.90 r	91.5	91.1	91.9	92.6	92.3	92.5			93.0	94.5	93.8	94.5
2.02			91.9			92.5			92.9			95.0
2.58 r	94.2	94.4	94.9	96.6	96.1	96.0			96.0	97.5	96.0	98.0
2.70 v			96.0			95.5			96.5			97.0
2.90 v	95.2	96.0		94.6	96.4					95.3	97.7	
Equiv. Width	1580			1415			1255			1145		
c	0.35			0.31			0.26			0.22_5		

	Corrected Central Intensities in per cent.			
	Mg 5172.7		Mg 5183.6	
sin ϑ	0.00	0.95	0.00	0.95
Cherrington	10	14	9	15
this thesis [1])	6	8	6	8

[1]) These intensities were read from Fig. 23 taking the whole of the centre-limb variation into account.

The two stronger lines were measured by G. Righini [9]) in 6 points of the sun's disc; generally speaking, the centre-limb variations are of the same nature as those found by me. It is, however, impossible to deduce finer details from his publication. A comparison of the equivalent widths (in A units), obtained by him and by me, is given in the following table:

sin ϑ = r/R		0.00	0.60	0.66	0.80	0.90	0.91	0.95	0.97	0.98	0.99	0.995	1.00
Mg 5173	Righini	1.34		1.09			1.31		1.05	0.98			0.74
	this thesis	1.41	1.37		1.38	1.38		1.36		1.24	1.07	1.00	
Mg 5184	Righini	1.58		1.44			1.48		1.23	1.19			0.86
	this thesis	1.77	1.75		1.71	1.66		1.58		1.42	1.25	1.15	

The quantities c were deduced by A. Unsöld from the Plaskett and Cherrington profiles [44]); his results do not agree with mine, although the centre-limb variations in the wings obtained by these two observers do not differ so pronouncedly from mine. The differences between Unsöld's results and mine are chiefly due to the manner in which the straight lines are drawn in the $i_0 - i$ versus $i/\Delta\lambda^2$-diagram. Unsöld draws these lines so as to fit as closely as possible the measured points between $i = 100$ % and $i = 70$ %, whereas I have always consistently tried to determine as well as possible the tangent in the point $i = 100$ % as the straight line. This makes, in particular for the centre-limb variation, some difference, because the curvature of the $i_0 - i$ versus $i/\Delta\lambda^2$-graph is appreciably larger for points near the limb than for the centre of the sun's disc. Fig. 24 shows the determination of the c's in the latter of the two ways. Their ratio deviates to some extent from the muliplet ratio. This may be due to the fact that the straight lines for the c's were

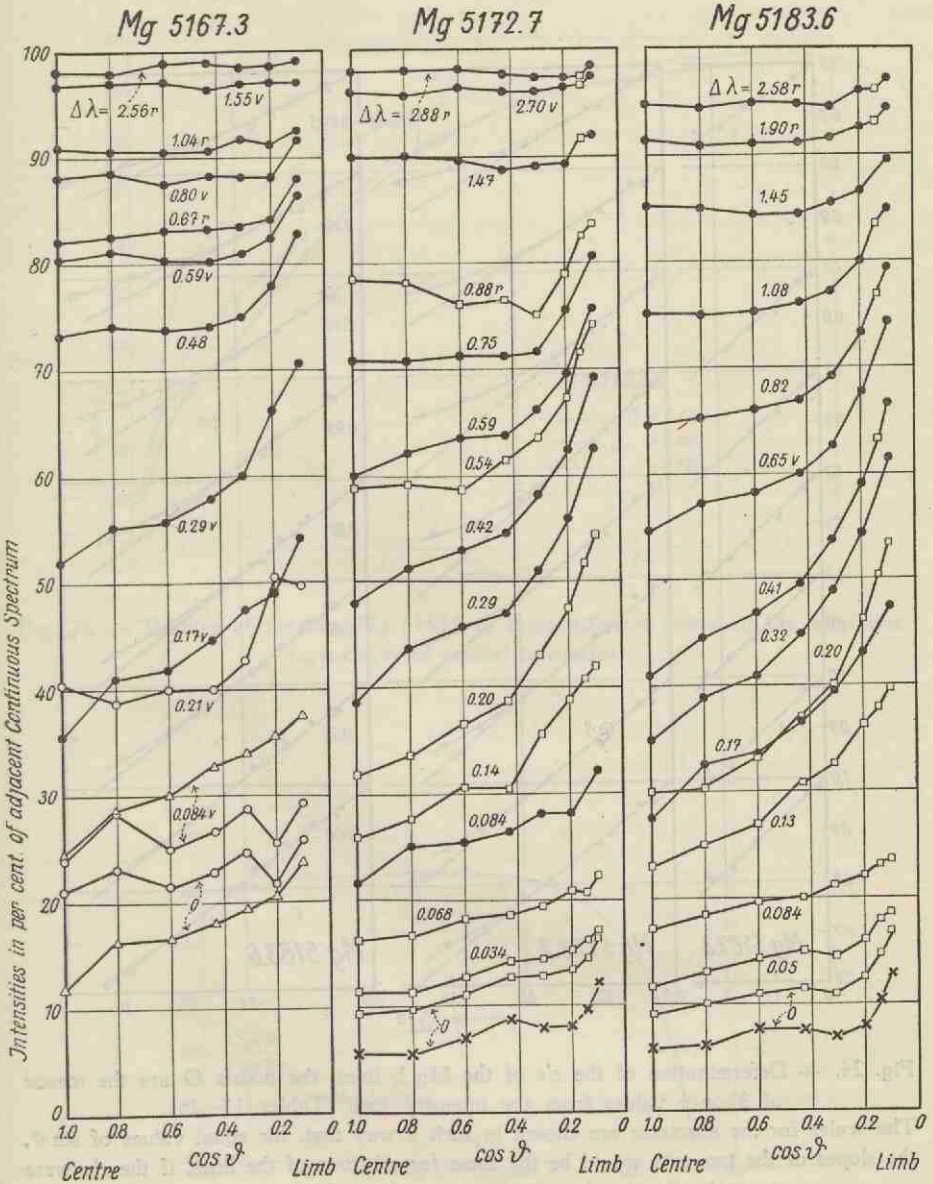

Fig. 23. — Centre-limb variations in the lines Mg 5167.3, Mg 5172.7 and Mg 5183.6; ○ Utrecht; △ Mount Wilson; □ Potsdam; ● mean of at least two of these; × corrected Potsdam central intensities (parameter $\Delta\lambda$ = distance in A from centre of line).

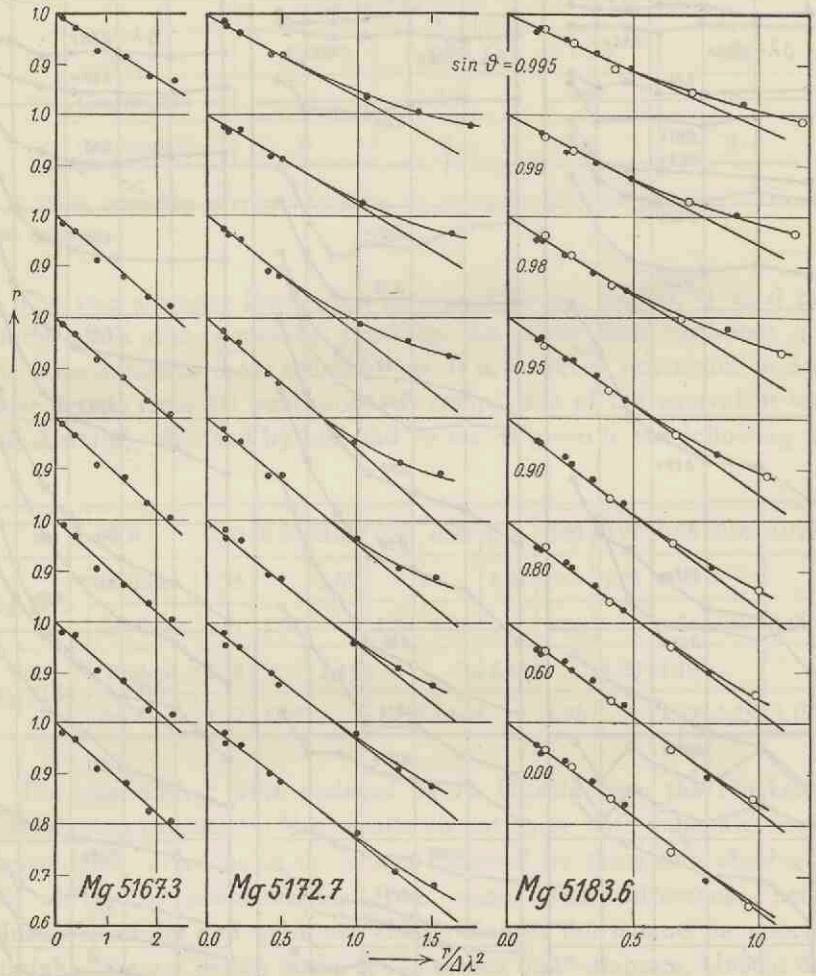

Fig. 24. — Determination of the c's of the Mg b lines; the points O are the means of 3 or 4 values from the intensity lists (Tables 13—15).
The scales for the abscissae are chosen in such a way that, for equal values of sin ϑ, the slopes of the tangents would be the same for all three of the lines, if the c's were to each other in the same ratio as the multiplet intensities.

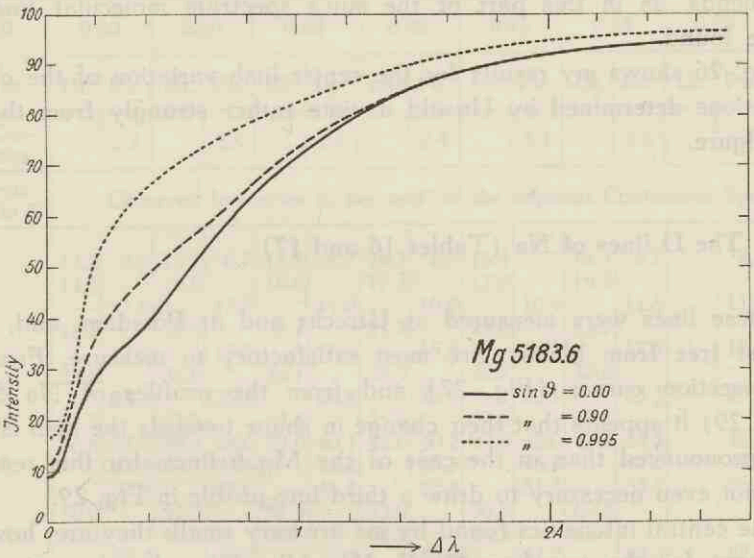

Fig. 25. — Profiles of the line Mg 5183.6 in three different points of the solar disc (non-corrected central intensities).

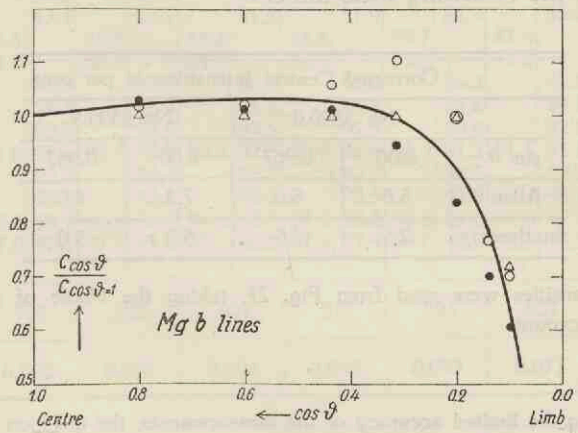

Fig. 26. — Centre-limb variations of the c's of the Mg b lines; ● Mg 5183.6; ○ Mg 5172.7; △ Mg 5167.3.

determined for the two weaker lines from points still slightly disturbed by blends, as in this part of the sun's spectrum molecular lines are to be found.

Fig. 26 shows my results for the centre-limb variation of the c's; the variations determined by Unsöld deviate rather strongly from those in the figure.

§ 16. The D lines of Na (Tables 16 and 17).

These lines were measured at Utrecht and at Potsdam, and, being almost free from blends, are most satisfactory to measure. From the cross-section curves (Fig. 27) and from the profiles of Na 5890.0 (Fig. 29) it appears that their change in shape towards the limb is much less pronounced than in the case of the Mg b lines; for this reason it was not even necessary to draw a third line-profile in Fig. 29.

The central intensities found by me are very small; they are, however, different for the two lines *). C. W. Allen [18], who determined the profiles of the D lines for the centre and the limb of the sun's disc, and who also applied a correction, though in a manner different from the one applied here, for the finite resolving power of the spectrograph, obtained results for the central intensities, which differ from mine, as appears from the following little table:

	Corrected Central Intensities in per cent.			
	Na 5890.0		Na 5895.9	
sin ϑ	0.00	0.967	0.00	0.967
Allen	6.6	6.0	7.2	6.0
this thesis[1])	2.5	3.5	5.0	5.0

[1]) These intensities were read from Fig. 27, taking the whole of the centre-limb variation into account.

*) Considering the limited accuracy of the measurements, the question arises whether this difference is real. From an examination, however, of the registrograms of the continuum-photographs, taken simultaneously of the D lines of Na and on others taken simultaneously of the lines Mg 5172.7 and Mg 5183.6, it appears at once that, independently of any photometric errors, there is a difference in this respect between the two pairs of lines.

Table 16. **Na 5890.0**

$\sin\vartheta = r/R$	0.00		0.60		0.80		0.90		0.95		0.98		0.99		0.995	
Observed at	Ut.	Po.	Ut.	Po.	Ut.	Po.	Ut.	Po.	Ut.	Po.	Ut.	Po.	Ut.	Po.	Ut.	Po.
Corrected Central Intensities		2.8		2.5		1.1		2.4		3.4		4.6		4.8		4.4
Distance from Line Centre in A	Observed Intensities in per cent. of the adjacent Continuous Spectrum															
0	13.2	7.0	15.2	6.7	15.5	5.7	16.3	6.7	16.8	7.5	18.3	8.7		8.9	20.6	8.7
0.041	14.3		16.6		16.6		17.2		17.9		19.3				22.2	
0.067		11.3		11.0		11.0		10.9		10.4		11.8		11.9		12.7
0.082	18.7		20.4		20.2		21.3		22.0		23.9				26.2	
0.10		17.5		17.5		17.3		15.9		16.5		17.9		17.3		16.9
0.12	24.6		26.0		26.1		28.9		29.7		30.8				32.6	
0.13		23.4		25.2		26.8		25.7		25.1		25.3		25.2		24.3
0.16	31.2		33.1		33.1		35.8		37.6		38.8				41.7	
0.20	36.8	38.1	38.4	38.0	39.0	40.1	42.0	40.2	43.9	42.0	47.1	45.8		46.3	50.1	46.9
0.27 v		*41.8*		*42.6*		*45.2*		*46.9*		*45.2*		*49.0*		*49.7*		*51.5*
r		47.8		47.0		48.8		50.4		51.1		55.7		56.8		58.6
0.29 r	50.0		51.3		51.5		53.9		56.0		60.8				63.9	
0.37 r	60.3		61.0		62.0		63.2		64.3		68.7				73.1	
0.40 v		*59.4*		*54.4*		*55.1*		*54.2*		*61.7*		*65.3*		*67.6*		*65.6*
r		65.9		64.4		64.0		65.3		67.0		70.5		71.8		72.6
0.45 v	66.0		66.0		66.3		66.9		68.4		72.6				74.3	
r	68.1		68.4		68.1		70.1		71.4		74.5				78.2	
0.53 v	75.0	75.4	75.0	73.6	74.4	72.7	74.7	72.6	76.0	75.5	78.8	77.1		79.6	82.0	79.9
r		75.9		74.7		75.3		73.1		74.7		79.0		77.7		80.5
0.61 v	81.0		80.2		79.6		80.8		81.5		83.0				85.6	
r	79.2		78.5		78.5		80.3		81.1		82.2				84.8	
0.67 v		84.2		81.6		82.5		82.3		82.4		87.3		85.2		87.0
r		83.1		82.2		81.5		81.9		82.3		85.9		85.2		85.8
0.74 v	85.5		85.2		85.1		85.5		85.7		87.4				90.1	
r	84.2		83.5		84.2		84.3		85.0		87.0				87.6	
0.80 v		88.3		88.7		86.8		86.2		86.2		89.8		88.4		89.2
r		87.3		86.9		86.8		86.3		84.8		89.1		88.6		87.9
0.99 v		93.0		92.9		92.5		91.8		89.8		92.3		91.9		93.0
r	91.0	92.6	90.5	92.5	90.5	92.5	90.9	91.8	91.2	91.2	91.5	94.7		93.4	93.1	93.7
1.33 v		93.9		93.4		93.9		92.2		94.5		93.2		93.7		93.3
r		93.4		92.1		92.2		92.5		93.5		94.7		93.9		94.2
1.73 v	96.4	98.2	96.4	99.9	97.5	98.7	97.5	98.8	97.3	97.6	97.0	97.8		99.9	99.6	99.0
2.07 r	97.0	97.1	97.0	96.6	97.7	96.6	97.9	97.4	98.0	98.0	98.3	98.5		97.6	98.6	97.6
Equiv. Width	906		921		927		917		891		807		814		758	
c	0.090		0.095		0.097		0.099		0.093		0.077		0.079		0.070	

Table 17. **Na 5895.9**

$\sin\vartheta = r/R$	0.00		0.60		0.80		0.90		0.95		0.98		0.99		0.995	
Observed at	Ut.	Po.	Ut.	Po.	Ut.	Po.	Ut.	Po.	Ut.	Po.	Ut.	Po.	Ut.	Po.	Ut.	Po.
Corrected Central Intensities		5.3		4.4		3.8		5.7		4.4		4.4		5.7		6.6
Distance from Line Centre in A	Observed Intensities in per cent. of the adjacent Continuous Spectrum															
0	18.2	10.8	19.1	10.1	18.7	9.9	21.0	11.3	20.9	10.1	22.2	10.5		11.2	25.0	12.1
0.033		11.6		11.5		11.4		12.0		11.3		11.3		12.3		12.8
0.041	20.2		20.9		21.3		23.0		22.6		24.4				26.9	
0.067		16.6		16.4		15.6		16.2		15.2		15.6		15.0		15.6
0.082	25.7		26.4		26.9		28.9		29.0		30.0				32.0	
0.10		24.9		26.3		24.5		24.5		23.7		24.1		22.9		24.3
0.12	34.2		34.2		34.4		37.2		38.2		39.8				40.8	
0.13		35.0		36.2		36.7		36.3		36.5		37.5		37.2		37.8
0.16 v	43.0	43.0	42.3	43.6	43.8	45.9	45.8	46.2	47.1	48.6	50.5	50.7		50.5	51.2	52.7
r	42.5	43.0	43.0	43.3	44.0	45.6	46.2	44.3	47 7	46.3	51.4	48.6		50.3	52.5	51.9
0.20 v	51.5	49.2	50.3	49.7	51.7	51.4	54.7	52.6	56.3	55.0	60.0	58.2		59.7	60.6	61.3
r	51.0	49.1	50.6	51.0	51.7	50.5	53.9	51.2	55.6	53.0	59.8	55.6		58.8	61.2	59.8
0.27 v		60.5		60.1		60.2		62.4		65.9		66.9		67.1		72.4
r		61.2		60.7		60.2		60.2		63.3		65.6		66.9		71.2
0.29 v	65.1		64.0		64.0		65.9		67.8		71.7				74.0	
r	63.4		63.4		63.0		65.2		67.0		70.3				73.3	
0.33 v		70.9		68.3		68.5		70.1		72.7		73.0		74.0		78.1
r		67.1		66.8		65.7		66.5		68.9		72.8		73.8		77.2
0.37 v	76.1		73.8		73.1		73.3		75.0		79.3				82.8	
r	71.2		70.4		70.4		71.8		72.8		76.0				79.0	
0.40 v		76.8		74.9		73.9		77.0		78.3		79.0		80.8		83.8
0.42 r		*72.7*		*70.6*		*70.0*		*69.1*		*73.1*		*74.6*		*75.4*		*78.4*
0.49 v	84.5		84.0		83.2		83.1		84.5		85.9				89.5	
0.53 v		86.7		85.2		85.8		84.8		87.6		87.5		86.8		90.3
0.61 v	89.2		88.6		88.1		87.8		89.1		89.4				91.5	
0.67 v		90.8		89.7		90.7		89.2		90.2		87.6		88.9		90.9
0.73 r	*87.1*	*86.7*	*86.4*	*86.2*	*86.8*	*89.1*	*87.0*	*86.1*	*87.5*	*88.3*	*88.5*	*87.8*		*85.9*	*89.5*	*89.5*
1.12 r	*92.3*	*91.6*	*92.4*	*91.5*	*92.8*	*92.0*	*92.7*	*91.6*	*94.4*	*93.6*	*93.6*	*92.3*		*92.0*	*95.4*	*93.5*
1.21 v	96.6	96.7	95.8	95.4	96.6	96.6	96.0	97.1	96.8	97.1	96.5	97.5		96.6	98.0	97.8
1.73 r		*95.9*		*94.7*		*95.6*		*96.6*		*96.2*		*96.8*		*96.0*		*97.8*
2.02 v	99.6	98.7	99.6	99.9	99.7	98.9	99.2	99.1	99.3	98.4	99.7	98.6		99.4	—	99.2
2.66 r	99.0		98.8		99.6		99.5		99.8		100				99.8	
Equiv. Width	636		658		665		652		623		596		601		532	
c	0.045		0.049		0.050		0.049		0.043		0.040		0.039		0.030	

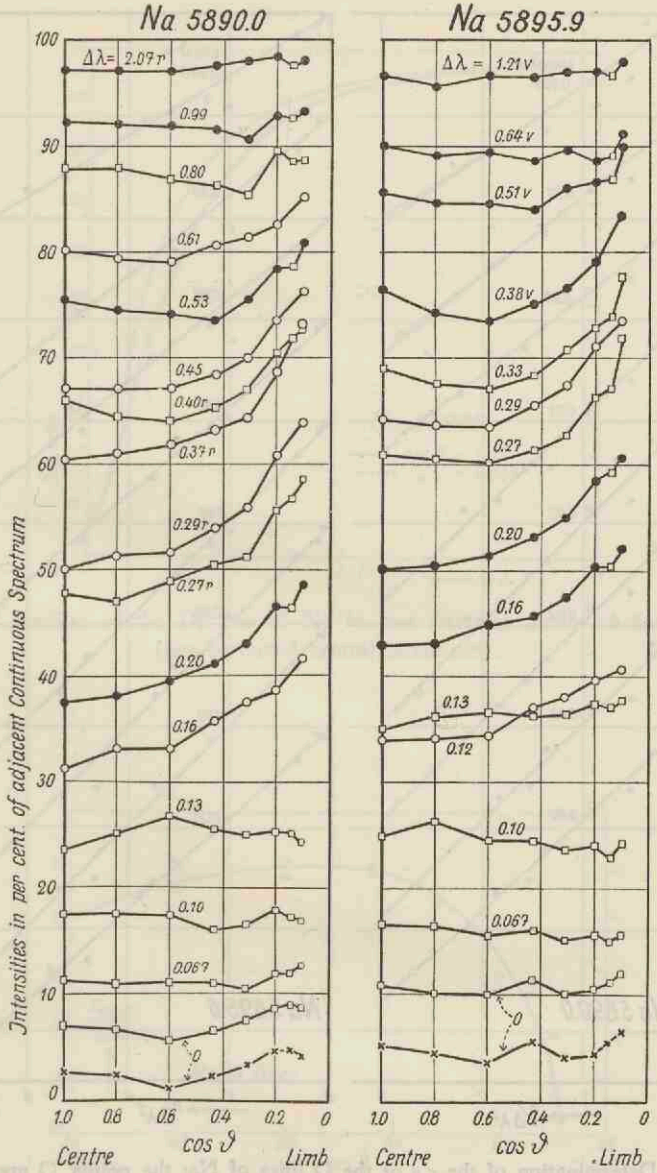

Fig. 27. — Centre-limb variations in the Na D lines; O Utrecht; □ Potsdam; ● mean; × corrected Potsdam central intensities (parameter $\Delta\lambda$ = distance in A from centre of line).

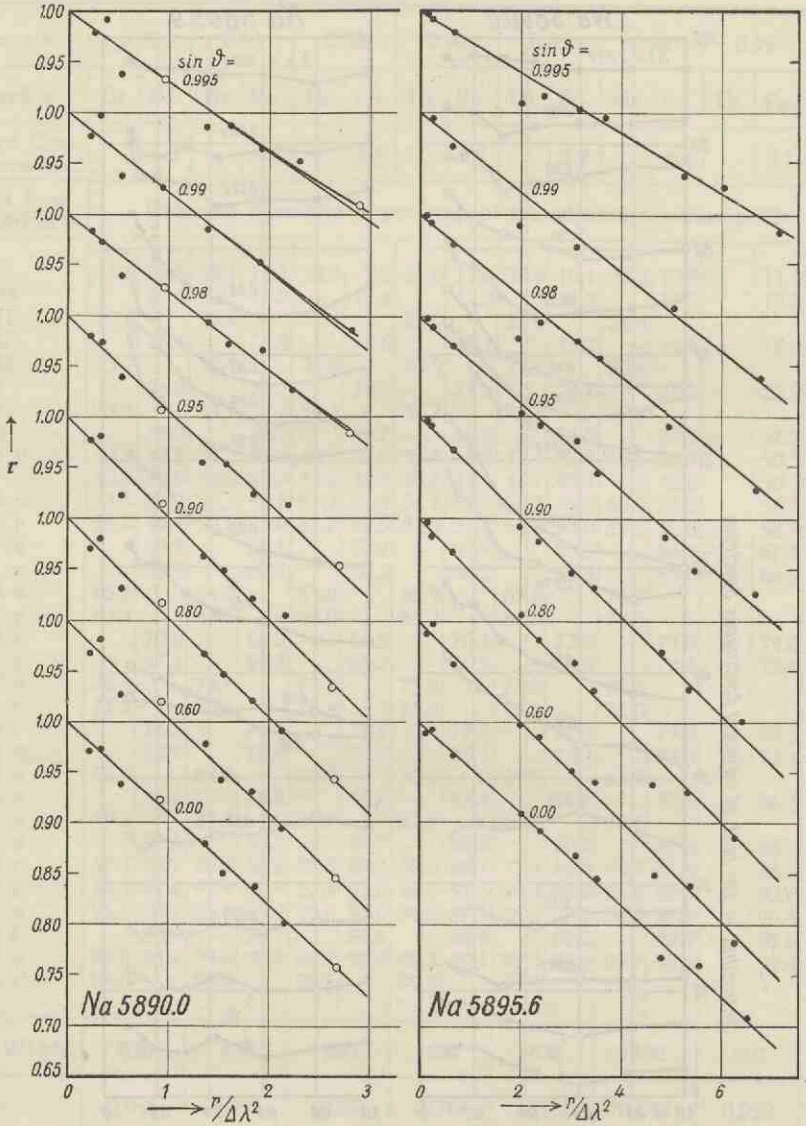

Fig. 28. — Determination of the c's of the D lines of Na; the points O are the means of 3 values from the intensity lists (Tables 16 and 17).
The scales for the abscissae are chosen in such a way that, for equal values of sin ϑ, the slopes of the tangents would be the same for both lines, if the c's were to each other in the same ratio as the doublet intensities.

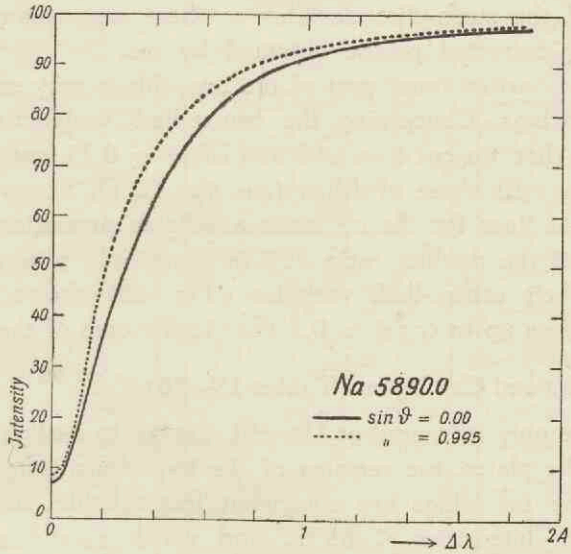

Fig. 29. — Profiles of the D_2 line of Na in two different points of the solar disc (non-corrected central intensities).

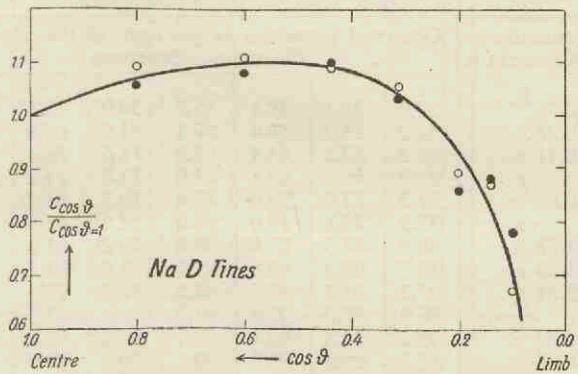

Fig. 30. — Centre-limb variations of the c's of the D lines of Na; ● Na 5890.0; ○ Na 5895.9.

From a comparison of Table II in Allen's publication with my Fig. 29 it appears further that, most remarkably, his corrected profile of D_2 for the centre of the sun's disc deviates nowhere more than about 2 % from the non-corrected profile obtained by me. As the correction is restricted to a narrow inner part of the line, this is very satisfactory as regards the wings. Concerning the centre-limb variations, it appears from Fig. 27, that, for $\cos \vartheta = 1.00$ and $\cos \vartheta = 0.25$, my results are in fair agreement with those of Allen (see also C. D. Shane [19a]).

The straight lines for the c's make a reliable determination possible (Fig. 28) and the doublet ratio 1 : 2 is beautifully reflected by these quantities. Their centre-limb variation (Fig. 30) shows a somewhat stronger increase up to $\cos \vartheta = 0.5$ than in the case of the Mg b lines.

§ 17. The infra-red Ca^+ lines (Tables 18—20).

These were only measured at Utrecht. Owing to a slight smudginess of some of the plates, the remains of the hypersensitizing process, the profiles in the far wings are somewhat less reliable. In those parts, however, with intensities < 85 %, and which extend over smaller, practically perfectly homogeneous, regions of the plates, the profiles are quite as reliable as those of the other Fraunhofer lines. The centre-limb variations show a decided character of their own, as appears from Fig. 31.

Table 18. Ca^+ 8498.0

$\sin \vartheta = r/R$	0.00	0.60	0.80	0.90	0.95	0.98	0.995
Distance from Line Centre in A	Observed Intensities in per cent. of the adjacent Continuous Spectrum						
0	33.9	35.1	38.8	38.8	39.0	38.8	38.5
0.27	51.0	54.2	56.8	59.2	61.0	62.8	62.9
0.41 v	60.3	62.6	64.4	68.0	71.6	74.4	75.8
r	61.9	65.2	68.1	71.0	73.2	74.2	73.8
0.68 v	71.3	73.8	74.6	77.8	79.7	84.2	84.8
r	73.5	75.8	78.0	82.0	82.5	85.3	85.8
1.37 v	86.4	87.3	87.6	88.7	89.2	91.0	91.3
1.50 r	89.5	90.2	90.8	91.5	92.0	93.7	93.2
2.74 v	97.2	97.2	97.3	97.5	97.3	97.9	98.5
r	96.9	97.0	97.5	97.2	96.9	97.5	97.3
5.20 v	99.0	98.8	99.1	99.1	99.3	99.5	99.0
6.58 r	98.8	99.2	98.3	99.1	99.9	99.9	99.6
Equiv. Width [1]	1250	1180	1120	1030	1000	910	910
c [1]	0.27	0.26	0.25	0.23	0.21	0.17	0.17

[1]) Values unreliable.

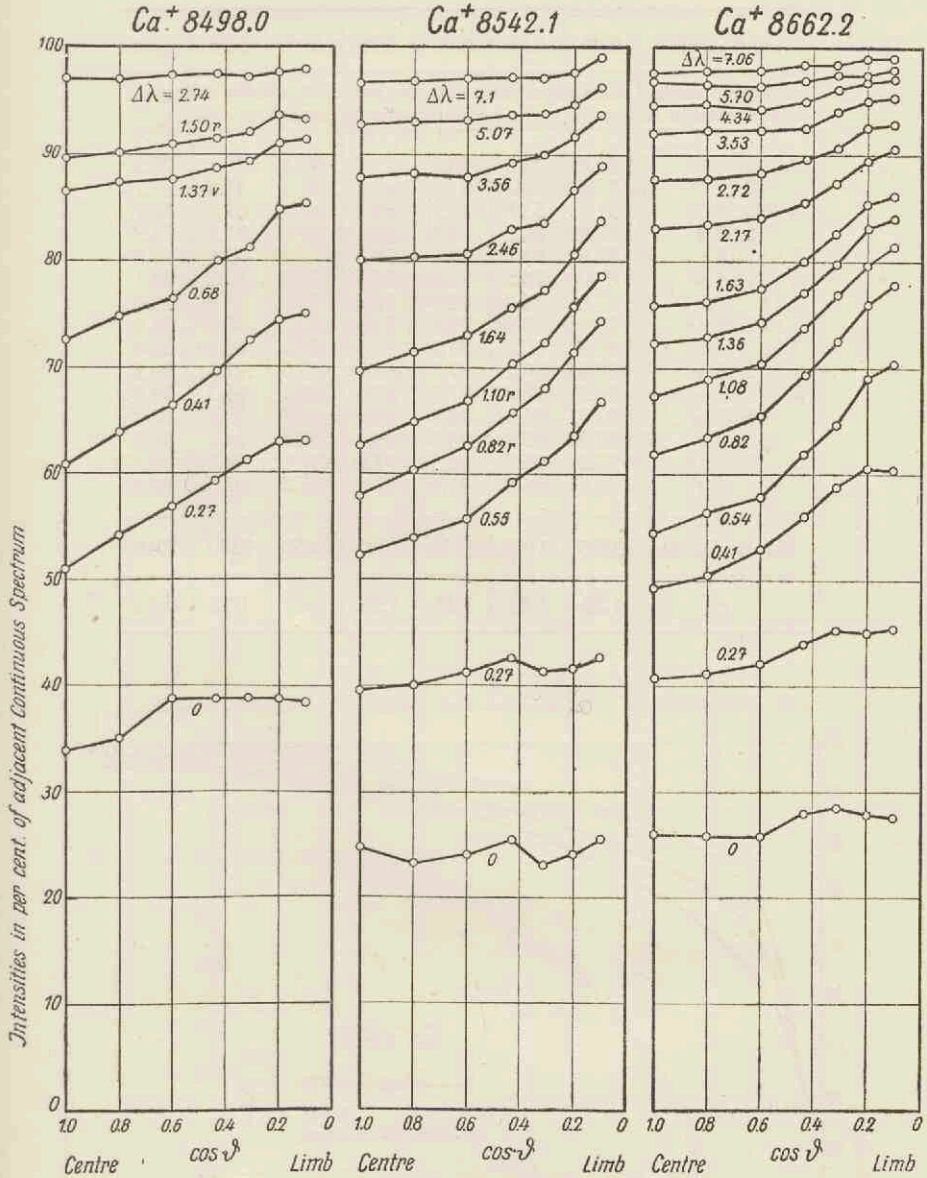

Fig. 31. — Centre-limb variations in the lines Ca+ 8498.0, Ca+ 8542.1 and Ca+ 8662.2; (parameter $\Delta\lambda$ = distance in A from centre of line).

Table 19. Ca^+ 8542.1

$\sin\vartheta = r/R$	0.00	0.60	0.80	0.90	0.95	0.98	0.995
Distance from Line Centre in A	Observed Intensities in per cent. of the adjacent Continuous Spectrum						
0	24.8	23.3	24.1	25.4	23.1	24.1	25.5
0.27	39.6	40.1	41.2	42.5	41.3	41.5	42.7
0.55	51.7	53.8	55.7	59.2	61.0	63.5	66.7
0.82 r	57.8	60.2	62.5	65.7	67.9	71.3	74.3
1.10 r	62.6	64.8	66.8	70.3	72.2	75.6	78.5
1.64 v	69.0	70.6	72 0	74.5	76.0	80.1	83.1
r	69.8	72.0	73.5	76.4	78.0	80.9	84.3
2.46 v	79.9	79.8	79.8	82.3	82.7	86.2	88.8
r	80.1	80.6	81.2	83.5	84.2	86.9	88.8
3.56 v	88.2	88.2	87.7	88.9	89.6	91.8	94.3
r	87.3	88.0	87.9	89.4	90.1	91.3	93.0
5.07 v	92.5	92.9	92.9	93.4	93.7	95.2	96.8
r	92.8	92.8	93.3	94.1	93.8	94.1	95.7
7.1 v	97.2	96.7	96.5	97.0	97.1	98.2	99.1
r	96.0	96.8	97.4	97.4	97.2	97.3	98.9
Equiv. Width	3295	3190	3110	2835	2650	2340	2010
c	1.86	1.85	1.81	1.59	1.49	1.22	0.85

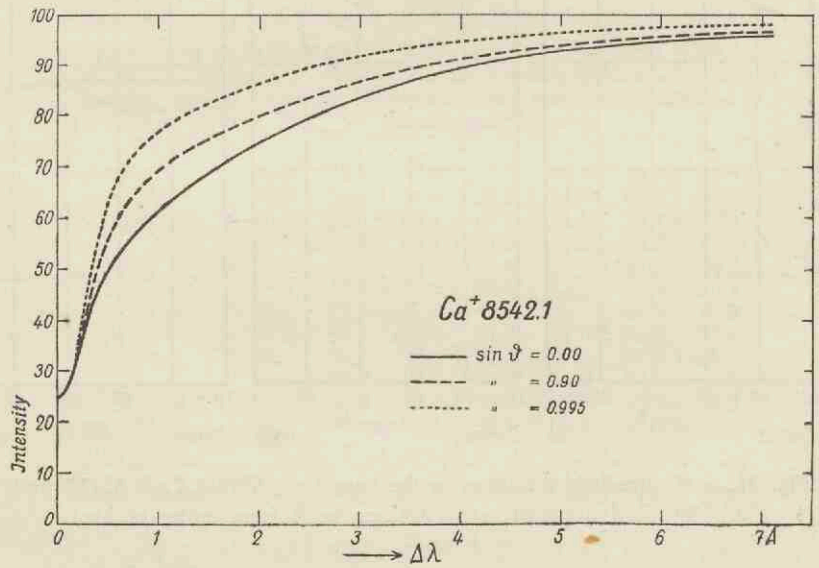

Fig. 32. — Profiles of the line Ca+ 8542.1 in three different points of the solar disc.

Table 20. **Ca+ 8662.2**

$\sin \vartheta = r/R$	0.00	0.60	0.80	0.90	0.95	0.98	0.995
Distance from Line Centre in A	Observed Intensities in per cent. of the adjacent Continuous Spectrum						
0	26.2	25.9	25.8	28.1	28.6	27.8	27.5
0.27	41.0	41.3	42.2	44.0	45.3	45.1	45.4
0.41	49.4	50.7	52.9	56.1	58.8	60.5	60.3
0.54	54.7	56.5	57.9	61.9	64.7	69.0	70.3
0.82	62.1	63.5	65.5	69.3	72.6	75.9	77.7
1.08	67.6	68.9	70.4	73.8	76.8	79.7	81.3
1.36	72.3	73.0	74.3	77.1	79.8	83.2	84.0
1.63	76.0	76.4	77.6	80.2	82.7	85.4	86.1
2.17	83.2	83.4	84.2	85.7	87.3	89.5	90.4
2.72 v	88.4	88.1	88.4	89.8	91.0	92.7	93.2
r	87.2	87.4	88.1	89.3	90.2	92.2	92.3
3.53 v	92.7	92.9	92.5	93.2	94.8	95.7	95.9
r	91.5	91.6	92.1	92.0	93.3	94.6	94.7
4.34 v	95.0	95.4	94.2	95.1	96.5	96.8	97.0
r	94.5	94.2	94.3	94.9	95.8	96.8	97.0
5.70 r	97.0	96.7	96.5	97.0	97.6	97.6	97.9
7.06 v	96.9	97.9	97.7	98.3	98.3	99.3	99.0
r	98.3	97.9	98.4	98.7	98.6	98.7	99.2
Equiv. Width	2500	2455	2356	2165	1960	1715	1645
c	1.05	1.06	1.01	0.91	0.78	0.63	0.58

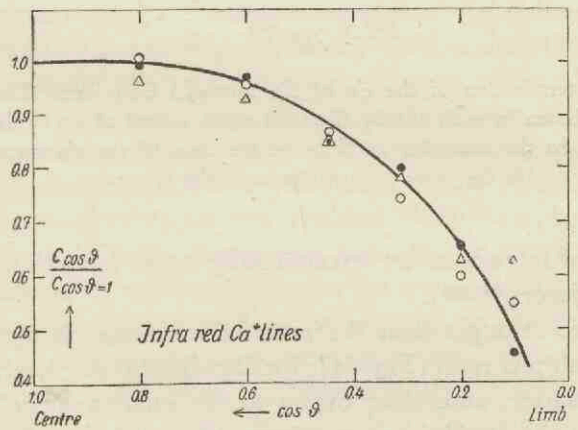

Fig. 33. — Centre-limb variations of the c's of the infra-red Ca+ lines; ● Ca+ 8542.1; ○ Ca+ 8662.2; △ Ca + 8498.0.

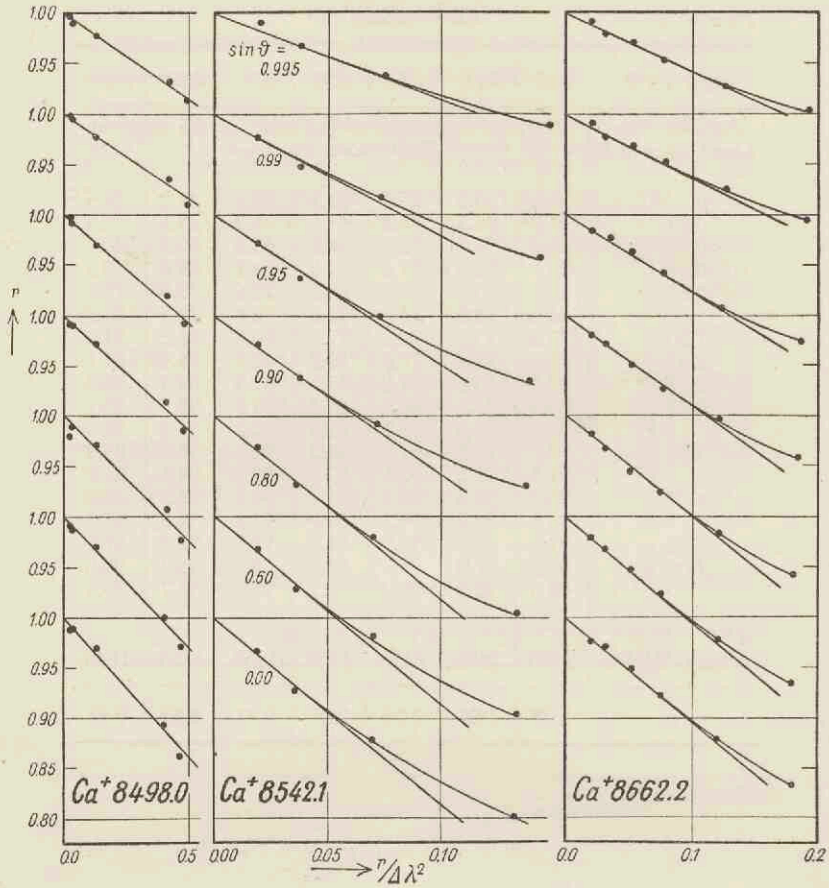

Fig. 34. — Determination of the c's of the infra-red Ca+ lines. The scales of the abscissae are chosen in such a way that, for equal values of $\sin\vartheta$, the slopes of the tangents would be the same for all three of the lines, if the c's were to each other in the same ratio as the multiplet intensities.

The central intensities are exceptionally large, as was also found by other investigators [18, 28].

For the two stronger lines the ratio between the c's agrees with the theoretical multiplet ratio (Fig. 34); for Ca+ 8498.0 the determination of c is, for that matter, unreliable, owing to the small number of measured points and to the smudginess mentioned above of the plates.

THEORETICAL PART

CHAPTER III

THE DERIVATION OF EXPRESSIONS FOR THE CENTRE-LIMB VARIATIONS IN A FRAUNHOFER LINE, WITH THE AID OF A SIMPLE MODEL OF THE SOLAR ATMOSPHERE

§ 18. Existing models.

One can attempt in various ways to trace the processes and the run of the quantities in the solar atmosphere, which serve to explain the behaviour of the Fraunhofer lines as found in the preceding chapter. When investigations in this field began, the pioneer work being done by A. Schuster [45]) and K. Schwarzschild [5]), later on continued by E. A. Milne [46, 47]) and A. S. Eddington [48, 49]), one started from schematized models of the solar atmosphere simplified in such a way that the equations for the exchange of radiation could be treated analytically and led to finite expressions for the emergent radiation. According to the point of view assumed by Schuster and Schwarzschild, a sharply defined boundary exists between the continuously radiating photosphere and the reversing layer, the solar atmosphere, properly speaking, where the selective properties of the atoms manifest themselves and the Fraunhofer lines are formed. A better knowledge of the behaviour of matter in conditions prevailing on the sun, enabled Milne [50]) to build up a more correct model of the solar atmosphere, according to which in the deeper layers the number of collisions between the particles and the absorption of the radiation are sufficiently large to establish an equilibrium which in each point is determined by the local temperature. This is what is called local thermodynamical equilibrium. This condition changes gradually into the one prevailing in the higher and less dense layers of the atmosphere. Here the continuous absorption and the number of collisions are considerably less and an energy-quant, absorbed by an atom, is in the majority of cases re-emitted by the same atom before a collision takes

place, the frequency of the radiation remaining practically the same. The limiting case, in which the radiation absorbed is re-emitted in exactly the same frequency, is called monochromatic equilibrium.

Owing to the increase of temperature and pressure with depth, the various Fraunhofer lines originate in different layers of the solar atmosphere, and Eddington, in his well-known article [49]) on the formation of Fraunhofer lines, elucidated the influence of the location and the depth of these layers on the intensity of the lines in the spectrum of the whole solar disc or of the stars.

The necessary restrictions imposed on the run of black-body radiation and in particular on that of the absorption- and scattering coefficients, in order to be able to solve the equations of transfer, were felt as hampering, when once it was thought possible to compute this run with the help of atomic theory, starting from a certain chemical composition of the solar atmosphere. This led to numerical models as constructed by A. Unsöld [51]) and A. Pannekoek [52. 16]). Starting from Eddington's differential equations one can, with the aid of the method developed by Pannekoek, compute the intensity of a Fraunhofer line for any arbitrary composition of a stellar atmosphere. An intermediate way was found by B. Strömgren [53]), who, for a rather arbitrary run of the quantities mentioned above, was still able to calculate analytically the intensity of a Fraunhofer line. In this way he took into account in these calculations the run of the concentration for that model of the sun's atmosphere, in which the continuous absorption is chiefly due to the negative hydrogen ions [54]).

One is struck immediately by a fundamental difference between the applications of the analytical method on the one hand and the numerical method on the other hand. The former makes it possible by means of incomparably less laborious computations to judge in a general way of the influence of the various factors in the final result. For that reason there is no lack of, occasionally very successful, attempts to find for the run of the absorption- and scattering coefficients more general expressions, adaptable to the actual conditions, by which the equations of transfer could still be solved [55–61]).

The above refers to the formation of a Fraunhofer line in its most general sense. The problem can be considerably simplified by restricting one's self to certain definite parts of the profile of such a line. This was done by Unsöld, who in two consecutive articles dealt with the intensity in the centre [2]) and the intensity in the far wings [62]) of a Fraunhofer line. In the first case the simplification arises from the fact that the selective absorption and scattering are very strong in comparison with

the continuous absorption, in the second case because this ratio is just the reverse. In the first case it is not necessary to know the conditions in the deeper layers of the sun's atmosphere, because for the radiation emerging in the central part of a Fraunhofer line only the conditions in the outermost layer are decisive. In the second case, on the contrary, it is the run of the various quantities down to comparatively great depth that matters, that depth namely, from which a still noticeable part of the continuous radiation emerges directly. With Unsöld's formulas one can take into account any run of $\sigma_\nu/\varkappa$ and $\varkappa_\nu/\varkappa$ with depth. For black-body radiation, however, he restricts himself to a linear function of the optical depth. In this respect a further development by M. Minnaert [63]) was a decided improvement and the expressions given by him are of excellent service in investigations of the wings.

Generally speaking, the various writers, in dealing with this problem, start from an equation of transfer in which, as far as scattering is concerned, monochromatic radiative equilibrium is taken into account. In that case the scattering is called coherent [64]). A few of them went a step further, not because they had observations at their disposal which for their explanation made it advisable to introduce the process of non-coherent scattering (see Chap. IV), but because one may, on physical grounds, assume that such a process does indeed take place (c.f. L. Spitzer [65]) and R. v. d. R. Woolley [66])). So long as we have no decisive answer to such fundamental questions, the time for numerical models has not yet come, and, likewise, the derivation of an observational model of the sun's atmosphere (P. ten Bruggencate [67]), P. Parchomenko [68, 69]), P. Wellmann [70]), H. H. Plaskett [71])) will remain uncertain, so long as we do not know from which equation of transfer we must start, that means so long as we have not sufficient information as to the active processes.

§ 19. Arguments for the construction of a model with an arbitrary layer-thickness, together with the introduction of an extinction-coefficient.

It appears to me that the testing of the observations by the predictions from a schematic model of the solar atmosphere has not yet been carried out to a sufficient extent, especially as regards the two following points:
a) the nature of the processes among which, more in particular, coherent- and non-coherent scattering and selective absorption claim our attention;
b) the effective thickness of the layer in which these processes take place

for a definite Fraunhofer line. The disadvantage of such a schematic model, namely, that it can never be more than an approximate representation of the actual conditions prevailing on the sun, is more than outweighed in the present state of the centre-limb investigations of Fraunhofer lines, by the advantage that one can by its means quickly form an idea of the influences of the points mentioned sub a) and b). If, by an appropriate choice of the quantities occurring in the model, one should find agreement with the observations (and in the following it will turn out that for a few typical centre-limb variations such a choice can indeed be made successfully) one can use this as a guide in the building up of the ultimate model of the sun's atmosphere.

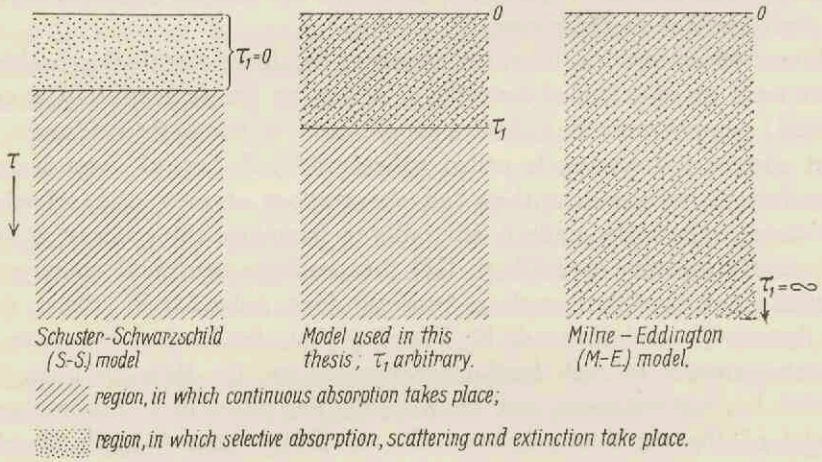

Fig. 35. — Three schematic models of the solar atmosphere.

In the model, now to be constructed, the boundary, above which selective absorption and scattering do take place, and below which they do not take place, is assumed at an arbitrary depth, whereas continuous absorption is supposed to occur everywhere (Fig. 35). In the extreme case that the boundary coincides with the surface of the sun, while at the same time the ratio between selective absorption and scattering on the one hand and continuous absorption on the other hand has become infinite, the model becomes identical with the S.-S. model, whereas it merges into the M.-E. model *), when the depth of the boundary is assumed to be infinite. For any location of the boundary the selective absorption and scattering can be simultaneously taken into account. The

*) See footnote, page 3.

degree of concentration at the sun's surface of the relevant atomic states can now be studied to any extent desired.

In the course of the present investigation it appeared that the behaviour of the wings can only be described on the assumption that non-coherent scattering takes place, i.e. that the light, absorbed in a certain frequency-range, is redistributed over the entire range of the Fraunhofer line. Anticipating future results, it may be stated here that the relative influence of this process on the far wings is comparatively strong, but in the central part only slight. In the wings such a non-coherent scattering is essentially equivalent to the partial disappearance or extra-emission of light from that frequency, so that one can take this process into account by introducing a coefficient (positive or negative) of extinction in the equation of transfer. It is true that this equation becomes thereby slightly more complicated, but its solution remains still equally well possible and from the final expressions for $r(0,\vartheta)$ one can deduce the relative importance of the three coefficients, describing together the selective processes, now supposed to be active, in any mutual proportion desired. In the next paragraph the formula for $r(0,\vartheta)$ will be deduced directly in a completely general way, as regards the combined role of the three coefficients of selective absorption, coherent scattering and extinction.

§ 20. The deduction of the general expression for $r(0,\vartheta)$.

Let τ be the optical depth in the solar atmosphere, defined by $\tau=\int_0^t \varkappa\varrho\,dt$, where t denotes the geometrical depth, $\varkappa$ the coefficient of continuous absorption for the wave length concerned per gram of matter and ϱ the density. We assume the coefficients of selective absorption, scattering and extinction to have respectively the values $\varkappa_\nu, \sigma_\nu$ and λ_ν from $\tau=0$ to $\tau=\tau_1$, and to be zero from $\tau=\tau_1$ to $\tau=\infty$. The layer of discontinuity for absorption, scattering and extinction is, therefore, assumed, for the time being, at one and the same depth $\tau=\tau_1$.

Neglecting the curvature of the atmosphere (which does not make any difference in the results, unless the observations are carried out closer to the sun's limb than can be done outside eclipses) and assuming further that the scattering is isotropic, the differential equation for the radiation of a definite wave length is *):

*) The equation of transfer, without coefficient of extinction, is amply explained in the No's [48, 72—77]) of the references.

$$\cos\vartheta\,\frac{\mathrm{d}I_\nu(t,\vartheta)}{\varrho\,\mathrm{d}t}=(\varkappa+\varkappa_\nu+\sigma_\nu+\lambda_\nu)\,I_\nu(t,\vartheta)-\sigma_\nu\int I_\nu(t,\vartheta)\,\frac{\mathrm{d}\omega}{4\pi}-(\varkappa+\varkappa_\nu)\,B \tag{1a}$$

No suffix ν is attached to the quantities $\varkappa$ and B, the black-body radiation, as they vary only slowly with wave length (an index of the notations used in this thesis is to be found on page 139).

Dividing the equation by $\varkappa$, putting $\varkappa_\nu/\varkappa=k$, $\sigma_\nu/\varkappa=s$, $\lambda_\nu/\varkappa=l$ and introducing τ as the independent variable, one obtains (omitting the suffix ν and the variables τ and ϑ):

$$\cos\vartheta\,\frac{\mathrm{d}I}{\mathrm{d}\tau}=(1+k+s+l)\,I-s\int I\,\frac{\mathrm{d}\omega}{4\pi}-(1+k)\,B. \tag{1b}$$

In order to be able to solve this equation, k, s and l are assumed to have constant values from $\tau=0$ to $\tau=\tau_1$, and to be zero from $\tau=\tau_1$ to $\tau=\infty$, while B must be given as a function of τ. In principle the differential equation can be solved for B being any power-series in τ; for the time being, however, B will be assumed to be a linear function of τ:

$$B=B_0\,(1+\beta_0\,\tau). \tag{2}$$

This simplifying assumption can be checked by the empirically determined darkening of the continuous spectrum towards the limb, from which it appears that equation (2) is approximately valid (§ 28). Later on (§ 35), the influence of a run of B, differing from (2) will be examined separately.

In solving the equation, Eddington's method of approximation [48]) will be used, which involves the introduction of the following quantities:

$$J=\int I\,\frac{\mathrm{d}\omega}{4\pi};\quad H=\int I\cos\vartheta\,\frac{\mathrm{d}\omega}{4\pi};\quad K=\int I\cos^2\vartheta\,\frac{\mathrm{d}\omega}{4\pi}. \tag{3}$$

Multiplication of (1b) respectively by $\mathrm{d}\omega/4\pi$ and $\cos\vartheta\,\mathrm{d}\omega/4\pi$, leads, after integration, to the differential equations:

$$\frac{\mathrm{d}H}{\mathrm{d}\tau}=(1+k+l)\,J-(1+k)\,B \tag{4}$$

$$\frac{\mathrm{d}K}{\mathrm{d}\tau}=(1+k+s+l)\,H,$$

or with $K=\frac{1}{3}J$:

$$\frac{\mathrm{d}J}{\mathrm{d}\tau}=3\,(1+k+s+l)\,H \tag{5a}$$

from which it follows that:

$$\frac{d^2J}{d\tau^2} = 3(1+k+s+l)\{(1+k+l)J-(1+k)B\}. \tag{6}$$

In order to be able to solve this equation in the same way as for the familiar case in which extinction is absent, we introduce:

$$B_1 = \frac{1+k}{1+k+l}B. \tag{7}$$

As B is a linear expression in τ, the same is true for B_1, so that one can write:

$$\frac{d^2(J-B_1)}{d\tau^2} = 3(1+k+s+l)(1+k+l)(J-B_1). \tag{8}$$

The solutions of this equation are:

for $\tau < \tau_1$, $J = B_1 + \mathrm{A}\,B_0\,e^{-p\tau} + \mathrm{B}\,B_0\,e^{p\tau}$ (9)

for $\tau > \tau_1$, $J = B + \mathrm{C}\,B_0\,e^{-\sqrt{3}\tau}$ (10)

where $p = \sqrt{3(1+k+s+l)(1+k+l)}$. (11)

Put $1+k+s+l = q$ (12)

then, from (5a), $H = \frac{1}{3q}\frac{dJ}{d\tau}$, (5b)

so that the solutions for H are:

for $\tau < \tau_1$, $H = \frac{B_0}{3q}\left\{\frac{\beta_0(1+k)}{1+k+l} - p\,\mathrm{A}\,e^{-p\tau} + p\,\mathrm{B}\,e^{p\tau}\right\}$ (13)

for $\tau > \tau_1$, $H = \frac{B_0}{3}\left\{\beta_0 - \sqrt{3}\,\mathrm{C}\,e^{-\sqrt{3}\tau}\right\}$. (14)

The constants of integration A, B and C can be determined from the boundary conditions. These are:
a) continuity of J and H for $\tau = \tau_1$; from (9) and (10) one finds:

$$\frac{B_1(\tau_1)}{B_0} + \mathrm{A}\,e^{-p\tau_1} + \mathrm{B}\,e^{p\tau_1} = \frac{B(\tau_1)}{B_0} + \mathrm{C}\,e^{-\sqrt{3}\tau_1} \tag{15}$$

and from (13) and (14):

$$\frac{1}{q}\left\{\frac{\beta_0\,(1+k)}{1+k+l} - p\,\mathsf{A}\,e^{-p\tau_1} + p\,\mathsf{B}\,e^{p\tau_1}\right\} = \beta_0 - \sqrt{3}\,\mathsf{C}\,e^{-\sqrt{3}\tau_1}; \qquad (16)$$

b) $J = 2H$ *) for $\tau = 0$; from (9) and (13) one finds:

$$\frac{1+k}{1+k+l} + \mathsf{A} + \mathsf{B} = 2\left[\frac{1}{3q}\left\{\frac{\beta_0\,(1+k)}{1+k+l} - p\,\mathsf{A} + p\,\mathsf{B}\right\}\right]. \qquad (17)$$

In the following only the constants A and B are necessary, for which one finds:

$$\mathsf{A} = \frac{\left(\sqrt{3}+\frac{p}{q}\right)\left(1-\frac{2\beta_0}{3q}\right)\frac{1+k}{1+k+l}\,e^{p\tau_1} + \left(1-\frac{2p}{3q}\right)\left\{\sqrt{3}\,(1+\beta_0\tau_1)\,\frac{l}{1+k+l} + \beta_0\left(1-\frac{1+k}{q\,(1+k+l)}\right)\right\}}{\left(\sqrt{3}-\frac{p}{q}\right)\left(1-\frac{2p}{3q}\right)e^{-p\tau_1} - \left(1+\frac{2p}{3q}\right)\left(\sqrt{3}+\frac{p}{q}\right)e^{p\tau_1}} \qquad (18)$$

while B is obtained from A by changing p into $-p$.

The intensity in a Fraunhofer line-profile in the integrated light of the solar disc follows from (13) by putting $\tau = 0$. From this $H(0)$ one obtains the relative intensity with respect to the neighbouring continuous spectrum by dividing by $H_0(0)$, which follows from $H(0)$ by putting k, s and l equal to zero.
One finds:

$$r(0) = \frac{H(0)}{H_0(0)} = \frac{1}{q}\,\frac{\beta_0\,\frac{1+k}{1+k+l} - p\,(\mathsf{A}-\mathsf{B})}{\beta_0 - \sqrt{3}\,(\mathsf{A}-\mathsf{B})_{k=s=l=0}} = \frac{2+\sqrt{3}}{q}\,\frac{\beta_0\,\frac{1+k}{1+k+l} - p\,(\mathsf{A}-\mathsf{B})}{\beta_0\sqrt{3}+3}, \qquad (19)$$

With the aid of this formula one can for the present model of an atmosphere with any arbitrary layer-thickness compute r as a function of the spectral region (β_0) and of the separate contributions from simultaneous selective absorption, scattering and extinction. When only coherent scattering occurs ($k = l = 0$), (19) transforms into the equation derived by P. Swings and S. Chandrasekhar [78], while in the case that only coherent scattering occurs and $\beta_0 = 1.5$, there appears a formula used by O. Struve [79].

For the radiation $I(0, \vartheta)$ emerging from the sun at an angle ϑ with the

*) A. Pannekoek [16]) puts here $J = 1.8\,H$; I have ascertained that this does not make any appreciable difference in the centre-limb variations (see also § 34).

normal, one can write down at once the expression in the shape of an integral:

$$I(0,\vartheta)=\int_0^\infty \{ s J + (1+k) B \}\, e^{-\int_0^\tau (1+k+s+l)\, d\tau \sec\vartheta}\, d\tau \sec\vartheta \qquad (20)$$

This integral is split into the parts from $0 - \tau_1$ and from $\tau_1 - \infty$ and one obtains, after some further calculations, with the expression for J from (9) — taking into account (7) — and dividing by the intensity of the continuous spectrum, $B_0\,(1+\beta_0\cos\vartheta)$, the expression for the relative intensity in a Fraunhofer line as a function of the angle of emergence:

$$r(0,\vartheta)=\frac{\left(1+\frac{\beta_0\cos\vartheta}{q}\right)\frac{1+k}{1+k+l}+e^{-q\tau_1\sec\vartheta}\left\{1+\beta_0\cos\vartheta+\beta_0\tau_1\frac{l}{1+k+l}-\frac{1+k}{1+k+l}\left(1+\frac{\beta_0\cos\vartheta}{q}\right)\right\}+ +s\left\{\frac{A}{q+p\cos\vartheta}\left(1-e^{-p\tau_1}e^{-q\tau_1\sec\vartheta}\right)+\frac{B}{q-p\cos\vartheta}\left(1-e^{p\tau_1}e^{-q\tau_1\sec\vartheta}\right)\right\}}{1+\beta_0\cos\vartheta} \qquad (21)$$

in which for A, B, p and q their expressions (18), (11) and (12) must be substituted. Apart from ϑ, the independent variables occurring in this formula are β_0, k, s, l and τ_1; before examining the centre-limb variations in their dependence on these quantities, we shall first discuss a few extreme cases.

§ 21. Various extreme cases, deduced from (21).

In the following, (21) will often be used for those cases in which only one of the factors k, s or l is not zero. In these cases (21) is considerably simplified, as are also the expressions for A and B, which then must only be calculated for the case of selective coherent scattering, because for $s=0$ they cancel out of (21).

1. *Selective absorption.* When only absorption occurs, (21) transforms into:

$$r(0,\vartheta)=\frac{1+\beta_0\cos\vartheta\left\{\frac{1}{q}+\left(1-\frac{1}{q}\right)e^{-q\tau_1\sec\vartheta}\right\}}{1+\beta_0\cos\vartheta} \qquad (22)$$

with $q=1+k$.

2. *Coherent scattering.* If only coherent scattering occurs, (21) becomes:

$$r(0,\vartheta)=\frac{1+\beta_0\cos\vartheta\left\{\frac{1}{q}+\left(1-\frac{1}{q}\right)e^{-q\tau_1\sec\vartheta}\right\}+}{+s\left\{\frac{A}{q+p\cos\vartheta}\left(1-e^{-p\tau_1}e^{-q\tau_1\sec\vartheta}\right)+\frac{B}{q-p\cos\vartheta}\left(1-e^{p\tau_1}e^{-q\tau_1\sec\vartheta}\right)\right\}}{1+\beta_0\cos\vartheta} \tag{23}$$

with $q=1+s$, $p=\sqrt{3(1+s)}$, while A and B are given by (18) with $k=l=0$. This formula can also be used in the case that selective absorption and coherent scattering are both active, while $l=0$; k and s will then remain in p, q, A and B, whereas l disappears.

3. *Extinction.* If only extinction occurs, (21) becomes:

$$r(0,\vartheta)=\frac{\left(1+\frac{\beta_0\cos\vartheta}{q}\right)\frac{1}{q}+e^{-q\tau_1\sec\vartheta}\left\{1+\beta_0\cos\vartheta+\beta_0\tau_1\left(1-\frac{1}{q}\right)-\frac{1}{q}\left(1+\frac{\beta_0\cos\vartheta}{q}\right)\right\}}{1+\beta_0\cos\vartheta} \tag{24}$$

with $q=1+l$.

The formulae (22) and (24) can also be derived directly, because in the case that only absorption resp. extinction takes place, the integral (20) can be written in a form which can be integrated at once.

4. *The Milne-Eddington model.* For $l=0$ and $\tau_1=\infty$, the model becomes identical with the M.-E. model in which throughout the whole atmosphere the coefficients of selective absorption and of scattering are in constant ratios to the coefficient of continuous absorption. Equation (21) transforms then into Unsöld's formula (65, 34) [77] and in Plaskett's formula (34) [8], which the latter has amply applied to his observations concerning the Mg b lines. The only difference between his formula and mine is that I have made no distinction between $\bar{\varkappa}$ and $\varkappa$, so that Plaskett's n is equal to my q. In the light of the most recent ideas, according to which the continuous absorption is assumed to be practically wholly due to hydrogen and to be substantially constant over the whole visible spectrum, one is indeed justified in putting $\bar{\varkappa}=\varkappa$.

5. *The Schuster-Schwarzschild model.* Another extreme case, also with $l=0$, is obtained by making τ_1 approach zero, at the same time increasing k and (or) s so as to approach ∞ in such a way that $k\tau_1=K$ and $s\tau_1=S$. Formula (21) transforms then into the formulas of the

S.-S. model with, at the surface, a layer in which only selective absorption and (or) scattering takes place and of which the optical depth amounts to K resp. to S. One should bear in mind, however that the deduction of the expression for $r(0,\vartheta)$, according to the S.-S. model, is here carried out in a way of approximation, different from that by previous writers, so that one need not expect for it the same expression as obtained by them. In the case of the S.-S. model with absorption only, (21) resp. (22) do indeed lead to the familiar expression, which one finds, for example, as Unsöld's formula (64, 24) [77]. For pure scattering, however, the expression is slightly different from the one deduced by Milne [46] (see also [77]), formula (64, 10)), though, numerically, there is hardly any difference. In this case it follows from (21)resp. (23) after some further transformations owing to the transition to the limit, that

$$r(0,\vartheta)=e^{-S\sec\vartheta}+\frac{\frac{1}{2}+\frac{\beta_0}{2\sqrt{3}}}{1+\beta_0\cos\vartheta}\,\frac{\left(1+\frac{3}{2}\cos\vartheta\right)\left(1-e^{-S\sec\vartheta}\right)-\frac{3}{2}Se^{-S\sec\vartheta}}{\frac{1}{2}+\frac{\sqrt{3}}{4}+\frac{3}{4}S} \tag{25}$$

This expression differs from the one deduced by Milne in that his factor $\dfrac{\frac{1}{2}+\frac{\beta_0}{3}}{1+s_1\varphi(s_1)}$ is replaced by $\dfrac{\frac{1}{2}+\frac{\beta_0}{2\sqrt{3}}}{\frac{1}{2}+\frac{\sqrt{3}}{4}+\frac{3}{4}S}$, where $S=s_1$, while φ changes from 1 to $\frac{3}{4}$, when s_1 varies from 0 to ∞ (c.f. Unsöld [77], formula (64, 10)). As can be seen from these expressions, the numerical difference is very small.

CHAPTER IV

NON-COHERENT SCATTERING

§ 22. Introduction.

The selective scattering of radiation by an atom *) is called coherent, if absorbed radiation of some definite frequency is re-emitted as radiation of that same frequency [64]). If, on the contrary, selectively absorbed radiation of a frequency-region $d\nu$ (small in comparison with the line-width) is distributed, on being re-emitted, over all frequencies within the spectral line, it is termed non-coherent scattering. The distribution-function governing this process depends on various factors.

We cannot say in what way the frequency-distribution of the absorbed radiation and that of the emitted radiation are connected with each other, if the interaction between the atoms and the field of radiation is disturbed by collisions, as is the case in the solar atmosphere. W. Orthmann and P. Pringsheim [80]) showed, however, by means of a resonance lamp that the frequency-distribution of the absorbed radiation can be practically independent of that of the emitted radiation. They found, namely, that when a gas is exposed to the radiation of a narrow resonance line, the re-emitted line, while being considerably wider than the first one, possesses a profile, which is completely determined by the Lorentz widening in the gas exposed to the radiation. One can, therefore, take it for granted that damping by collision gives rise to non-coherent scattering.

Theoretical physics has not yet formulated in detail in what way the exchange of radiation takes place in the case of damping by collision and for that reason two different conceptions will be worked out in the following paragraphs. In the first conception the redistribution of the emitted radiation over the frequencies of the spectral line is assumed

*) Experimentally, the scattering can only be measured for a great number of atoms in a certain volume of gas; the reasoning in the present chapter is directly applicable to this case by substituting "a gas" for "an atom"; the coefficient of absorption is then the one for the gas as a whole.

to be proportional to the value of the absorption-coefficient†) and independent of the frequency-distribution of the absorbed radiation. Henceforth this case will be called *complete redistribution*. In the second conception one starts from a model of an atom in which the transfer of energy between the levels, widened by damping by collision, takes place in the same way as in the case of radiation-damping, of which the theory has been developed by V. Weisskopf [81, 82]. Henceforth this conception will be designated as the one of the *widened energy-levels*.

§ 23. Non-coherent scattering based on complete redistribution.

The amount of radiation absorbed by an atom within a frequency-region between ν and $\nu + d\nu$, which is small in comparison with the line-width, is proportional to the radiation-density J_ν *) and to the coefficient of absorption α_ν, so that it can be put equal to $J_\nu \alpha_\nu d\nu$.

Let us now consider an enclosure with radiation and atoms inside; between them a state of equilibrium will set in, for which $J_\nu = J$, constant over the spectral line. The radiation absorbed in each region $d\nu$ is then equal to the radiation emitted in $d\nu$ (detailed balancing); we shall put this amount equal to $e_\nu d\nu$, so that $e_\nu = J\alpha_\nu$. Under well-defined exterior conditions α_ν will vary over the frequency-region of the spectral line in a way, which is characteristic of the atomic states concerned. It is, therefore, clear that in the

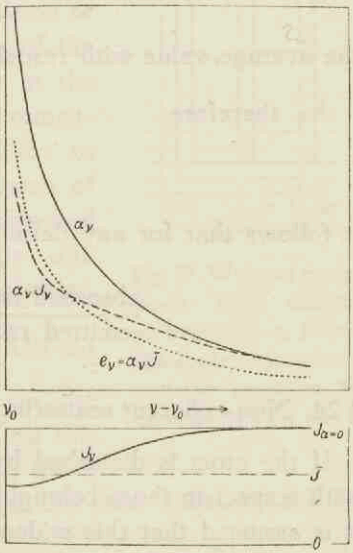

Fig. 36. Complete redistribution: absorption ($\alpha_\nu J_\nu$) and emission ($e_\nu = \alpha_\nu \bar{J}$) as functions of $\nu - \nu_0$ in the frequency-range of a Fraunhofer line.

†) One must carefully distinguish between: a) absorption = taking in of radiation (as in the present instance); b) absorption = transformation of radiant energy into kinetic energy. See also p. 139.

*) Strictly speaking the radiation-density ought to be denoted by $\frac{4\pi}{c} J_\nu$, while J_ν represents the mean radiation-intensity, averaged over all directions, but we shall omit the factor $\frac{4\pi}{c}$.

state of equilibrium e_ν varies proportional to a_ν. Now we start from the assumption that in the general case, in which J_ν is not constant (Fig. 36), e_ν will, all the same, vary over the frequencies of the spectral line in the same way as in the case of equilibrium, so that $e_\nu = \mu a_\nu$. The factor of proportionality μ is found from the equilibrium of the radiation for the whole Fraunhofer line,

$$\int J_\nu a_\nu \, d\nu = \int e_\nu \, d\nu = \mu \int a_\nu \, d\nu,$$

so that:

$$\mu = \frac{\int J_\nu a_\nu \, d\nu}{\int a_\nu \, d\nu} = \bar{J}, \tag{26}$$

the average value with respect to the coefficient of absorption of J_ν †).

As, therefore,

$$e_\nu = a_\nu \bar{J}, \tag{27}$$

it follows that for any definite frequency-region $d\nu$ the ratio:

$$\frac{\text{absorbed radiation}}{\text{emitted radiation}} = \frac{a_\nu J_\nu}{e_\nu} = \frac{J_\nu}{\bar{J}}. \tag{28}$$

§ 24. Non-coherent scattering based on widened energy-levels.

If the atom is disturbed by collisions, the spectral lines are widened with respect to those belonging to its undisturbed state. In the following it is assumed that this widening can be described by means of energy-levels, widened by damping by collisions, in exactly the same way as Weisskopf has developed for radiation-damping. That in our case the lowest or fundamental level must be included in this widening is obvious and follows also from the experiments by Orthmann and Pringsheim mentioned in § 22.

The effect of the non-coherent scattering depends on the distribution of the radiation-density over the line. In the solar atmosphere the radiation incident on an atom is not black-body radiation, for it has,

---

†) If the radiation-density in the centre of the line, J_c, is not very small compared with those in the others parts of the line, $\bar{J}$ will be practically equal to J_c, owing to the large value of a_ν in the centre of the line.

among other factors, been modified by the Fraunhofer lines. The relation between the absorbed and the emitted radiation will now be computed for a simplified case, in which for the frequencies of the far wings the radiation-density J_ν is greater than in the more central parts of the line, where it is assumed that it is constant and equal to J_c. Owing to this excess of radiation in the far wings, a deviation arises from the state of equilibrium, in which J was constant over the whole line and in which for each frequency equal amounts of radiation were emitted and absorbed. Let us now consider the effects of exposing the atom to the excess-radiation $(J_\nu - J_c)$ of a wing-frequency (Fig. 37, transitions a); we see then that, analogous to Weisskopf's results, two maxima occur in the frequency-distribution of the emission, one at the frequency $\nu_0 + \Delta\nu$ of the incident radiation (transitions b) and one at the frequency ν_0 of the centre of the line (transitions c). The intensities of these maxima are to each other as γ_n to γ_m, the damping constants of the higher, resp. lower level. What is absorbed of the excess-radiation in the far wings will, therefore, be re-emitted in the same frequency-region to the fraction $\frac{\gamma_n}{\gamma_m + \gamma_n}$*). The total amount of radiation absorbed in the far wings in the frequency-region $d\nu$ is $\alpha_\nu J_\nu \, d\nu$. On dividing this into two parts: $\alpha_\nu J_c \, d\nu$ and $\alpha_\nu (J_\nu - J_c) \, d\nu$, it follows from the above considerations that the total emission will be:

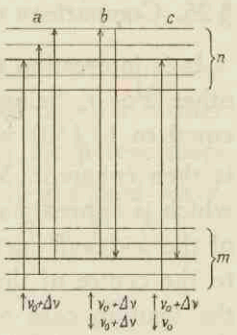

Fig. 37. Widened energy-levels; when radiation of frequency $\nu_0 + \Delta\nu$ is absorbed, maxima of emission occur at frequencies $\nu_0 + \Delta\nu$ and ν_0.

$$\alpha_\nu J_c \, d\nu + \alpha_\nu \frac{\gamma_n}{\gamma_m + \gamma_n} (J_\nu - J_c) \, d\nu = \alpha_\nu \frac{\gamma_n J_\nu + \gamma_m J_c}{\gamma_m + \gamma_n}, \qquad (29)$$

*) It is assumed here that the half-width of the emission is small compared with the region considered of the far wings, for which the radiation-density is equal to J_ν. This is justified because the constitution of the emission is similar to that of an emission-line, emerging from an optically thin layer, and whose width is very narrow compared with that of a strong Fraunhofer line.

The remaining fraction of the excess-radiation which is emitted in the centre of the line does not concern us further, because the process described here takes place in those layers of the solar atmosphere, in which the damping by collisions is important; these layers, however, lie deeper in that atmosphere than those, in which the observed light of the central frequencies of a Fraunhofer line originates.

so that in the far wings the ratio:

$$\frac{\text{absorbed radiation}}{\text{emitted radiation}} = \frac{(\gamma_m + \gamma_n) J_\nu}{\gamma_n J_\nu + \gamma_m J_c}. \tag{30}$$

As the radiation of the far wings interacts mainly with the radiation of the centre of the line, one can put J_c approximately equal to the value of J for that centre which in its turn is practically equal to $\bar{J}$ (see (26)).

§ 25. Comparison of (28) with (30).

It is interesting to compare the expressions (28) and (30) with each other. For J_ν being constant, both of them become, as a matter of course, equal to 1. (30) will also be equal to 1, when $\gamma_m = 0$; the scattering is then coherent. When $\gamma_n = 0$, (28) and (30) will agree, if $J_c = \bar{J}$, which is approximately the case (see the end of § 24). In the conception of the widened energy-levels the removal of radiation from the far wings to the centre of the line is then a maximum. (28) represents, therefore, the limiting case of (30), in which, owing to non-coherent scattering, the transfer of radiation from the far wings to the centre is a maximum.

Attention must here be drawn to a difference between (28) and (30). If the radiation-density in the far wings is less than in the centre of the line, (28) holds as it stands, whereas (30) does not apply to this case, as is evident from the way it was obtained. There will then be an excess of radiation of the central frequencies and, on re-emission, a small part of it will find its way to the frequencies of the far wings, so that, if $\gamma_m \neq 0$, (28) and (30) agree, in so far that in that case more radiation is emitted than absorbed in the far wings. A quantitative test of the non-coherent scattering by means of (28) and (30) is impossible, so long as the ratio γ_m / γ_n is not known. The qualitative application of (27) and (29), resp. (28) and (30) to the Fraunhofer lines will, however, be already sufficient to establish beyond any doubt the occurrence of non-coherent scattering.

§ 26. The equation of transfer for non-coherent scattering.

In order to be able to apply the results obtained in the above paragraphs, we start from the equation of transfer in its general form:

$$\cos\vartheta \frac{\mathrm{d}I_\nu}{\varrho\,\mathrm{d}t} = \text{total absorption} - \text{selective emission} - \text{continuous emission}$$

or: $$\cos\vartheta \frac{\mathrm{d}I_\nu}{\varrho\,\mathrm{d}t} = (\varkappa + \alpha_\nu) I_\nu - \text{selective emission} - \varkappa B. \qquad (31)$$

1. *Complete redistribution.* As shown by (27), the total selective emission is in this case $\alpha_\nu \bar{J}$. The equation of transfer becomes, therefore, introducing τ:

$$\cos\vartheta \frac{\mathrm{d}I_\nu}{\mathrm{d}\tau} = (1 + a_\nu) I_\nu - a_\nu \bar{J} - B \qquad (32)$$

with $a_\nu = \alpha_\nu/\varkappa$.

The run of $\bar{J}$ with τ must be obtained from a closer investigation of the solar atmosphere; this investigation will be carried out in a further chapter. For the time being we proceed to solve (32) for a few cases in which $\bar{J}$ changes relatively to B and J_ν in definitely assigned ways.

The simplest solutions of (32) are obtained for $J = B$ or $\bar{J} = J_\nu$.

a. $\bar{J} = B$. In this case (32) becomes:

$$\cos\vartheta \frac{\mathrm{d}I_\nu}{\mathrm{d}\tau} = (1 + a_\nu) I_\nu - a_\nu B - B \qquad (33)$$

and this is, formally, the equation of transfer for selective absorption.

b. $\bar{J} = J_\nu$. In this case (32) becomes:

$$\cos\vartheta \frac{\mathrm{d}I_\nu}{\mathrm{d}\tau} = (1 + a_\nu) I_\nu - a_\nu J_\nu - B \qquad (34)$$

which is, formally, the equation of transfer for coherent scattering.

In general, however, $\bar{J}$ will be different from B and from J_ν. One can then express $\bar{J}$ either in B or in J_ν. In the first case the equation of transfer acquires a form which can be interpreted as a combination of selective absorption and extinction (if $\bar{J} < B$) or increased emission (if $\bar{J} > B$). In the second case as a combination of coherent scattering and extinction (if $\bar{J} < J_\nu$) or increased emission (if $\bar{J} > J_\nu$). In two cases, namely, for $B < \bar{J} < J_\nu$ and $B > \bar{J} > J_\nu$ it is possible to obtain a combination of selective absorption and coherent scattering by expressing $\bar{J}$ simultaneously in B and J_ν. If, however, one expresses in general

$\bar{J}$ simultaneously in B and J_ν, one obtains a combination of the three effects, selective absorption, coherent scattering and extinction or increased emission. By this procedure, however, the results become unduly complicated, as one can always suffice with at most two effects.

We shall now proceed to work out a few of these cases, to which we shall refer again later on in explaining the centre-limb variations of the Fraunhofer lines.

c. $\bar{J} < B$. Put $a_\nu \bar{J} = k_\nu B$ and $a_\nu = k_\nu + l_\nu$, then (32) becomes:

$$\cos\vartheta \frac{\mathrm{d}I_\nu}{\mathrm{d}\tau} = (1 + k_\nu + l_\nu) I_\nu - k_\nu B - B \tag{35}$$

which is, formally, the equation of transfer for a combination of selective absorption and extinction. The ratio between the two coefficients is:

$$\frac{l_\nu}{k_\nu} = \frac{a_\nu - k_\nu}{k_\nu} = \frac{B}{\bar{J}} - 1. \tag{36}$$

d. $\bar{J} < J_\nu$. Put $a_\nu \bar{J} = s_\nu J_\nu$ and $a_\nu = s_\nu + l_\nu$, then (32) becomes:

$$\cos\vartheta \frac{\mathrm{d}I_\nu}{\mathrm{d}\tau} = (1 + s_\nu + l_\nu) I_\nu - s_\nu J_\nu - B \tag{37}$$

which is, formally, the equation of transfer for a combination of coherent scattering and extinction. The ratio between the two coefficients is:

$$\frac{l_\nu}{s_\nu} = \frac{a_\nu - s_\nu}{s_\nu} = \frac{J_\nu}{\bar{J}} - 1. \tag{38}$$

e. $B > \bar{J} > J_\nu$. In terms of B, this leads to selective absorption and extinction, in terms of J_ν, to coherent scattering and increased emission. One can, however, express $\bar{J}$ simultaneously in B and J_ν, as follows: put $a_\nu = a_{\nu,1} + a_{\nu,2} = k_\nu + s_\nu$ and $a_{\nu,1} \bar{J} = k_\nu B$, $a_{\nu,2} \bar{J} = s_\nu J_\nu$, then (32) becomes:

$$\cos\vartheta \frac{\mathrm{d}I_\nu}{\mathrm{d}\tau} = (1 + k_\nu + s_\nu) I_\nu - s_\nu J_\nu - k_\nu B - B. \tag{39}$$

This is, formally, a combination of selective absorption and coherent

scattering. For the ratio between the two coefficients one finds, with the aid of the conditions which $a_{\nu,1}$, $a_{\nu,2}$, k_ν and s_ν must satisfy:

$$\frac{s_\nu}{k_\nu} = \frac{B - \bar{J}}{\bar{J} - J_\nu}. \tag{40}$$

2. *Widened energy-levels.* Starting from the conception of the widened energy-levels, the equation of transfer is modified to a certain extent. The selective emission is now (see (29)): $a_\nu \frac{\gamma_n J_\nu + \gamma_m J_c}{\gamma_m + \gamma_n}$. Write n for $\frac{\gamma_n}{\gamma_m + \gamma_n}$ and m for $\frac{\gamma_m}{\gamma_m + \gamma_n}$, then the equation of transfer becomes:

$$\cos\vartheta \frac{dI_\nu}{d\tau} = (1 + a_\nu) I_\nu - n a_\nu J_\nu - m a_\nu J_c - B. \tag{41}$$

The term $n a_\nu J_\nu$ represents a contribution to the coherent scattering. As regards the term $m a_\nu J_c$ the following statement can be made. If $J_c = B$, the term contributes solely to selective absorption, if $J_c = J_\nu$, it contributes solely to coherent scattering. If, however, $J_c \neq B$ and $\neq J_\nu$, one can first compare J_c with B, and the term will then give rise to selective absorption and extinction, while, comparing J_c with J_ν, it will give rise to extinction and to a contribution to coherent scattering. The ratios between these various effects depend on the ratio between J_c and B and on the ratio between J_c and J_ν. This can be investigated in the same way as was carried out sub 1) for various cases of the complete redistribution. One finds, for example, for the case that $J_c \leq B$:

$$s : k : l = B\,\gamma_n/\gamma_m : J_c : (B - J_c). \tag{42}$$

The ratio of the other effects to that of coherent scattering is now, moreover, dependent on γ_m/γ_n, which enters into the problem as still another unknown quantity, but whose influence can be accounted for by a suitable modification of the meaning of s, k and l.

The conclusion to be drawn from the present chapter is, therefore, that the non-coherent scattering must be considered as the general process of scattering which can be formally described by means of the

three coefficients, of selective absorption, coherent scattering and extinction, while the mutual ratios between these coefficients depend on various quantities. In the case of complete redistribution these are the densities of radiation of the various frequencies in the region of a Fraunhofer line and the black-body radiation, in the case of the widened energy-levels they are these same quantities and the ratio γ_m/γ_n as well.

CHAPTER V

DETERMINATION OF THE QUANTITIES OCCURRING IN THE EXPRESSION FOR THE CENTRE-LIMB VARIATIONS

§ 27. Introduction.

In the preceding chapter it is shown, that in the case of non-coherent scattering the equation of transfer takes the form, from which one started in § 20. This means, that it must indeed be possible to describe the behaviour of the Fraunhofer lines by means of (21), in so far as the applied approximations are allowed. Before proceeding to a comparison with the observations, one must first form an idea of the values of the parameters occurring in (21), namely β_0, τ_1, k, s and l. The ratios between k, s and l are, in their turn, dependent on B, J_ν and $\bar{J}$, and on certain atomic constants, as shown in § 26. Reversely, however, the functions B, J_ν and $\bar{J}$ are again determined by β_0, τ_1, k, s and l. It will be clear, that under these conditions it is only possible to make headway by means of successive approximations to be carried out according to the following scheme. — Concerning the constants β_0, τ_1, k, s and l of the solar atmosphere and γ_m/γ_n of the atoms very plausible simplifying assumptions are made. Taking this as our starting point, we can assign a general run to the functions $B/\bar{J}$ and $J_\nu/\bar{J}$, which in the further development play the essential part, from which again more accurate statements concerning the ratios between k, s and l will follow. Once these are known, we are in a position to compute the radiation-density J_ν at any depth in the solar atmosphere, and, from that density, to compute in the well-known way the radiation emerging from any point of the solar disc.

Owing to the, as yet, too scanty knowledge of the actual state in the solar atmosphere and of various atomic constants it would be futile to work out completely the scheme of approximation. What is chiefly lacking is a sufficient knowledge of the run with depth of the black-body

radiation, the concentration, the damping and the ratio between the total damping-constants of the two energy-levels, which correspond to the Fraunhofer line in question.

§ 28. The determination of β_0.

The black-body radiation was supposed to be, for every wave length, a linear function of τ, given by (2), i.e. $B = B_0\ (1 + \beta_0\ \tau)$. The run of B in the various wave-length regions is, therefore, characterised by β_0. If (2) holds, the run of the intensity of the continuous spectrum along

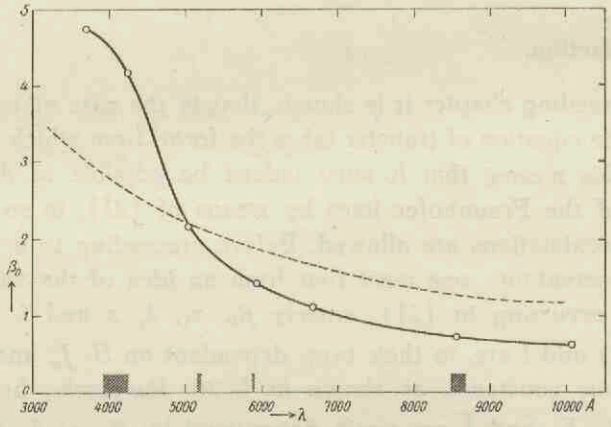

Fig. 38. — Run of β_0 with wave length; —— deduced from C. G. Abbot's measurements of the darkening of the continuous spectrum towards the limb; — — — theoretical run in the case of local thermodynamical equilibrium and when $\varkappa\ (\lambda, \tau) =$ constant (A. Unsöld). Along the λ-axis are marked the locations of the measured Fraunhofer lines.

a radius of the solar disc is for a given wave length, represented by $I_0\ (0, \vartheta) = B_0\ (1 + \beta_0 \cos \vartheta)$ [72]). I have determined the way in which β_0 depends on the wave length from the measurements by C. G. Abbot and collaborators [83]) concerning the darkening of the continuous spectrum towards the limb. If one plots their observed values for $I_0(0, \vartheta)/I_0(0, 0)$ against $\cos \vartheta$, the resulting curves are fairly closely approximated by the straight lines $I_0(0, \vartheta)/I_0(0, 0) = (1 + \beta_0 \cos \vartheta)/(1 + \beta_0)$ *). The

*) If the results of the measurements by W. J. H. Moll, H. C. Burger and J. v. d. Bilt [84]), and by H. Raudenbusch [85]) concerning the darkening towards the limb are plotted in the same way, their representation by straight lines is slightly less satisfactory.

factor β_0 was now computed from the values for $I_0(0, \vartheta)$ with $\cos\vartheta = 1$, and 0.312. Fig. 38 shows the run of $\beta_0(\lambda)$, determined in this way, to which is added, for comparison, the run of $\beta_0(\lambda)$ computed by A. Unsöld [86]) for the case of local thermodynamical equilibrium, while, moreover, $\varkappa\,(\lambda, \tau) =$ constant.

In order to restrict our calculations to a certain extent, a preliminary comparison was carried out of the observational results from the various lines with the results from the formulas (22), (23) and (24) for the values of β_0 chosen as follows:

Lines:	Wave Lengths in A:	β_0:
Ca^+ H and K,	3968.5 and 3933.7	4.5
Fe multiplet,	4045.8 etc.	
Ca line,	4226.7	
Mg b lines,	5167.3 and 5183.6	1.75
Na D lines,	5890.0 and 5895.9	
Ca^+ infra-red lines,	8498.1, 8542.1 and 8662.2	0.75

§ 29. The choice of τ_1.

If one accepts the occurrence of non-coherent scattering the behaviour of the Fraunhofer lines can be formally described by means of a combination of absorption, coherent scattering and extinction or increased emission. One must then bear in mind that the run of the concentration of the atomic state, to which the Fraunhofer line in question is due, is completely determined by the conditions of the atmosphere, but that the individual runs with depth of k, s and l may mutually differ. Consequently three different values for τ_1 which we can denote by $\tau_{1,k}$, $\tau_{1,s}$, and $\tau_{1,l}$ are correlated to one and the same Fraunhofer line. By way of a guidance in discussing the results and in selecting from the numerous possibilities, one can avail oneself of the conditions imposed on the choice of these τ_1's by what is known of the upper layers of the sun. To this end one needs, first of all, to know something about the run of $a(\tau) = k(\tau) + s(\tau) + l(\tau)$. In order to obtain this knowledge one can first compute from Strömgren's model of the solar atmosphere and from the theory of ionization the run of the concentration for various lines. On carrying out these computations, it appears that for the different atoms the run with depth of the concentration does not vary much so far as the lower energy-levels are concerned. One can schematize the run with depth of the ratio (concentration) : (coefficient of continuous absorption) by putting the effective layer-thickness τ_1 equal to 0.5. This run is not yet identical with

that of the function $a(\tau)$, because both the damping and the Doppler effect are each time different at different depths, but a computation of these changes would only be possible by extended investigations of the various Fraunhofer lines separately. For the far wings of the Na D lines B. Strömgren [54]) found a run for $a(\tau)$ — which he denotes by η — which can be described by $\tau_1 = 1.5$ *) (see § 34, Fig. 43). Especially as the computations are still rather uncertain, we cannot do better than assume that the damping influence is of the same order of magnitude for the other atomic lines. For the Ca^+ lines $\tau_1 = \infty$ will yield a fair approximation, the more so as it will appear that the centre-limb variation is practically independent of τ_1, once this quantity is larger than 3.

According to § 26, $a = k + s + l$ can be split up into these three quantities in various ways as a consequence of the non-coherent scattering. Once $a(\tau)$ is known, $k(\tau)$, $s(\tau)$ and $l(\tau)$ are obtained with the aid of the formulae in § 26. From their run one can then estimate $\tau_{1,k}$, $\tau_{1,s}$ and $\tau_{1,l}$. As will appear in the next paragraph the value of $\tau_{1,l}$ is considerably less than those of $\tau_{1,k}$ and $\tau_{1,s}$.

If, however, collisions of the second kind also play a part in the formation of the Fraunhofer lines, this will lead to the occurrence of true selective absorption and in this case $\tau_{1,k}$ has a different, larger, value which can be estimated by taking into account that the run of $k(\tau)$ differs from that of $a(\tau)$ by a factor which increases with the pressure.

As regards the simultaneous action of the various formal processes the following statement can be made. In the far wings each result of one of the processes with its own τ_1 can be combined directly with the result of another process also with its own τ_1, owing to the additivity of the small depressions.

In the more central parts of the lines the final formula (21) in § 20 applies only to the computation of the three effects together on condition that their three τ_1's coincide. This is mostly not the case; it will appear, however, that important qualitative information concerning the processes in action can, nevertheless, be obtained.

§ 30. The runs of $B(\tau)$, $J_\nu(\tau)$ and $\bar{J}(\tau)$.

In the schematized model of the solar atmosphere designed in Chapter III, the run of $B(\tau)$ is given by (2) and that of $J_\nu(\tau)$ by (9) and (10).

*) In the other parts of the line the run of $a(\tau)$ is different from that in the far wings, owing to Doppler effect and damping.

The run of $B(\tau)$ is linear and depends further solely on β_0. The run of $J_\nu(\tau)$ depends on the contrary on all parameters, with the exception of ϑ, occurring in the equation of transfer, namely β_0, τ_1, k, s and l. Guided by what was stated in this connection in §§ 28 and 29, we shall use for β_0 and τ_1 the values which fit in in a plausible way with the Fraunhofer lines investigated and which represent the behaviour of these lines as closely as possible. For β_0 the values given in § 28 are taken; for τ_1, the values by which in all probability the run of $k(\tau)$ and $s(\tau)$ for the far wings can be best schematized (see § 29). That the run of these quantities in the far wings in particular is taken is based on the fact that for the points of the profile closer to the centre of the line, the value of τ_1 grows less and less important, as practically all the light corresponding to these points originates in layers of the atmosphere located above the boundary $\tau = \tau_1$.

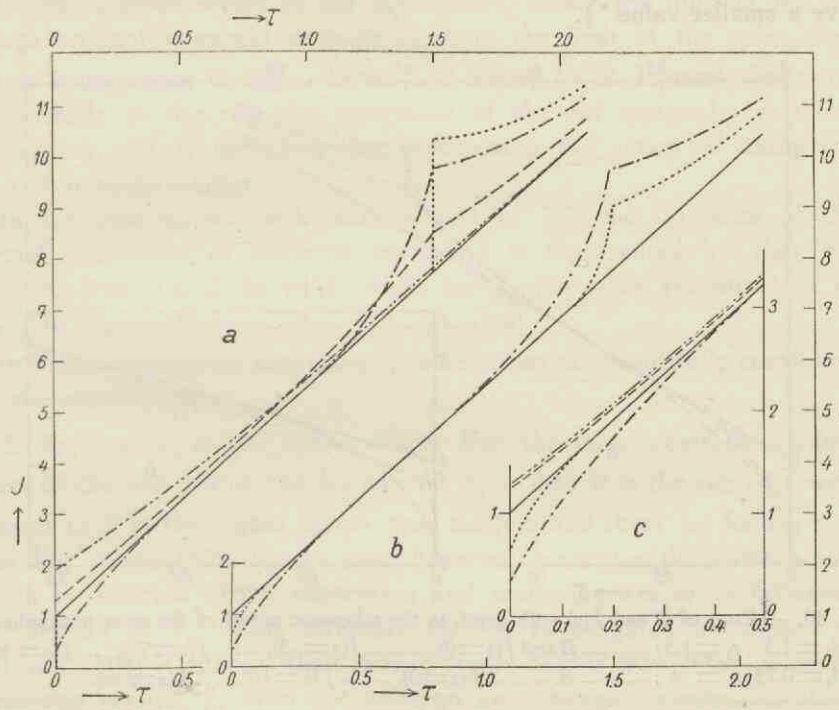

Fig. 39. — Runs of B, $J(s)$ and $J(k)$ with depth in the schematic model of the solar atmosphere for $\beta_0 = 4.5$ (all of them in terms of B_0).

a) $\tau_1 = 1.5$; ——— B, — . . — $J(s = 0)$, — — — $J(s = 1)$, — . — $J(s = 16)$, ... $J(s = \infty)$.

b) $\tau_1 = 1.5$; ——— B, — . — $J(s = 16)$, ····· $J(k = 16)$.

c) $\tau_1 = \infty$; ——— B, — ···· $J(s = 1)$, — — — $J(k = 1)$, — . — $J(s = 16)$, ... $J(k = 16)$.

A clear ordered investigation of the dependence of J_ν on k, s and l is impossible by any other means than by the successive determination of $J_\nu(\tau)$ as a function of each of these three quantities separately.

Figures 39 and 40 show for a few selected values of s the curves for $J_\nu(s, \tau)$ belonging to the added values of β_0 and τ_1. When one compares these curves for each set of values for β_0 and τ_1 with each other and with the run of $B(\tau)$, it appears that in the various spectral regions the runs of the J_ν's and B differ essentially from each other. It is, however, possible to make an important *general statement:* for all sets of values of β_0 and τ_1, the curve for $J_\nu(s \to \infty)$ coalesces with the one for B except for $\tau = 0$ and for $\tau \lessgtr \tau_1$. For other large values of s, J_ν deviates from B only for small values of τ and $\tau_1 - \tau$ and for $\tau > \tau_1$. This gives already an indication for the run of $\bar{J}(\tau)$, which, between $\tau = 0$ and $\tau = \tau_1$, where the J_ν's coincide for larger s-values with B, is practically equal to B, whereas in the highest layers $\bar{J}$ will have a smaller value *).

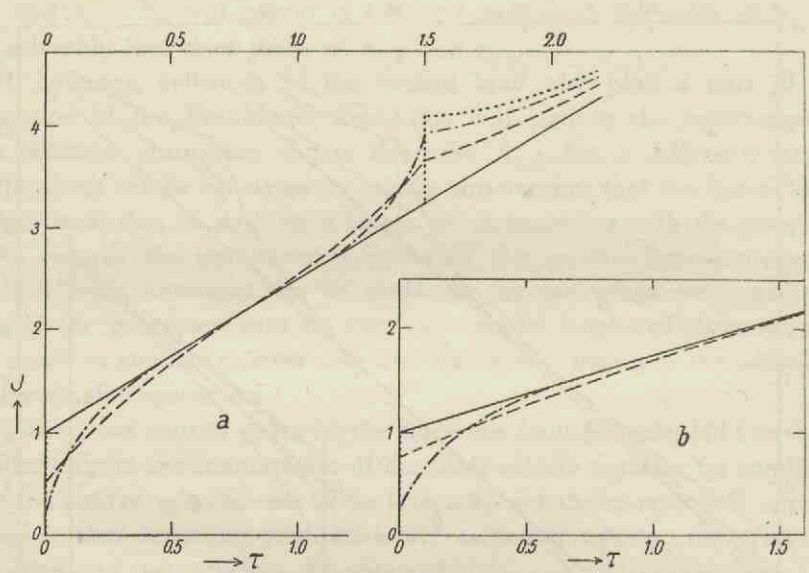

Fig. 40. — Runs of B and $J(s)$ with depth in the schematic model of the solar atmosphere. *a*) $\beta_0 = 1.5$, $\tau_1 = 1.5$; ——— B and $J(s=0)$, – – – $J(s=3)$, –.– $J(s=29)$, ... $J(s=\infty)$. *b*) $\beta_0 = 0.75$, $\tau_1 = \infty$; ——— B, – – – $J(s=0)$, –.– $J(s=10)$, ... $J(s=\infty)$.

*) The differences between $\bar{J}$ and B in those layers, for which τ is slightly smaller than τ_1 and $> \tau_1$ need not be taken into account, because they become large only for larger values of s and k; the observed light in those parts of the Fraunhofer lines where s and k have these larger values originates, however, chiefly in higher layers of the atmosphere.

For comparison the run of $J_\nu(k, \tau)$ for a few values of k is drawn in Fig. 39 b and c together with the run of $J_\nu(s, \tau)$. Although both these runs are of a similar nature, the $J_\nu(k)$'s differ less from B than the $J_\nu(s)$'s, and this is true for all values of β_0 and τ_1. This means that $\bar{J}(k)$ will deviate appreciably from B only in still higher layers than $\bar{J}(s)$ does.

1. *Application to the far wings.* So long as one may assume that $\bar{J}(\tau)$ coincides with $B(\tau)$, the behaviour of the Fraunhofer lines in the case of complete redistribution can be described by absorption (see § 26, a). This description is purely formal (one need not at all have in mind, for example, collisions of the second kind) and signifies that the selective emission is connected with the absorption in the same way as in the case of selective absorption; the run of the formally introduced $k(\tau)$ agrees then with that of the actual $a(\tau)$. The condition $\bar{J} = B$ is satisfied in those layers of the atmosphere, where the light in the far wings originates, except perhaps close to the limb of the solar disc, where it originates in higher layers and where $\bar{J} < B$. It must, therefore, be possible to describe the behaviour of the far wings by selective absorption and, if necessary, by superposing the action of extinction in a thin surface-layer.

In the case of widened energy-levels (§ 26) the influence of the formal coefficient of coherent scattering is represented by the first emission-term $n a_\nu J_\nu$ in (41), while for J_c the same remains true as for $\bar{J}$ in the case of complete redistribution.

In § 32 it will appear that these considerations are beautifully confirmed by the observations.

2. *Application to the inner wings.* For the more centrally located parts of the line-profile (as far as $r(0, \vartheta) = 0.5$) it is the run of $\bar{J}$ with respect to B in the higher layers, that matters and there we have $\bar{J} < B$ (see Fig. 39 and 40). In this case, however, extinction does also occur, which in addition to the absorption and scattering exerts its influence on the run of J_ν. This influence can be investigated by means of (9) and (10); it appears then that in layers deeper than those in which extinction occurs, J_ν does not undergo any change (whereas in these same layers coherent scattering and absorption do influence J_ν). As soon, however, as extinction sets in, the value of J_ν decreases. In that case $\bar{J}$ will decrease obviously also, so that in the high layers the influence of the extinction is still greater than followed already from

the runs of $\bar{J}(s, \tau)$ and $\bar{J}(k, \tau)$. The true run of $\bar{J}$ can only be approximated by successive steps. One can start from $\bar{J}(\tau) = B(\tau)$. Then, according to § 26, 1a: $\cos\vartheta \, dI_\nu/d\tau = (1 + k_\nu) \, I_\nu - k_\nu \, B - B$. By assuming one or other definite run of $k(\tau)$ one can then calculate $J(k, \tau)$. If, for instance, one assumes $k(\tau)$ according to the schematic model, one arrives for $J(k, \tau)$ at (9) and (10). In order then to obtain $\bar{J}$ from the J_ν's, it is necessary to know the run of $k(\nu)$ over the spectral line. This $k(\nu)$ depends on Doppler effect and damping. The damping constant γ, occurring in the expression for $k(\nu)$ and which is the sum of the damping constants for radiation and for collisions, varies with the depth in the solar atmosphere. If γ were known, one would be able to compute $\bar{J} = \dfrac{\int J_\nu \, k_\nu \, d\nu}{\int k_\nu \, d\nu}$ for every τ. The ratio between the coefficients of extinction and absorption is then $\dfrac{l_\nu}{k_\nu} = \dfrac{B}{\bar{J}} - 1$ (§ 26, 1c) and the equation of transfer becomes, once more:

$$\cos\vartheta \frac{dI_\nu}{d\tau} = (1 + k_\nu + l_\nu) \, I_\nu - k_\nu \, B - B. \tag{35}$$

If this approximation should be sufficient, one can then compute the emerging radiation $r(0, \vartheta)$; this cannot be carried out by means of (21), since in general the effective $\tau_{1,l}$ and $\tau_{1,k}$ will be different. The solution must, therefore, be obtained by a numerical method, most readily with the integral expression (20), in which s must then be equal to 0. If a second approximation should prove the first one to be insufficient, one must, with the aid of (35), compute again the J_ν's, after which the whole scheme must be worked through once again.

If the point of view of the widened energy-levels is adopted, one must in a first approximation start from the equation of transfer (41), in which also s occurs and where the ratio γ_m/γ_n appears as an unknown quantity.

It is evident that in the present stage of our knowledge concerning, on the one hand the run of the black-body radiation, the concentration of the various atomic states in the solar atmosphere and the damping, and, on the other hand, the non-coherent scattering, it is not possible to pass on to a quantitative calculation, such as is outlined in the above.

3. *Application to the parts of the line-profile close to the centre.* If, now, one examines those parts of the profile of a Fraunhofer line, that

are located still closer to its centre and where $r(0,0) = 0.30$, it is known that in the high layers where, this time, the light chiefly originates, the deviation of $\bar{J}$ from B increases more and more. $\bar{J}$ will now, however, differ less from the corresponding J_ν (because the coefficient of absorption for these parts of the Fraunhofer line is larger, see (26), the definition of $\bar{J}$) and the comparison of $\bar{J}$ with J_ν now suggests itself. If $\bar{J}(\tau)$ should be equal to $J_\nu(\tau)$, the behaviour of the Fraunhofer lines could be described by means of coherent scattering. This equality, however, cannot be expected to exist over the entire τ-region in question, so that according as $\bar{J} < J_\nu$ or $> J_\nu$, extinction or increased emission must be superposed to a certain extent on the coherent scattering. One can expect, however, that for these parts of the lines a description by means of absorption must make room for a description, if only an approximate one, by means of coherent scattering. This way of viewing our problem will also be confirmed by the observations.

4. *Application to the central intensities.* Finally one comes to deal with the central intensities; the light originates now in the uppermost layers of the solar atmosphere, where the damping by collisions is very slight. The coefficient of absorption has, for that reason, a sharp maximum at the centre of the line and, since it is known from the observations that the radiation-density in the line centre, J_c, is not zero, it follows from the definition of $\bar{J}$, that $\bar{J} \approx J_c = J_\nu$. In the light of the considerations in § 26 the central intensities should, therefore, be formally described by means of coherent scattering, which, as is well-known, would lead to the value zero for the centre of the line, but this is at variance with the observations. The central intensities can, however, be explained in another way, as shown by A. Unsöld [2]) and B. Strömgren [3]); we shall enter into further detail on this point in Chapter VIII.

CHAPTER VI

THE TESTING OF THEORETICAL STATEMENTS BY MEANS OF OBSERVATIONS PERTAINING TO THE FAR WINGS

§ 31. Manner of comparing theory and observation.

Fig. 41 shows theoretical curves, representing for the selected values of β_0 (§ 28) and a set of four values of τ_1 the centre-limb variations for absorption, coherent scattering and extinction separately. These curves were obtained by computing by means of the formulae (22), (23) and (24) the *depressions* $1-r(0,\vartheta)$, assigning to k, s and l such values that for $\cos\vartheta = 1$ (centre of the sun's disc) the depression is 5 % or less. The depressions computed in this way for various values of $\cos\vartheta$ are then replaced by their ratios to the depressions for $\cos\vartheta = 1$ and these ratios are plotted against $\cos\vartheta$. Greater ordinates of the curves obtained in this way represent, therefore, deeper depressions of the line-profile. Table 21 gives, for each set of values for β_0 and τ_1 for which a curve is drawn in Fig. 41, the values for k, s and l, which cause a depression of 5 % in the profile of the line for the centre of the sun's

Table 21. **Values of k, s and l which, for the Centre of the Sun's Disc, cause a Depression of 5 % in the Line-Profile according to (21).**

β_0	4.5				1.75				0.75			
τ_1	0.1	0.5	1.5	∞	0.1	0.5	1.5	∞	0.1	0.5	1.5	∞
k	0.64	0.16	0.084	0.065	0.88	0.21	0.108	0.086	1.3	0.30	0.162	0.130
s	0.81	0.18	0.092	0.072	0.89	0.21	0.111	0.086	1.0	0.25	0.139	0.114
l	0.51	0.11	0.045	0.029	0.52	0.11	0.048	0.033	0.5	0.12	0.053	0.037

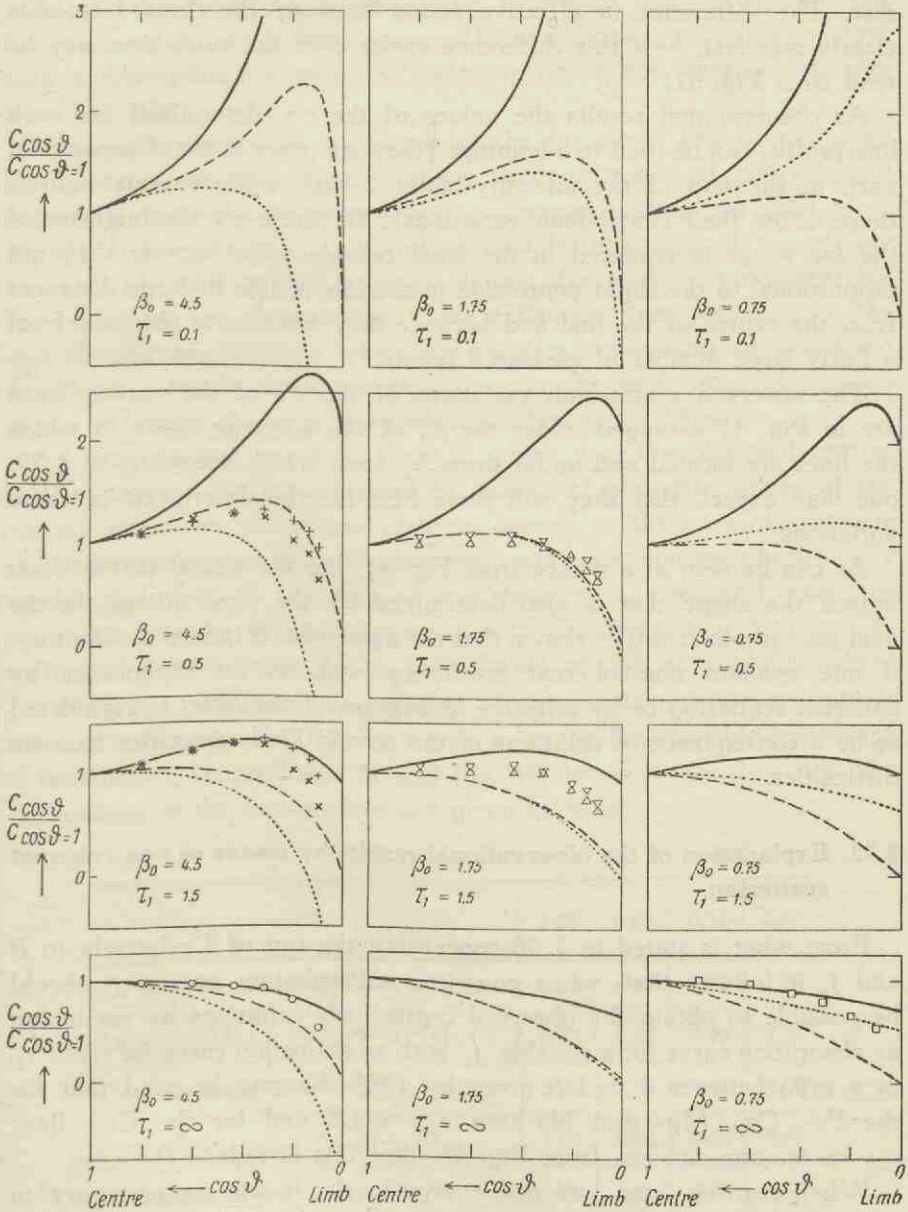

Fig. 41. — Computed centre-limb variations of c: ——— absorption, ... coherent scattering, —— extinction. Observations added: ○ K line of Ca+, + Fe multiplet at 4100 A, × Ca 4226.7, △ Mg b lines, △ Na D lines, □ infra-red lines of Ca+.

disc. The difference in effective action between the three factors is clearly manifest; how this difference varies over the sun's disc may be read from Fig. 41.

As observational results the values of the c's, determined for each line-profile, can be used to advantage (they are given in the observational part, at the end of the intensity-tables 2—20, while various figures, there, show their centre-limb variations). By these c's the intensity of the far wings is rendered in the most reliable way, because they are proportional to the slight depression in the line-profile at large distances from the centre of the line and because they have been obtained from a fairly large number of measured points.

The observed centre-limb variations of the c's of the various lines are in Fig. 41 arranged under the β_0 of the spectral region in which the lines are located and under those τ_1 from which according to § 29, one may expect, that they will serve best for the description of these variations.

As can be seen at a glance from Fig. 41, the theoretical curves show indeed the shape that is also determined by the observations. In the next paragraphs it will be shown that the agreement is indeed satisfactory, if one assumes non-coherent scattering, whereas an explanation by coherent scattering or by selective absorption, if the latter is considered to be a consequence of collisions of the second kind, gives rise to some difficulties.

§ 32. Explanation of the observational results by means of non-coherent scattering.

From what is stated in § 30 concerning the run of $\bar{J}$ relatively to B and J_ν it follows that, when complete redistribution occurs, it should be possible to obtain the observed centre-limb variations by combining an absorption curve for a suitable τ_1 with an extinction curve for small τ_1, in a ratio between k and l, given by (36). Bearing in mind that for the Fe-, Ca-, Mg- and Na-lines $\tau_{1,k} \approx 1.5$ and for the Ca^+ lines $\tau_{1,k} \approx \infty$, one can see from Fig. 41, that this is indeed the case.

When starting from widened energy-levels, it will be necessary to add to every combination of an absorption curve and an extinction curve also a scattering curve (see § 26, 2), for which the value of $\tau_{1,s}$ is the same as that of $\tau_{1,k}$ mentioned above. As can be seen, the observations can also be described in this way, provided the share of the coherent scattering be not too great.

As yet the values of τ_1 cannot be absolutely reliable (§ 29), and for values smaller than those assumed here, the observations fit in better with a description by means of selective absorption only, as appears from Fig. 41.

When the centre-limb behaviour of the far wings can be described by means of absorption, this proves the occurrence of non-coherent scattering, in so far as true selective absorption does not take place (§ 33). If one is willing to accept as reliable the values of τ_1, as they are made plausible in § 29, a certain degree of extinction is indispensable for explaining the observations. Since extinction does not occur in the case of coherent scattering, whereas in the case of non-coherent scattering it follows naturally from the conditions in the solar atmosphere, *this proves a fortiori the occurrence of non-coherent scattering.*

An example may serve to show in which way the observed centre-limb variations can be explained by means of plausible values of the various quantities, when one restricts oneself to the case of complete redistribution, so that selective absorption and extinction must be formally combined. For the K line of Ca^+ was assumed $\tau_{1,k} \approx \infty$; further one can take by way of an estimate $\tau_{1,l} = 0.1$, since it is known that extinction sets in only in the high layers of the atmosphere, where $\bar{J} < B$ (§ 30). An exact computation of $\tau_{1,l}$ would only be possible in the way indicated in § 30, 2, for which, however, the available knowledge is insufficient. Using Table 21 and Fig. 41, one finds for $\beta_0 = 4.5$ (the depressions in the line-profiles are given in %):

$\cos\vartheta$	1.00	0.60	0.31	0.10
For $\tau_{1,k} = \infty$, $k = 0.065$: $1-r(0,\vartheta)$ . .	5.00	4.50	3.55	1.85
For $\tau_{1,l} = 0.1$, $l = 0.032$: $1-r(0,\vartheta)$ . .	0.32	0.52	0.96	2.24
Total depression: $1-r(0,\vartheta)$	5.32	5.02	4.51	4.09
From which: $c_{\cos\vartheta}/c_{\cos\vartheta} = 1$ . . .	1.00	0.94	0.85	0.77
Observation, K line	1.00	0.96	0.87	0.49

By slightly modifying the choice of $\tau_{1,l}$ and l, a better agreement with the observations can be certainly attained. As, however, for the present only an orientation concerning this kind of computations is meant, the

above will suffice. The value assumed for l leads to $\frac{l}{k} = 0.5$, from which it follows by (36) that $B/\bar{J} = 1.5$, this being a very plausible result for this ratio in the extreme part of the solar atmosphere between $\tau = 0$ and $\tau = 0.1$. In an analogous way the centre-limb variation of the far wings of the other lines can be qualitatively explained.

It is still of some importance to remark that the observed centre-limb behaviour of the resonance lines does not differ from that of the subordinate lines, a fact which can be seen particularly clearly when one compares the resonance line Ca 4226.7 with the lines of the Fe multiplet in the neighbourhood of 4100 A. This is in accordance with the conception of the origin of non-coherent scattering as arising from a widening, due to collision damping, of the distribution of the absorption-coefficient over the frequencies, such as underlies the reasonings in Chapter IV, so that this must occur for resonance- and subordinate lines in an analogous manner.

§ 33. Impossibility of an explanation by means of coherent scattering and true selective absorption.

From Fig. 41 it is clear, that an explanation by means of coherent scattering only, is not possible. This is chiefly apparent in the case of the violet lines, where the theoretical centre-limb variations, due to absorption and scattering differ mutually to a sufficient extent.

In a number of publications selective absorption due to collisions of the second kind *) has been called to the rescue in elucidating the conceptions concerning the origin of the Fraunhofer lines. One might, perhaps, feel inclined to make use of this explanation also in the present connection, since it turns out that the centre-limb variations can be described by means of a coefficient of selective absorption. This idea becomes the more tempting when one considers that the observed radiation in the far wings originates in the deeper layers of the atmosphere, so that, if collisions of the second kind contribute anywhere to the formation of the Fraunhofer lines, it must be in these parts of their line-profiles. Now from the observations it is obviously not possible to distinguish between a description by means of a formal coefficient of absorption which is due to non-coherent scattering and a description by means of a coefficient of absorption, which is due to collisions of

*) This is what is called true absorption.

the second kind. From the following considerations, however, one can safely conclude, that the conception of non-coherent scattering, which is directly inherent to the use of a formal coefficient of absorption, is indispensable. Indeed, one must expect the number of collisions of the second kind to become gradually less in the higher, less dense, layers of the atmosphere. Now, on the assumption that in these layers the Fraunhofer lines originate chiefly through coherent scattering, the centre-limb observations should show a transition from selective absorption to coherent scattering from the centre to the limb of the sun's disc, and no trace of such a transition is to be found in the case of the well-determined centre-limb variations of the violet lines ($\beta_0 = 4.5$, Fig. 41). For $\beta_0 = 1.75$ no information is to be gained in this respect from theory because no distinction can be made between absorption and scattering.

That this effect ought to have been noticeable for $\beta_0 = 4.5$, appears from the following estimate. For the optical depth τ_m a value is fixed in such a way, that for the wave length in question, the amounts of emerging light, that originate in the layers for which $\tau > \tau_m$, and in those for which $\tau < \tau_m$, are equal. For the far wings τ_m is practically the same as the one for the adjacent continuous spectrum, so that we can write for the far wings of the violet Fraunhofer lines:

$$\int_0^{\tau_m} B(\tau)\, e^{-\tau \sec\vartheta} \sec\vartheta \, d\tau = 0.5 \int_0^{\infty} B(\tau)\, e^{-\tau \sec\vartheta} \sec\vartheta \, d\tau,$$

from which, with $B = B_0 (1 + \beta_0 \tau)$, $\beta_0 = 4.5$ and $\cos\vartheta = 1$ resp. 0.1; one obtains $\tau_m = 1.25$ resp. 0.1.

In B. Strömgren's [54]) model of the solar atmosphere a transition from $\tau = 1.25$ to 0.1 causes a decrease of the pressure of the gas with a factor 4 and of the electron pressure with about a factor 10. These differences are sufficient to justify the expectation of the above-mentioned transition from absorption to scattering.

Summarizing we can conclude that *true selective absorption is of no importance* whatever in the explanation of the centre-limb variation in the far wings of Fraunhofer lines.

§ 34. The influence of the run of the concentration.

In this and the next paragraph the influence will be investigated of the variations in the run with depth of concentration and black-body radiation, in order to obtain at least some idea of the influence of deviations from our very simple model. If the preceding statements are to remain valid, they must hold equally well for other cases, which

might likewise approximate the true state of things, and in which the run of concentration and of black-body radiation differs from what, for simplicity, has been assumed so far. It will be proved more in particular that not any plausible run with depth of concentration and of black-body radiation can explain the observed centre-limb variations of the quantity c, that means, of the far wings, by means of coherent scattering.

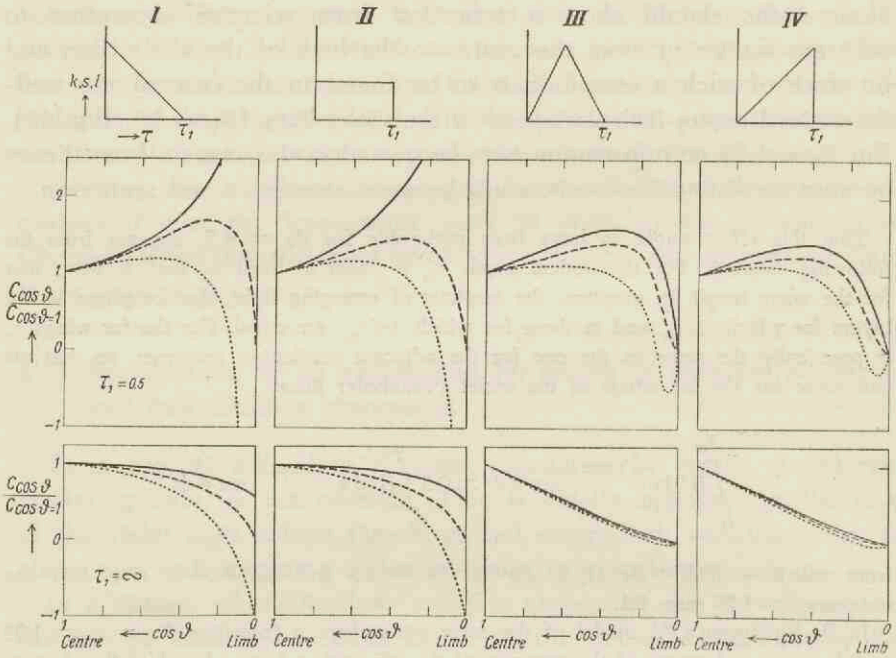

Fig. 42. — Computed centre-limb variation of c for various cases of the run with depth of k, s and l, all of them for $\beta_0 = 4.5$ (violet part of the spectrum): — — — absorption, ... coherent scattering, —— extinction. As appears from the drawings at the top, the four models are arranged according to decreasing concentration at the surface; in each of the models τ_1 can vary from 0 — ∞, from this range the values 0.5 and ∞ have been selected for the construction of the figures.

In our simple model the concentration of the active atomic state was assumed each time in such a way that the ratios between the selective absorption and the scattering on the one hand and continuous absorption on the other hand, were constant down to a certain definite optical depth τ_1, whereupon it dropped abruptly to zero. We shall now examine three cases, where this is not so, though for the time being we still assume B to increase linearly with τ. Together with our first model

we have then four models at our disposal, by means of which we can judge the influence of the run of k, s and l respectively. The investigation is carried out for the violet spectral region only, characterized by $\beta_0 = 4.5$. This region was selected for the following reasons: the theoretical runs of selective absorption, coherent scattering and extinction differ, here, mutually to a sufficient degree (Fig. 41); in this region reliable observational results from a number of lines are available, which could not be explained with the aid of coherent scattering only, for which, moreover, s would be assumed to be constant down to τ_1. The run of k, s and l respectively is adopted as represented in the graphs at the top of Fig. 42 *). In passing from model I to model IV we imagine, therefore, the active atoms to be less and less strongly concentrated at the surface. In each of the models the layer containing the atoms can be assumed to have any thickness desired. It appeared sufficient to carry out the computations for $\tau_1 = 0.5$ and ∞; in between one can interpolate qualitatively. In the latter case, the models I and II, respectively III and IV merge, as a matter of course, into each other.

The numerical computations for the extinction were carried out by means of formula (20), whereas, since we are here concerned with the small depressions of the profile in the far wings, for the selective absorption and the coherent scattering were used the formulas of M. Minnaert [63]). These are, for absorption:

$$\frac{i_0 - i}{i_0} = 1 - r(0,\vartheta) = \int_0^\infty \frac{\beta_0 \cos\vartheta}{1 + \beta_0 \cos\vartheta} e^{-\tau \sec\vartheta} \sec\vartheta \, k(\tau) \, d\tau \qquad (43)$$

and for scattering:

$$1 - r(0,\vartheta) = \int_0^\infty \frac{\beta_0 \cos\vartheta + (0.49 - 0.29\,\beta_0)\, e^{-\sqrt{3}\tau}}{1 + \beta_0 \cos\vartheta} e^{-\tau \sec\vartheta} \sec\vartheta \, s(\tau) \, d\tau. \qquad (44)$$

The models I—IV have been chosen in such a way, that, while the runs with depth differ mutually as much as possible, they all lead to expressions in the above formulas, admitting of an easy integration. In deducing his formulas Minnaert uses the boundary conditions

*) The runs of k, s and l will not, in general, be identical for the same Fraunhofer line. Strictly speaking, therefore, we deal with three differently constituted atmospheres in each of the four "models".

$J_{\tau=0} = 1.8\, H_{\tau=0}$, in accordance with A. Pannekoek [16]), whereas in the present thesis constant use is made of $J_{\tau=0} = 2\, H_{\tau=0}$. The difference in the results is insignificant, as appears from a comparison with previous computations for model II, carried out by means of the more detailed formulas (22) and (23). The values of c differ by no more than 1 %, except for scattering at the outermost limb, where the difference amounts to a few percents. The satisfactory agreement justifies our relying on Minnaert's formulas for the other models as well.

The character of the centre-limb variation can be understood in all cases shown in Fig. 42; for example, the value $c_{\cos\vartheta=0} = 0$, for absorption and scattering as well as for extinction, in the models II and IV arises from the fact that, here, the concentration at the sun's surface becomes zero, so that in looking grazingly along the atmosphere the selective action of the atoms vanishes and the intensity of the lines, and likewise c, become zero.

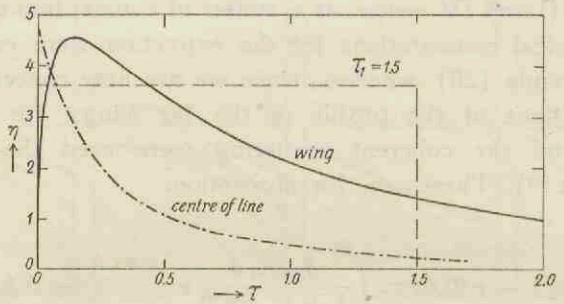

Fig. 43. — Run of η, the ratio of the summed up selective absorption and scattering to the continous absorption, deduced by B. Strömgren for the Na D lines. The ordinates are expressed in arbitrary units, which differ for the wings and the centre of the line but are the same for the run in the wing and the schematic run with $\tau_1 = 1.5$.

We shall restrict ourselves to the following conclusion: even if the run of the concentration be strongly varied, *the centre-limb variation of the wings cannot be explained by means of coherent scattering only*, and, because the considerations in § 33 apply to each of the four models (these models showing, namely, qualitatively the same centre-limb variation), true selective absorption is out of the question.

Based on the most recent ideas concerning the constitution of the solar atmosphere B. Strömgren [54]) has computed the run of $a(\tau)$ — which he denotes by η — for the Na D lines (Fig. 43). We shall examine

what the centre-limb variation in the wings is like on the assumption of this fairly well-founded run with depth, and we shall compare this variation with the one from the simple model for $\tau_1 = 1.5$. The numerical computations, using Strömgren's run, were carried out with the aid of Minnaert's formulas (43) and (44) for absorption and scattering and of the formula (20) applied to extinction only. Here again B was still assumed to be linear in τ while, for simplicity, β_0 was taken equal to 1.69, so that the factor $0.49—0.29\beta_0$ in formula (44) becomes zero, and absorption and scattering yield, thereby, the same expression. In the simple model β_0 was taken equal to 1.75, so that, as a matter of course, the results do not differ appreciably from those for $\beta_0 = 1.69$. How little it matters whether one uses Strömgren's run or the constant value down to $\tau_1 = 1.5$ in the simple model, can be seen from Fig. 44.

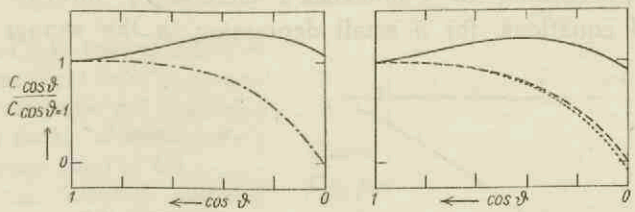

Fig. 44. — Centre-limb variations of the c's for the Na D lines. Left: computed with a run of k, s and l which is the same as that of Strömgren's η (using run for wing of Fig. 43). Right: k, s and l according to our simple model with $\tau_1 = 1.5$, computed with formula (21) (c.f. Fig. 43).
— — — absorption, ... coherent scattering, —— extinction.

It appears, therefore, that, for $\beta_0 = 4.5$ as well as for $\beta_0 = 1.75$, the actual run of k, s and l, can be fairly well approximated by a rectangular run, so that, so far as the run of the concentration is concerned, the conclusion already drawn remains valid, namely, that the observed behaviour of the far wings can only be described by means of non-coherent scattering.

§ 35. The influence of the run of the black-body radiation.

So far, it has in the present thesis invariably been assumed for the black-body radiation, that its run with depth is given by $B = B_0 (1 + \beta_0 \tau)$. It is quite possible that in some wave-length regions considerable deviations occur, although little can be said as yet, as regards the nature and the amount of these deviations. The darkening towards the limb, according to Abbot's measurements, for example, is

especially in the region round 4000 A such a practically perfect linear function of $\cos\vartheta$ (see [86])), that the deviation of B from a linear run with τ cannot be serious, apart, perhaps, from the highest layers, which, however, are of no concern in this problem. Contrary to this run, there is the more or less curved run for other wave lengths. From measurements by W. H. J. Moll, H. C. Burger and J. van der Bilt [84]) of the darkening towards the limb, H. H. Plaskett [87]) and I. W. Busbridge [88]) deduced for 5500 A a run of $B(\tau)$, deviating strongly from a linear run with τ. With the $B(\tau)$, as found by Plaskett (Fig. 45), I have once again computed the centre-limb variations, making use of the run of concentration with depth according to Strömgren and only taking into account *coherent* scattering (Fig. 46). The numerical computations were carried out by subdividing τ into little steps and finding first the run of $J(\tau)$ (Fig. 45) according to Pannekoek's method [52]) directly from the differential equations, for a small depression in the wings.

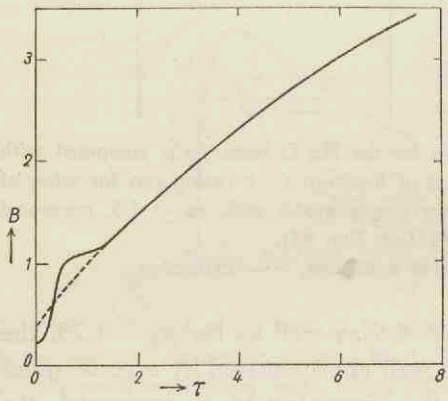

Fig. 45. — Run of B, computed by H. H. Plaskett from the observations of W. J. H. Moll, H. C. Burger and J. v. d. Bilt; ---- J, the radiation-density in the far wings of a Fraunhofer line.

From a comparison of the centre-limb variation computed with $B = B_0\ (1 + 1.69\ \tau)$ and with Plaskett's B, both times using the same steps in τ, it appears (see Fig. 46) that the run of the black-body radiation with depth has a rather considerable influence, but that neither with the $B(\tau)$, deduced by Plaskett, is any agreement with the observations obtained, so long as one restricts oneself to coherent scattering. Nor is this to be expected with the $B(\tau)$ run, deduced by Busbridge. One would have to assume $B(\tau)$ in such a way, that, in rising from the deeper layers, it first decreases and then remains constant in the outer layers, or even increases again. This is strongly at variance with everything known theoretically of B and with what is deduced from

the continuous darkening towards the limb, so that it is impossible to find herein an explanation of the observed centre-limb variation of the wings. For Plaskett's run of $B(\tau)$ the deviations from the observations are restricted to those points for which $\cos\vartheta < 0.25$, that means close to the limb, but here the deviations are appreciable. The cause of the difference between the centre-limb variations computed with a linear $B(\tau)$ and with Plaskett's $B(\tau)$ can be seen at once: for points close to the sun's limb it is the B run in the upper layers that chiefly matters, where, according to Plaskett it rises more rapidly than according to $B = B_0 (1 + 1.69\,\tau)$; in other words, we have to expect that, there, the centre-limb variation computed with Plaskett's B will agree with a linear run of B, in which β_0 has a larger value, and this is indeed the case, as appears from a comparison of Fig. 46 with Fig. 41.

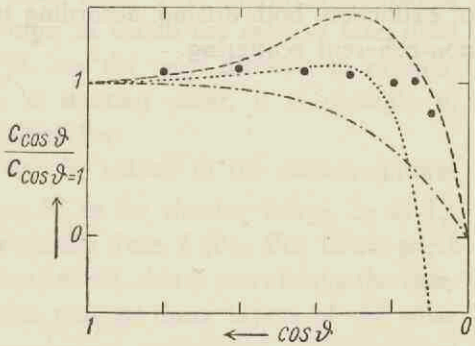

Fig. 46. — Centre-limb variations of the c's for the Na D lines. Theoretical curves, for which the run of k and s is the same as that of Strömgren's η in the far wings (see Fig. 43): — . — absorption and coherent scattering with $B = B_0 (1 + 1.69\,\tau)$; - - - - absorption, ... coherent scattering, both with B according to Plaskett (c.f. Fig. 45). ● From observations.

If, however, non-coherent scattering is assumed instead of coherent scattering, one must expect that the centre-limb variations can be partly described by means of a coefficient of absorption (§ 26). As the share of the absorption is unknown, the computations are carried out for absorption only, in order at least to be able to judge the extent to which the agreement with the observations has improved. In these computations the same subdivision of τ was used as in the preceding computations for coherent scattering; the result is the centre-limb variation shown in Fig. 46. It appears, once again, that $B(\tau)$ has a strong influence, which can be seen by a comparison with the curve for linear $B(\tau)$ likewise computed for the case of absorption. The gratifying point, however, is now, that this time the observations lie between the centre-limb variations computed in the two ways.

For various reasons the description by means of complete absorption may not be the right one. In the first place extinction also must still be

taken into account for the outermost layers of the solar atmosphere, in the second place also coherent scattering, namely, if the conception of the widened energy-levels should be the right one, while in the third place the question remains how closely the $B(\tau)$ run, derived by Plaskett, approximates its true run. Yet, for all that, it is once again clear that *non-coherent scattering furnishes a better description of the observations than that given by coherent scattering.*

Summarizing the two preceding paragraphs one can state that neither plausible changes in the run of the concentration, nor those in the run of the black-body radiation enable one to explain the observations by means of true selective absorption or coherent scattering or by a combination of these two, and that this can only be done by the introduction of a formal coefficient of selective absorption and a coefficient of extinction, both arising, according to the considerations in § 26, from non-coherent scattering.

CHAPTER VII

COMPARISON OF THE THEORY WITH THE OBSERVATIONS CONCERNING THE INNER WINGS

§ 36. Introduction.

The centre-limb variations of those parts of a line-profile between the centre of the line and the far wings, in which the relative intensities have amounts between 30 and 80 %, are the most difficult to explain. Taking non-coherent scattering as a starting point, it is possible to indicate accurately where the difficulties lie.

Indeed, the equation of transfer can be solved in the easiest manner if $\bar{J}$ admits of a simple expression in B, as for the far wings, or in J_ν, as for the central parts of the line-profile (see § 30). For those parts of the line-profile, that will now be considered, this is not always the case. The observed radiation originates this time in those layers of the solar atmosphere, for which, for the time being, nothing of a quantitative nature can be stated as regards the run of $\bar{J}(\tau)$ relatively to $B(\tau)$ and $J_\nu(\tau)$. Fortunately, however, one can make *two qualitative statements,* which can be tested. As the first, one can state that towards the centre of a line, the influence of the formal coefficient of coherent scattering becomes more and more predominant over that of the selective absorption (§ 30). The second one is based on a comparison between Fraunhofer lines in the various spectral regions for which the run of $\bar{J}(\tau)$, with respect to $B(\tau)$ and to $J_\nu(\tau)$ is essentially different (§ 30) which manifests itself characteristically in the centre-limb variations.

§ 37. Manner of comparing theory with observation.

The comparison of the theory with the observations is again performed by means of figures, showing theoretical curves for various values of β_0 and τ_1, each time for absorption, coherent scattering and extinction

separately, while the observational results are given in various sub-figures (Fig. 47 and 48). These results have been obtained by first tracing with the aid of the data from Tables 2—20 the complete undisturbed line-profiles. If, now, it was thought advisable to draw for example in Fig. 47 for a Fraunhofer line a centre-limb series of observations, which

Table 22. **Values of k, s and l belonging to the Curves in Fig. 47.**

β_0	4.5				1.75				0.75			
τ_1	0.1	0.5	1.5	∞	0.1	0.5	1.5	∞	0.1	0.5	1.5	∞
k	7	2	1	1	10	3	2	1.5	∞	∞	∞	10
s	7	2	1	1	10	3	2	1.5	15	4	3	3
l	6	1.3	0.5	0.4	5	1.3	0.7	0.4	6	1.3	0.7	0.4

Table 23. **Values of k, s and l belonging to the Curves in Fig. 48.**

β_0	4.5		1.75		0.75	
τ_1	0.5	∞	0.5	∞	0.5	∞
k	7	5	∞	∞	∞	∞
s	7	5	10	7	15	10
l	3	1	3	1	3	1

starts from $r = 0.60$ at $\cos\vartheta = 1$, the $r(0, \vartheta)$'s were determined in points of the profiles of the centre-limb series of this line at the same $\Delta\lambda$, as found for $r = 0.60$ at $\cos\vartheta = 1$. In the case of a multiplet the results of this procedure from the components were averaged and were drawn in the figures as one single observational series. As the observed centre-limb variations of the Fe multiplet and of Ca 4226.7 differ only slightly, they have, likewise, been averaged (see also remark, end of § 32).

Two different places in the inner wings have been selected. Fig. 47 shows the theoretical curves, computed for a relative intensity of about 60 % in the centre of the sun's disc, Fig. 48 those for a relative intensity of about 30 %. Tables 22 and 23 give the values of k, s and l, which with the aid of (22), (23) and (24) have served for the computation of these theoretical curves. In the infra-red, where $\beta_0 = 0.75$, the minimum relative intensity for selective absorption amounts for $k = \infty$ still to 57 %, so that is was impossible for this case to draw a curve in Fig. 48, which for 30 % starts at $\cos\vartheta = 1$. The number of values for τ_1 in Fig. 48 is limited to two, because, practically speaking, τ_1 has no longer an appreciable influence on the centre-limb variation, owing to the fact that the observed radiation originates predominantly in high layers. The theoretical curves for the values of τ_1, that for a given line deserve in the first place to be compared with the observations (according to § 29) are marked with an asterisk.

In this connection one should once more bear in mind that, for the parts of the line-profile now discussed, in addition to the coefficient of coherent scattering, the coefficient of extinction must be chiefly introduced in the computations referring to the higher layers of the atmosphere, where the difference between $\overline{J}$ and J_ν is greatest, which is why the observations must be described by means of a combination of coherent scattering and extinction, in which $\tau_{1,l}$ is considerably smaller than $\tau_{1,s}$ (§ 30).

From a comparison with the drawn curves one can decide whether or not the observations can be explained by means of one of the processes considered. If the explanation requires the simultaneous action of more processes, only qualitative statements can be made, owing to the fact that for the already deep depressions in the line-profile, it is no longer allowed directly to combine the various curves of Fig. 47, resp. 48. It remains in that case, however, possible to ascertain qualitatively, whether or not the tendency of the difference between the observed centre-limb variation and a certain definite theoretical curve agrees with the variation indicated by another curve.

By means of (21) one can, however, compute the centre-limb variation for any mutual ratio of the three processes, provided only that their individual τ_1's are the same and one would then be able to draw in the figure the curves representing a simultaneous influence of absorption, scattering and extinction, in order to compare them with the observational

results. If, however, the τ_1's are mutually different, this is no longer possible and one has to resort to numerical computations.

A qualitive statement is also obtained when one of the processes (A) must be considered as the principal one and another one (B) as subsidiary, so that in a first approximation it will act additively. The effect of this slight addition (B) can be read from the curves for the far wings (Fig. 41), bearing in mind, that one is free to multiply these by an arbitrary factor, depending on the extent to which the process (B) is active. When (B) means scattering or absorption, this factor will in any case be positive; when, however, the process (B) can be described by the coefficient l, this factor can a priori be positive as well as negative (the effect of a positive l has been called extinction, the effect of a negative l may be called increased emission). From a further discussion in the §§ following next it will appear, that in the wings of the lines considered, a small negative coefficient may be expected only for the infra-red lines, whereas for the other lines, it is positive.

§ 38. Explanation of the centre-limb variations of those parts in the line-profile for which $r(0,0) \approx 0.60$.

If, now, we study Fig. 47 first, it appears that the centre-limb variations of the violet lines cannot be rendered by the theoretical curves for the appropriate $\tau_{1,k}$ and $\tau_{1,s}$ which for the H- and K line have the value ∞, and for the Fe lines and the line Ca 4226.7 values from 0.5 to 1.5. From a comparison with the extinction-curves, it is clearly apparent, that here the influence of the extinction in a thin surface layer is still fairly strongly present. For the Mg b lines and the Na D lines the agreement with the curve of scattering is much more satisfactory, while for the infra-red Ca^+ lines the deviations of the observations from the curves of scattering are in a direction opposite to the one in which they deviate for small $\tau_{1,l}$ from the extinction-curve. We shall now proceed to relate how this can be explained in the light of the conceptions concerning non-coherent scattering.

Considerations obviously following from § 30 furnish a qualitative explanation. For $\beta_0 = 4.5$, J_ν is larger than $\bar{J}$ for those values of k and s, that give a relative intensity of about 60 % for the centre of the sun's disc (Table 22), and this difference increases fairly strongly close to the surface (Fig. 39). For that reason, the coefficient of extinction must, in the higher layers of the atmosphere, occur in addition to the coefficient of coherent scattering in the description of the behaviour of the Fraun-

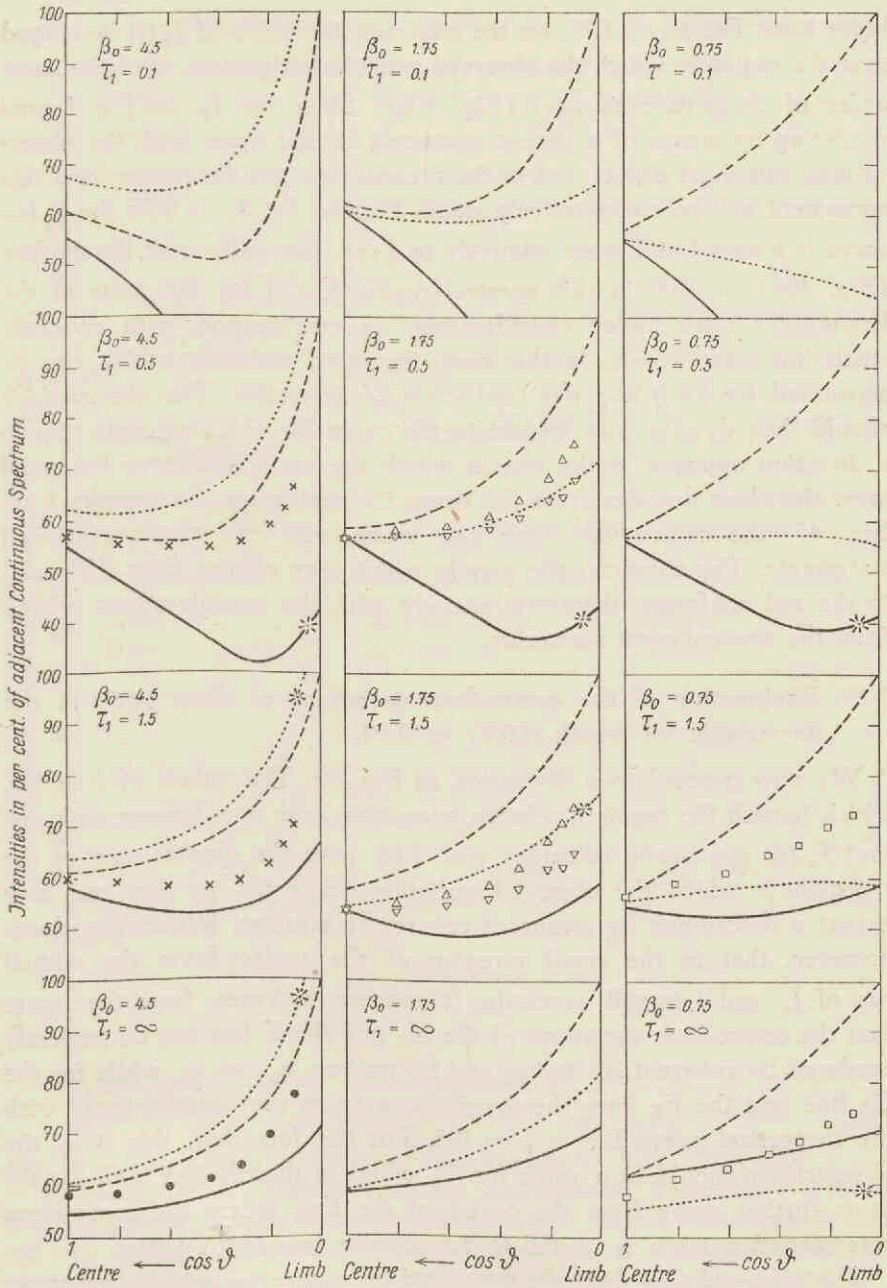

Fig. 47. — Centre-limb variations in the wings of the Fraunhofer lines. Theoretical curves: — — — absorption, ... coherent scattering, —— extinction. Observations: ● H- and K line of Ca+, × Fe multiplet and Ca 4226.7, △ Mg b lines, ▽ Na D lines, □ infra-red lines of Ca+. For further explanations see Fig. 48.

hofer lines. For $\beta_0 = 1.75$, on the contrary, the value of $J_\nu(\tau)$ averaged over the region in which the observed radiation originates, is of the same order of magnitude as $\overline{J}(\tau)$ (Fig. 40a). Since for $J_\nu = \overline{J}$ a formal rendering by means of coherent scattering should agree with the observations, one must expect that in the present case the deviations from this agreement will be comparatively small. Finally, for $\beta_0 = 0.75$ the $J_\nu(\tau)$-curve is lowered still more relatively to $\overline{J}(\tau)$, especially near the surface (Fig. 40b), so that in this spectral region $J_\nu < \overline{J}$ for the parts of the Fraunhofer lines under consideration. In combination with coherent scattering there occurs, in this case, increased emission, which can be accounted for by a negative coefficient of extinction. The observations should then deviate with respect to the curve for coherent scattering in a direction opposite to the one in which the extinction-curve for small layer-thickness deviates from the curve for scattering. As appears from Fig. 47, the centre-limb variations agree with the above-mentioned statements. The characteristic way in which they change from the violet to the red conforms, therefore, entirely with the considerations arising from the non-coherent scattering.

§ 39. Explanation of the centre-limb variations of those parts in the line-profile for which $r(0,0) \approx 0.30$.

We now proceed to a discussion of Fig. 48. The values of k and s, which furnish the required relative intensities have now become so large, that $J_\nu(\tau)$ practically coincides with $\overline{J}(\tau)$ over the greater part of the τ-region in which the observed radiation originates, so that one may expect a description by means of coherent scattering. We cannot deny, however, that in the small τ-region of the surface-layer the mutual run of J_ν and $\overline{J}$ is still uncertain. It appears, however, from the figure that the centre-limb variations of the H- and the K line can be perfectly rendered by coherent scattering and by putting $\tau_{1,s} = \infty$, while for the Ca line and the Fe lines these variations agree very satisfactorily with the theoretical curve for $\tau_{1,s} = 0.5$. For the fact that, this time, the observations should fit a value for τ_1, which is slightly less than for the parts further away from the centre of the line, where the comparison was carried out for $\tau_1 = 0.5$ to 1.5, can be refered to § 29.

The infra-red Ca^+ lines fit the curve for $\tau_{1,s} = \infty$ within the errors of observation, while the observations of the Mg b lines and the Na D lines deviate in opposite directions from the curves for $\tau_{1,s} = 0.5$. These deviations can be due to different causes. In the first place, owing

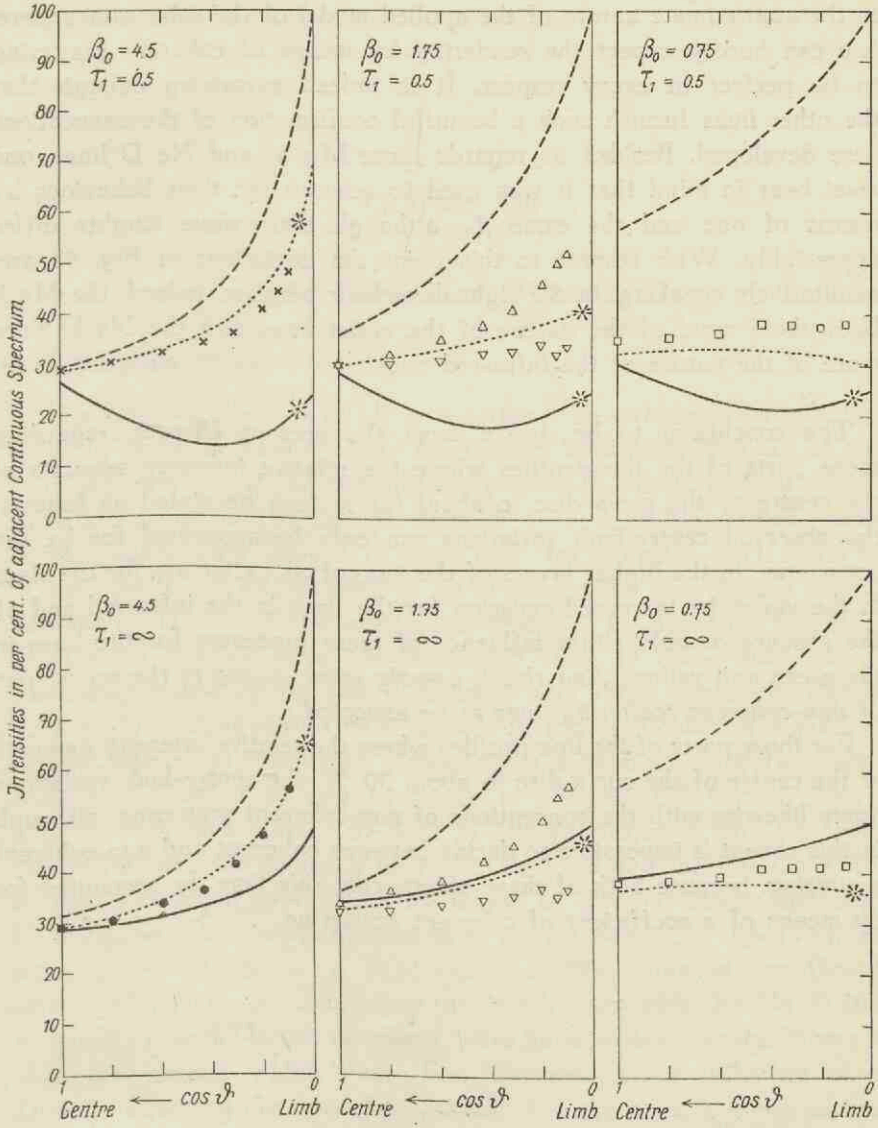

Fig. 48. — Centre-limb variations in the Fraunhofer lines. Theoretical curves: — — — absorption, ... coherent scattering, —— extinction. Observations: ● H- and K line of Ca+, × Fe multiplet and Ca 4226.7, △ Mg b lines, ▽ Na D lines, □ infra-red lines of Ca+. The theoretical curves, appropriate to a comparison with the observations, are marked with an asterisk (extinction is only to be expected in a comparatively thin surface-layer); the comparison concerns the centre-limb *variations;* the heights of the various theoretical curves and of the observational points are, therefore, adapted as well as possible to each other.

to the approximate nature of the applied model of the solar atmosphere, one can hardly expect the rendering by means of coherent scattering to be perfect in every respect. It is indeed surprising enough that the other lines furnish such a beautiful confirmation of the conceptions here developed. Besides, as regards these Mg b- and Na D lines, one must bear in mind that it was tried to account for their behaviour by means of one and the same β_0, although their wave lenghts differ appreciably. With respect to this point the deviations in Fig. 48 are, qualitatively speaking, in the right directions, because, indeed, the Mg b lines show more of the nature of the violet lines and the Na D lines more of the nature of the infra-red ones.

The conclusion to be drawn from the present chapter, regarding those parts of the line-profiles where the relative intensity amounts at the centre of the sun's disc to about 60 %, can be stated as follows: the observed centre-limb variations can only be accounted for by the occurrence in the higher layers of the sun, of a) extinction for the lines in the violet, b) increased emission for the lines in the infra-red and c) the absence or only slight influence of these processes for the lines in the green and yellow. *And this is exactly what, owing to the occurrence of non-coherent scattering, was to be expected.*

For those parts of the line-profiles where the relative intensity amounts at the centre of the sun's disc to about 30 %, the centre-limb variations agree likewise with the conceptions of non-coherent scattering, although in this case it is impossible to decide between coherent and non-coherent scattering, because both of these effects can, this time, be accounted for by means of a coefficient of coherent scattering.

CHAPTER VIII

THE CENTRAL INTENSITIES

§ 40. Doppler effect.

The Doppler effect, in so far as it arises from turbulence, would cause a filling up of the centre of the Fraunhofer lines to an amount of more than 0.5 percent., if the turbulence-elements at the surface of the sun have a velocity in the line of sight of 1 to 2 km/sec, which various investigations have proved to exist (see, for example, [89]). This fact is used by R. O. Redman [39]) as an argument for providing a possible explanation of the central intensities, measured by him on a few strong Fraunhofer lines. I have also measured some of these lines and the intensities found are in fair agreement with those found by Redman (see § 13). Yet, it should be remarked that in particular as regards the central intensities turbulence plays only a subsidiary part. In order to make this clear, it is only necessary to compare the various lines in Fig. 49, with each other. The wide H and K lines have stronger central intensities than the so much narrower Fe lines and the line Ca 4226.7, so that a common explanation by means of Doppler effect, appears to be excluded. The central intensities of the infra-red Ca^+ lines are, likewise, much too strong to have their possible origin in the Doppler effect only, while on comparing the Mg b lines with the Na D lines, it appears that the latter, narrower, ones have weaker central intensities than the former, wider, ones. For that reason the influence of the Doppler effect on the central intensities is in the present thesis assumed to be small, while they themselves are ascribed to a different cause, but this does not mean, that part of the central intensities might not be due to the Doppler effect.

§ 41. Extra-emission.

A. Unsold [2]), A. Pannekoek [90, 91, 92]), R. v. d. R. Woolley [93]) and B. Strömgren [3]) have given explanations of the formation of central in-

tensities, all to the effect that extra-emission occurs in the proper and in the adjacent higher and lower frequencies of the spectral line. This extra-emission arises from the fact, that more light of the other frequencies is switched over to the central ones than the other way round. This is a consequence of the small radiation-density in the centre of a strong Fraunhofer line, which causes the cycle of energy-transferences of which absorption of light of the central intensity forms part, to occur less often than the reversed cycle accompanied with emission of that light.

In the exchange of radiation between different frequencies, one must distinguish between the two following possibilities:

a) the two frequencies are located, as in the case of non-coherent scattering, in the region of one and the same Fraunhofer line; the transitions of energy in the atom are then only those between the two energy-levels, corresponding to the Fraunhofer line in question,

b) the two frequencies are *not* located in the region of one and the same Fraunhofer line, as in the case of fluorescence; this time also other discrete levels or the energy-continuum play their part in the transitions of energy.

The various writers mentioned above have investigated the influence of these processes on the central intensities.

Unsöld examined the influence of the transitions from the higher of the two energy-levels, that correspond with the Fraunhofer line in question, to the discrete more highly located levels such as will occur under the influence of the prevailing field of radiation, and the subsequent transitions in the reversed direction. He showed that, assuming a Boltzmann-partition for the occupations of the higher levels, one can account for this process by a formal coefficient of selective absorption, and from transition-probabilities of atomic theory he succeeded in deriving an estimate of the ratio between this selective absorption and the selective scattering. From this ratio he calculated values for the central intensities, and their centre-limb variations, which in their general features, agree with the observations.

Pannekoek considered, as did Unsöld, fluorescence-coupling between discrete stationary states, without, however, assuming that the occupations are adapted to a Bolzmann-partition [91]; for resonance-lines his calculations did not lead to appreciable amounts for the central intensities. He also examined the exchange of radiation between the centre and the wings of the lines in a similar way as done in § 24 of the present thesis. As Pannekoek did not assume a widening of the fundamental level, he finds, also in this way, that for a resonance-line the

central intensity is zero[90]). On taking into account the run of the coefficient of scattering in the core of the line, he was, however, led to the result[92]) that in the centre an emission-peak may occur, whose influence on the central intensities is, however, difficult to trace.

Woolley calculated the influence of the cyclic transitions, which occur in the fluorescence-process, on the central intensities of the Balmer lines $H\alpha$ and $H\beta$ and he finds values which agree with the observations.

Strömgren explained the central intensities by means of an extra-emission due to free electrons being caught via the higher level subsequent to direct photo-ionization from the lower level. Owing to the less dense radiation in the centre of a strong Fraunhofer line this cycle of transitions will, namely, occur more often than the reversed one. Strömgren, too, was successfull in making his results agree, as regards the order of magnitude, with the observations. Unsöld applied to Strömgren's explanation the same reasoning as to his own, and was, therefore, able to account here, too, phenomenologically for the central intensities by means of a finite s/k.

It will now be shown that a finite s/k provides one of the ways to account for the behaviour of a Fraunhofer line, if a frequency is concerned, for which extra-emission occurs, as, according to the above mentioned investigators, happens in the centre of the lines *). This follows already from the case dealt with in § 26e of which the treatment can also be started in a slightly modified way so as to make it apply directly to the central intensities, where coherent scattering and extra-emission take place; the equation of transfer can then be written as follows:

$$\cos\vartheta \frac{\mathrm{d}I}{\mathrm{d}\tau} = (1 + s_1) I - s_1 J - E - B \tag{45}$$

where s_1 denotes the coefficient of coherent scattering and E the selective extra-emission.

The equation of transfer for coherent scattering and absorption is:

$$\cos\vartheta \frac{\mathrm{d}I}{\mathrm{d}\tau} = (1 + s_2 + k) I - s_2 J - k B - B. \tag{46}$$

If these two equations are to merge into each other, the conditions

*) Pannekoek [92]) drew already a similar conclusion.

$s_1 = s_2 + k$ and $s_1 J + E = s_2 J + k B$ must be satisfied, from which it follows that

$$\frac{s_2}{k} = \frac{s_1 (B - J)}{E} - 1. \tag{47}$$

It is, therefore, indeed possible to describe the combined effects of coherent scattering and extra-emission by means of a finite ratio s/k, and its value is known when the value of $B - J$ and the ratio between the coefficient of scattering and the emission are known.

§ 42. Comparison with the observations.

In the present paragraph will be shown first how the observed centre-limb variations of the central intensities can be formally accounted for by means of certain definite values of s/k, which possibility must be regarded as corroborating the theories of the extra-emission. Next, the values obtained for s/k will be compared with those determined by Unsöld.

In the line-centre the coefficient of scattering has a very large value and, as it will turn out that for all investigated Fraunhofer lines $s/k < 2000$, we have $k \gg 1$. It follows from this, that, when the values of τ_1 are not too small, — the values $\tau_1 > 0.5$ deduced from the centre-limb variations of the wings, are sufficiently large —, the products $p\tau_1$ and $q\tau_1$ are likewise large, so that formula (21) transforms into an expression, in which, beside β_0 and $\cos\vartheta$, only s/k occurs. In this limiting case we have:

$$r(0,\vartheta) = (1 + \beta_0 \cos\vartheta)^{-1} \left\{ 1 - \frac{\frac{s/k}{s/k+1}}{\left(1 + \frac{2}{\sqrt{3}} \sqrt{\frac{1}{s/k+1}}\right)\left(1 + \sqrt{3} \sqrt{\frac{1}{s/k+1}} \cos\vartheta\right)} \right\} \tag{48}$$

When $s/k \gg 1$, this can be simplified to:

$$r(0,\vartheta) = \frac{\frac{2}{\sqrt{3}}\left(1 + \frac{3}{2}\cos\vartheta\right)}{1 + \beta_0 \cos\vartheta} \sqrt{k/s}. \tag{49}$$

These two expressions have already been deduced by Unsöld. It follows from the above, that the value of τ_1, the optical thickness of the

layer in which the absorbing atoms occur, does not matter if only s and k be sufficiently large, because, in passing to the limit, not τ_1 itself, but $p\tau_1$ and $q\tau_1$ are the decisive quantities. This can be readily understood, considering that in the case of only a thin layer of atoms but with large scattering- and absorption coefficients, no radiation from deeper layers can emerge at the surface. For the three different spectral regions characterized by $\beta_0 = 4.5$, 1.75 and 0.75, a few centre-limb variations were computed by means of (48) for different values of s/k. These values were chosen in such a way, that the computed *values* of the central intensities of the various lines agreed as well as possible with the observed ones. The criterion for the correctness of the explanation of the central intensities is in that case the centre-limb *variation*, which, once the values of β_0 and s/k have been chosen, is unambiguously determined. The observed and computed centre-limb variations are represented in Fig. 49. As observational results are taken the central intensities of the lines corrected for the instrumental broadening, except for the Ca^+ lines, to which this correction could not be applied, the instrumental curve for the Utrecht apparatus not being sufficiently known; fortunately these happen to be broad lines, so that the influence of the apparatus will presumably be small (c.f. in this connection the observational part).

It serves a useful purpose to carry out the comparison of the observations with theory in another way too. As is evident (48) restricts the influence of β_0 to the darkening towards the limb of the continuous spectrum, since it occurs only in the denominator $1 + \beta_0 \cos\vartheta$. This darkening can, however, be represented only approximately by $1 + \beta_0 \cos\vartheta$ and it suggests itself to use the *observed* darkening towards the limb of the continuous spectrum for predicting the centre-limb variations of the central intensities. For this purpose the results from the measurements by W. J. H. Moll, H. C. Burger and J. v. d. Bilt have been used, as of all observations these were continued the farthest up to the limb. If, now, the centre-limb variations are computed by substituting for the denominator in (48) the values observed by the investigators mentioned, one obtains the ——— curves of Fig. 49. The height of these curves was fixed in such a way, that in the various graphs the relative intensities at $\cos\vartheta = 1$ coincide with those computed directly from (48). It appears, that in a few cases, the observations are now better accounted for (H- and K line and Mg b lines), though in a few other cases (infrared Ca^+ lines) the agreement becomes slightly less. Generally speaking, one can state that the observations lie in between the centre-limb variations computed in the two ways.

The comparison of the observed central intensities with the theoretical curves of Fig. 49, yields the values of s/k, given under „observed" in Table 24. In the column headed „theoretical" one finds the values of s/k, computed by Unsöld or in the way indicated by him. The observational results, as well as the values predicted from theory can still be improved,

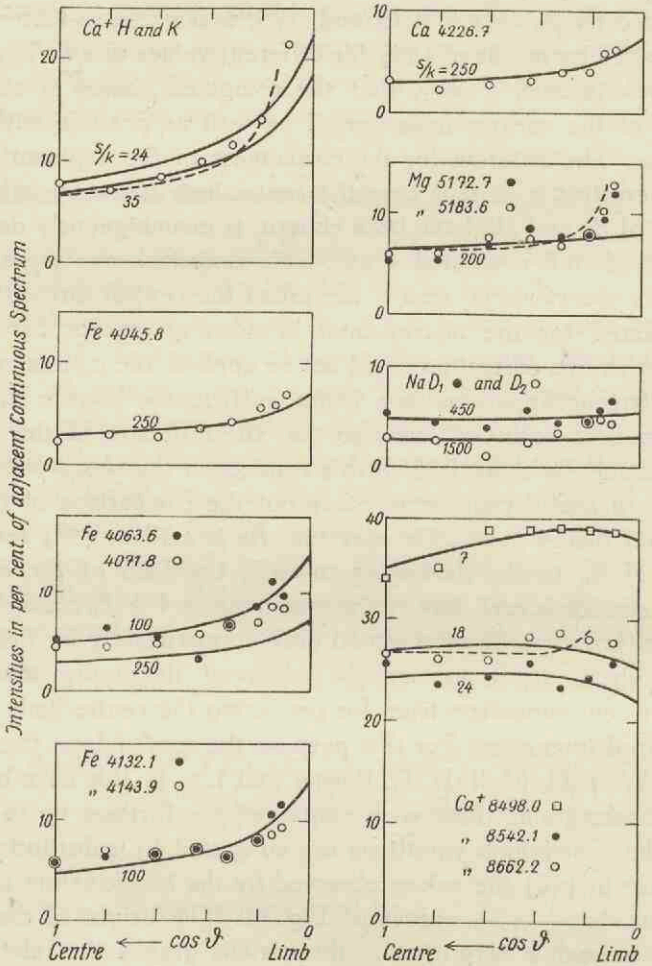

Fig. 49. — Centre-limb variations of the central intensities; —— computed with the aid of formula (48); the values of s/k belong to these curves; — — — computed with the numerator of (48) and the darkening of the continuous spectrum towards the limb, according to the observations by W. J. H. Moll, H. C. Burger and J. v. d. Bilt; these curves have been made to coincide for $\cos\vartheta = 1$ with one of the curves computed from (48); for lines located in the same spectral region the ratios between the ordinates of —— and — — — are the same for corresponding $\cos\vartheta$.

the former because the observations on which the present thesis is based may be impaired by the sources of error mentioned in § 9, (for a comparison with other observers see Chapter II), the latter because Unsöld's theory is only an approximative one. Besides one should bear in mind that the other processes contributing to the central intensities have not been taken into account.

The differences beween theory and observation become less striking, when one compares the values of the central intensities themselves, instead of those of s/k, because for large s/k the former are proportional to $\sqrt{k/s}$, so that for the weak central intensities an error of a few percents in the observational results corresponds to a large difference in s/k.

The results obtained in this chapter can be summarized as follows:

1) The centre-limb variations secured can be explained with the aid of a finite value of s/k, that is to say with the theories of extra-emission.

2) For a few lines the theoretical and observational absolute values do not agree; a striking feature as regards this discrepancy is that for some multiplet components the values found observationally are mutually different, whereas Unsöld's theory requires them to be equal.

3) The fact that for all Ca^+ lines investigated, the values of s/k are small, and deviate strongly from those for the other lines, points to a common cause. This is further evidence for the conception that the extra-emission is due to the particular nature of the higher level common to all these lines; these properties might for example, lead to a great multiplicity of transitions to and from the higher energy-levels.

Table 24. **Observed and Theoretical Values of s/k and $r(0,0)$.**

Lines	s/k		$r_{\cos\vartheta=1}$ (in %)	
	Observed	Theoretical (Unsöld)	Observed	Theoretical (Unsöld)
Ca^+ H- and K line	30	$467-1.74 \cdot 10^7$	7.4	0.013—2.2
Ca 4226.7 . . .	250	23.6—338	3.0	2.6—7.7
Mg b lines . . .	200	43—513	5.5	4.1—14.0
Na D lines . . .	450; 1500	15.9—132	2.5; 5.0	8.7—25.0
Ca^+ 8498.0 . .	7	$24.6-0.92 \cdot 10^6$	35	0.17—24.0
Ca^+ 8542.1 . .	24	$187-7.0 \cdot 10^6$	24	0.06—10.6
Ca^+ 8662.2 . .	18	$158-5.9 \cdot 10^6$	27	0.07—11.4

FINAL CONSIDERATIONS

The uncertainty as regards the exchange of radiation in the Fraunhofer lines which has prevailed for years in astrophysics, and on which light has been thrown by various investigators, cannot be better characterized than by what Eddington [49]) wrote 13 years ago: „The crucial question is whether light absorbed in one part of a line is re-emitted in precisely the same part of the line. If so, the blackening in this frequency is independent of what is happening in neighbouring frequencies. The alternative is that the re-emission has a probability distribution, and is correlated to, but not determined by, the absorbed frequency. For example, if the process is regarded as one of transition between two energy levels which are not sharp but are composed of narrow bands of energy, the atom is not likely to return to the precise spot in the lower level from which it started, and the re-emission will not be the exact reverse of the absorption. In that case the line can only be studied as a whole. Modern attempts to interpret the contours of absorption lines assume (rightly or wrongly) that there is no such redistribution of frequencies. . . . . If this assumption is untrue, the usual treatment of line-contour is entirely unsound."

Since then, the consequences of the redistribution, meant by Eddington have, as yet, never been compared with the observational results. In the present thesis, however, non-coherent scattering, which comprises also the redistribution mentioned by Eddington, is put foremost and is then applied in order to be able to explain the centre-limb variations of the wings of the strong Fraunhofer lines. The difference between non-coherent and coherent scattering manifests itself, however, only if the intensity of radiation varies over the region of a spectral line. This is, however, exactly what happens in stellar atmospheres, so that in dealing with the various problems, it will always be necessary to trace its influence. As regards the centre-limb variations of the wings of the strong Fraunhofer lines, this influence is very appreciable; it is just by their characteristic behaviour that the present writer has been forced to investigate fully the effects of non-coherent scattering.

When Schwarzschild [5]) was lead by his observations to the conclusion that it is scattering and not absorption that plays the chief part in the formation of Fraunhofer lines, the first step was made towards the attainment of an explanation of the centre-limb variations. This thesis has shown that especially the lines in the blue and violet parts of the spectrum vanish at the limb of the sun's disc to a still less pronounced degree than would follow from coherent scattering, and that, finally, non-coherent scattering furnishes here the solution. The remarkable point, however, is now that, nevertheless, the behaviour of the far wings can, in this case, be partly accounted for, be it only formally, by absorption. A similar conclusion was already reached by Woolley [66]), who, however, did not investigate its consequences in further detail. After absorption was rejected by Schwarzschild, it is now, at least formally, re-introduced for the wings of the strong Fraunhofer lines.

Finally, a few effects of non-coherent scattering will here be discussed, pertaining to equivalent widths. They follow at once from the considerations in this thesis, and refer more especially to the difference from coherent scattering, because up to the present time, practically all statements concerning stellar atmospheres were based on the latter process.

In the first place it appears from the Chapters VI and VII, that, if the same number of atoms contributes to their formation, the Fraunhofer lines if due to non-coherent scattering will be stronger in the violet and weaker in the red parts of the spectrum than if due to coherent scattering. This must be taken into account when one compares lines which lie in different parts of the spectrum with a view to obtaining from their mutual strengths data concerning the temperature and the degree of ionization.

In the second place the difference between the two kinds of scattering will be more pronounced for strong Fraunhofer lines than for weak ones. Indeed, of the stronger lines the wings, which are the only parts where the effects of non-coherent scattering are noticeable, furnish a larger relative contribution to the equivalent width, than the wings of the weaker lines, because they are determined in the case of the former by damping, in the case of the latter by Doppler effect. This influence makes itself, therefore, already felt when one compares lines in the same spectral region. As its effect on lines of different strength varies with their strength, it will modify, among others, the shape of the curve of growth [94]).

In terms of the equivalent width, however, the differences mentioned

attain at the most values of a few tens of percents, so that, generally speaking, the conclusions drawn from coherent scattering are not endangered. This is indeed obvious, because, otherwise, one would surely have investigated the effects of non-coherent scattering sooner.

As, however, the fact is now firmly established that non-coherent scattering predominates in the formation of the Fraunhofer lines, it is worth while to subject this process to a closer theoretical and experimental study and to investigate it more in particular in the case of spectral lines disturbed by collisions, thereby enabling one to arrive at a quantitative treatment of the problems connected with it.

λ wave length in A units.

ν frequency of light.

γ damping constant.

ϑ angle with positive direction of normal to the solar surface.

ω solid angle.

Quantities referring to the sun's disc.

r distance from the centre of the sun's disc
R radius of the sun's disc
} $r/R = \sin \vartheta$.

Quantities referring to the line-profiles.

$r(0,\vartheta) = r_\nu(0,\vartheta) = i/i_0 = I_\nu(0,\vartheta)/I_0(0,\vartheta)$, intensity at frequency ν in the profile of a Fraunhofer line, in terms of the intensity of the adjacent continuous spectrum.

c quantity, measuring the depression $1-r(0,\vartheta)$ in the far wings according to: $(i_0-i)/i = c/\Delta\lambda^2$.

$\Delta\lambda$ distance in A from the centre of a Fraunhofer line.

Quantities referring to the solar atmosphere.

ϱ local density.

t geometrical depth.

τ optical depth, defined by $\tau = \int_0^t \varkappa \varrho \, dt$.

τ_1 optical depth of the layer in the schematic model of the solar atmosphere in which the selective processes take place.

Coefficients of absorption etc.

$\alpha = \alpha_\nu(\tau)$ total line absorption coefficient per gram of matter at frequency ν and optical depth τ. This quantity can be split up into the three coefficients $\varkappa$, σ and λ.

$\varkappa = \varkappa_\nu(\tau)$ coefficient of selective absorption; the part of the absorbed radiation corresponding to this quantity is transformed into

kinetic energy (by non-elastic collisions) and subsequently into temperature radiation.

$\sigma = \sigma_\nu(\tau)$ coefficient of coherent scattering; the part of the absorbed radiation corresponding to this quantity is re-emitted in the same frequency.

$\lambda = \lambda_\nu(\tau)$ coefficient of extinction; the part of the absorbed radiation corresponding to this quantity is re-emitted in a different frequency; a negative value of λ means that the radiation absorbed in a frequency different from ν is re-emitted in the frequency ν; this is called increased- or extra-emission.

$\varkappa = \varkappa(\tau)$ coefficient of continuous absorption, practically constant with ν.

$a = a_\nu(\tau) = \alpha_\nu(\tau)/\varkappa(\tau) = k + s + l$
$k = k_\nu(\tau) = \varkappa_\nu(\tau)/\varkappa(\tau)$
$s = s_\nu(\tau) = \sigma_\nu(\tau)/\varkappa(\tau)$
$l = l_\nu(\tau) = \lambda_\nu(\tau)/\varkappa(\tau)$

$p = \sqrt{3(1+k+s+l)(1+k+l)}$; $q = 1 + k + s + l$.

$\eta = \eta_\nu(\tau) = k + s$, is the notation used by B. Strömgren [54]); in the absence of extinction η corresponds to our a.

$e = e_\nu$ amount of emitted radiation.

Quantities referring to the radiation.

$I = I_\nu(\tau, \vartheta)$ intensity of radiation in a Fraunhofer line at frequency ν in optical depth τ, making an angle ϑ with the normal to the solar surface.

I_0 the same as I, but in the continuous spectrum.

$J = J_\nu(\tau)$ mean intensity over all directions, defined by $J = \int I \, d\omega/4\pi$; in this thesis J is called radiation-density.

$\bar{J} = \bar{J}_\nu(\tau)$ mean value of J with respect to α_ν, defined by $\bar{J} = \int J_\nu \alpha_\nu \, d\nu / \int \alpha_\nu \, d\nu$.

$H = H_\nu(\tau)$ net flux of radiation at frequency ν in a Fraunhofer line, defined by $H = \int I \cos\vartheta \, d\omega/4\pi$.

H_0 the same, but in the continuous spectrum.

$B = B(T)$ black-body radiation of temperature T (in the absence of thermodynamical equilibrium B deviates from the black-body radiation properly speaking)

$B_0 = B(T_0)$ black-body radiation at the surface

$\beta_0 = \beta_0(\lambda)$ constant which determines the schematic run of B

$B = B_0(1 + \beta_0 \tau)$.

B_1 auxiliary quantity, related to B by the formula: $B_1 = B(1 + k)/(1 + k + l)$.

REFERENCES

1. P. ten Bruggencate, J. Houtgast und H. von Klüber, *Publ. Ap. Obs. Potsdam* Nr. 96, **29**, 1939.
2. A. Unsöld, *Zs. f. Ap.* **4**, 319, 1932; *Physik der Sternatmosphären*, J. Springer, Berlin 1938 *), Abschnitt 74.
3. B. Strömgren, *Zs. f. Ap.* **10**, 237, 1935.
4. G. E. Hale and W. S. Adams, *Ap. J.* **25**, 300, 1907.
5. K. Schwarzschild, *Sitzgsber. Preuss. Ak. d. Wiss.* **II**, 1914, S. 1183.
6. A. Unsöld, *Zs. f. Ap.* **44**, 793, 1927.
7. ——, *ibid.* **46**, 765, 1928.
8. H. H. Plaskett, *Mon. Not. R. A. S.* **91**, 870, 1931.
9. G. Righini, *Pubbl. Arcetri* **48**, 29, 1931; *Mem. Soc. Astr. Ital.* **5**, 283, 1931.
10. E. Cherrington, *Lick Obs. Bull.* No. 477, **17**, 161, 1935.
11. G. Righini, *Pubbl. Arcetri* **51**, 57, 1933; *Mem. Soc. Astr. Ital.* **7**, 19, 1933.
12. T. Royds and A. L. Narayan, *Kodaikanal Obs. Bull.* **109**, 375, 1936.
13. M. G. Adam, *Mon. Not. R. A. S.* **98**, 112, 1937.
14. ——, *ibid.* **98**, 544, 1938.
15. M. Minnaert und J. Houtgast *Zs. f. Ap.* **12**, 81, 1936.
16. A. Pannekoek, *Publ. Astr. Inst. Univ. Amsterdam* Nr. **4**, 1935.
17. J. Houtgast, *Zs. f. Ap.* **16**, 43, 1938.
18. C. W. Allen, *Mon. Not. R. A. S.* **100**, 10, 1939.
19. D. S. Evans, *ibid.* **100**, 156, 1939.

19a. C. D. Shane, *Lick Obs. Bull.* No. 507, **19**, 119, 1941.

20. R. O. Redman, *Mon. Not. R. A. S.* **96**, 488, 1936.
21. M. Minnaert und J. Genard, *Zs. f. Ap.* **10**, 377, 1935.
22. A. Unsöld, *ibid.* **12**, 56, 1936; *Physik der Sternatmosphären*, S. 278.
23. P. ten Bruggencate und J. Houtgast, *Zs. f. Ap.* **20**, 149, 1940.
24. M. Minnaert, *ibid.* **10**, 40, 1935.
25. W. H. Julius, *Bull. Astr. Inst. Netherl.* **1**, 119, 1922; *Hemel en Dampkring* **21**, 57, 1923.
26. P. H. van Cittert, *Zs. f. Phys.* **65**, 547, 1930; **69**, 298, 1931.
27. G. Abetti e I. Castelli, *Pubbl. Arcetri* **53**, 25, 1935.
28. M. Minnaert, G. F. W. Mulders, J. Houtgast, *Photometric Atlas of the Solar Spectrum*, Kampert en Helm, Amsterdam 1940, p. 6.
29. A. Unsöld, *Physik der Sternatmosphären*, S. 216.
30. M. Minnaert, *Zs. f. Phys.* **45**, 610, 1927.
31. A. D. Thackeray, *Mon. Not. R. A. S.* **95**, 293, 1935.
32. R. O. Redman, *ibid.* **95**, 742, 1935.

*) Further to be referred to as „*Physik der Sternatmosphären*".

33. E. Strohbusch, *Zs. f. Instr.* **59**, 417, 1939.
34. E. Freundlich, *Das Turmteleskop der Einstein-Stiftung*, J. Springer, Berlin 1927.
35. H. C. v. d. Hulst, *Bull. Astr. Inst. Netherl.* **9**, 225, 1941.
36. P. Kremer, *ibid.* **9**, 229, 1941.
37. C. E. Moore, *A Multiplet Table of Astrophysical Interest*, Princeton, N. J. 1933.
38. C. E. St. John, C. E. Moore, L. M. Ware, E. F. Adams, H. D. Babcock, *Revision of Rowland's preliminary Table*, Washington 1928.
39. R. O. Redman, *Mon. Not. R. A. S.* **97**, 552, 1937.
40. C. W. Allen, *Mem. Comm. Sol. Obs.* **5**, part II, 1934.
41. R. B. King and A. S. King, *Ap. J.* **82**, 377, 1935.
42. R. v. d. R. Woolley, *Mon. Not. R. A. S.* **92**, 806, 1932.
43. M. Minnaert und G. F. W. Mulders, *Zs. f. Ap.* **1**, 192, 1930.
44. A. Unsöld, *Physik der Sternatmosphären*, Abschnitt 61.
45. A. Schuster, *Ap. J.* **21**, 1, 1905.
46. E. A. Milne, *Phil. Trans. Roy. Soc. London* **A 223**, 201, 1922.
47. ——, *Mon. Not. R. A. S.* **89**, 3, 1928.
48. A. S. Eddington, *The Internal Constitution of the Stars*, Cambridge, Univ. Press, 1926, Chapter XII.
49. ——, *Mon. Not. R. A. S.* **89**, 620, 1929.
50. E. A. Milne, *ibid.* **88**, 493, 1928.
51. A. Unsöld, *Zs. f. Ap.* **8**, 225, 1934.
52. A. Pannekoek, *Mon. Not. R. A. S.* **91**, 139 and 519, 1931.
53. B. Strömgren, *Ap. J.* **86**, 1, 1937.
54. ——, *Festschrift E. Strömgren*, Einar Munksgaard, Kopenhagen 1940, S. 218.
55. R. v. d. R. Woolley, *Mon. Not. R. A. S.* **90**, 170, 1930.
56. ——, *ibid.* **92**, 482, 1932.
57. ——, *ibid.* **98**, 3, 1937.
58. L. Spitzer, *Ap. J.* **87**, 1, 1938.
59. P. Swings and L. Dor, *ibid.* **88**, 516, 1938.
60. M. Krook, *Mon. Not. R. A. S.* **98**, 477, 1938.
61. H. R. Hulme, *ibid.* **99**, 730, 1939.
62. A. Unsöld, *Zs. f. Ap.* **4**, 339, 1932.
63. M. Minnaert, *ibid.* **12**, 313, 1936.
64. S. Rosseland, *Theoretical Astrophysics*, Oxford, Clarendon Press, 1936, § 41.
65. L. Spitzer, *Mon. Not. R. A. S.* **96**, 794, 1936.
66. R. v. d. R. Woolley, *ibid.* **98**, 624, 1938.
67. P. ten Bruggencate, *Zs. f. Ap.* **4**, 159, 1932.
68. P. Parchomenko, *Russ. Astr. J.* **12**, 140, 1935.
69. ——, *Astr. Nachr.* **270**, 193, 1940.
70. P. Wellmann, *Zs. f. Ap.* **12**, 140, 1936.
71. H. H. Plaskett, *Mon. Not. R. A. S.* **96**, 402, 1936; **101**, 3, 1941.
72. E. A. Milne, *Handbuch der Astrophysik* **III**, **1**, J. Springer, Berlin 1930, S. 65.
73. A. Pannekoek, *ibid.* S. 256.
74. S. Rosseland, *Astrophysik*, J. Springer, Berlin 1931, § 33.
75. B. Strömgren, *Handbuch der Astrophysik* **VII**, S. 203.
76. S. Rosseland, *Theoretical Astrophysics*, Chapter IX.
77. A. Unsöld, *Physik der Sternatmosphären*, Kapitel XII.
78. P. Swings and S. Chandrasekhar, *Mon. Not. R. A. S.* **97**, 24, 1936.

79. O. Struve, *Proc. Nat. Ac. Sc. U.S.A.* **26**, 120, 1940.
80. W. Orthmann und P. Pringsheim, *Zs. f. Phys.* **43**, 9, 1927.
81. V. Weisskopf, *Obs.* **56**, 291, 1933.
82. ——, *Zs. f. Phys.* **85**, 451, 1933.
83. C. G. Abbot, F. E. Fowle, L. B. Aldrich, *Ann. Ap. Obs. Smithsonian Inst.* **3**, 157, 1913; **4**, 221, 1922.
84. W. J. H. Moll, H. C. Burger, J. v. d. Bilt, *Bull. Astr. Inst. Netherl.* **3**, 83, 1925.
85. H. Raudenbusch, *Astr. Nachr.* **266**, 301, 1938.
86. A. Unsöld, *Physik der Sternatmosphären*, Abschnitt 31.
87. H. H. Plaskett, *Mon. Not. R. A. S.* **101**, 3, 1941.
88. I. W. Busbridge, *ibid.* **101**, 26, 1941.
89. P. ten Bruggencate, *Zs. f. Ap.* **18**, 316, 1939.
90. A. Pannekoek, *Proc. Ak. Amsterdam* **34**, 1352, 1931.
91. ——, *Bull. Astr. Inst. Netherl.* **7**, 151, 1933.
92. ——, *Mon. Not. R. A. S.* **95**, 725, 1935.
93. R. v. d. R. Woolley, *ibid.* **94**, 631, 1934.
94. M. Minnaert, *Obs.* **57**, 331, 1934.

CONTENTS

THEORETICAL PART

STELLINGEN

I

Onvolmaaktheden van het menselijk evenwichtsorgaan zijn mede oorzaak van verkeerde uitkomsten bij het schatten van de hoogten der hemellichamen.

II

De scintillatie der hemellichamen kan behulpzaam zijn bij het vaststellen van meteorologische toestanden. De interpretatie hunner waarnemingen door Gallisot en Bellemin moet evenwel betwijfeld worden.

C. Gallisot et E. Bellemin, *J. d. Phys.* **8**, 29, 1927.
M. Minnaert en J. Houtgast, *Zs. f. Ap.* **10**, 86, 1935.
J. Houtgast, *Hemel en Dampkring*, **34**, 169, 1936.

III

Wolkenbanden, zoeklichtbundels en andere dergelijke verschijnselen aan het hemelgewelf, die in werkelijkheid recht zijn, hebben een schijnbare vorm, die voorgesteld kan worden door de vergelijking $h = \text{bgtg}\ (a \cos A)$, waarin h en A de coördinaten aan het hemelgewelf zijn (hoogte en azimuth).

IV

Het is niet nodig om, zoals Unsöld doet, bij het oplossen van de integraal

$$\int_0^\infty \left(1 - e^{-\frac{1}{x^2}}\right) dx$$

een benaderingsmethode toe te passen.

A. Unsöld, *Physik der Sternatmosphären*, Berlin 1938, S. 167.

V

Het is mogelijk om bij zelfregistrerende microfotometers op een eenvoudige en toch nauwkeurige wijze de voortgaande beweging van de fotografische plaat met de roterende beweging van de trommel direct te koppelen, zonder gebruik te maken van tandraderen.

VI

De wijze, waarop N. Thompson zijn directe intensiteitsmetingen van fotografisch opgenomen spectra uitlegt, getuigt van een ernstig gemis aan inzicht in de werking van het door hem geconstrueerde apparaat.

N. Thompson, *Proc. Phys. Soc.* **45**, 441, 1933.

VII

Over de apparaatfunctie van een spectraalapparaat bestaan bij Unsöld en Evans nog onjuiste voorstellingen.

A. Unsöld, *Physik der Sternatmosphären*, Berlin 1938, S. 211.
D. S. Evans, *Obs.* **62**, 231, 1939.

VIII

De intensiteiten van de spookbeelden van een buigingsrooster kunnen met voordeel bepaald worden door intensiteitsmetingen in absorptielijnen, gebruik makend van een monochromator met voldoende „oplossend vermogen" (zie blz. 15 van deze dissertatie).

IX

In het probleem van de verstrooiing van licht door gestoorde atomen zou door bepaalde physische experimenten klaarheid gebracht kunnen worden.

X

Voor de toetsing van de niet-coherente verstrooiing is het van belang, het verloop van de zwarte straling met de diepte in de zonneatmosfeer te kennen in het violette spectraalgebied.